Electronic Thesis and Dissertation Repository

8-19-2015 12:00 AM

Self-Sustaining Smouldering Combustion as a Novel Disposal Destruction Method for Waste Water Biosolids

Tarek L. Rashwan
The University of Western Ontario

Supervisor
Dr. Jason I. Gerhard
The University of Western Ontario

SELF-SUSTAINING SMOULDERING COMBUSTION AS A NOVEL DISPOSAL
DESTRUCTION METHOD FOR WASTE WATER BIOSOLIDS

(Thesis format: Integrated Article)

by

Tarek L. Rashwan

Graduate Program in Engineering Science
Department of Civil and Environmental Engineering

A thesis submitted in partial fulfillment
of the requirements for the degree of
Master of Engineering Science

The School of Graduate and Postdoctoral Studies
The University of Western Ontario
London, Ontario, Canada

© Tarek L. Rashwan 2015

Abstract

Managing biosolids, the major by-product from wastewater treatment plants (WWTPs), persists as a major global challenge that often constitutes the majority of WWTP operating costs. Self-sustained smouldering is a new approach for organic waste treatment, in which the waste (i.e., the fuel) is destroyed in an energy efficient manner after mixing it with sand. Smouldering has never been applied to biosolids. Column experiments, using biosolids obtained from a WWTP, were employed to identify if - and under what conditions - smouldering could be used for treating biosolids. The parameter space in which smouldering was self-sustaining was mapped as a function of key system metrics: (1) sand/biosolids mass fraction, (2) biosolids moisture content, and (3) forced air flux. It was found that a self-sustaining reaction is achievable using biosolids with water content as high as 80% (with a biosolids lower heating value greater than 1.6 MJ/kg). Moreover, results suggest that operator-controlled air flux can assist in keeping the reaction self-sustaining in response to fluctuations in biosolids properties. An economic analysis suggests that smouldering could be a cost-effective management approach for WWTP biosolids in a number of scenarios by providing on site destruction with minimal energy input and limited preliminary dewatering.

Keywords

Smouldering, self-sustaining, STAR, biosolids, wastewater treatment, economic analysis

Co-Authorship

This thesis was written in accordance with regulations and guidelines for integrated-article format by the Faculty of Graduate and Postdoctoral Studies at the University of Western Ontario. All the experiments and relevant data was collected, analyzed and interpreted by the candidate under the supervision and guidance of Dr. Jason I. Gerhard.

Chapter 3: Self-sustaining Smouldering Combustion as a Novel Destruction Method for Biosolids

By Tarek L. Rashwan, Jason I. Gerhard, Gavin Grant

Contributions:

Tarek L. Rashwan: initiated the research topic, performed all the experiments, analysis and interpretation of experimental results, and wrote the draft chapter.

Jason I. Gerhard: initiated the research topic, supervised experiments, assisted in data interpretation, and reviewed/revised the draft chapter.

Gavin Grant: assisted in data interpretation, assisted in data collection for the economic analysis, and reviewed/revised the draft chapter.

Acknowledgements

I have had the incredible fortune to spend the last two years within the RESTORE group officially as a graduate student and the prior two years interloping as a summer researcher and undergraduate thesis student. During my time with such an outstanding group, I have grown in surprising directions and had the immense pleasure of co-creating many meaningful relationships with friends who are the most intelligent and virtuous people I have ever met. These four years have been some of my most enjoyable and have opened my eyes and my mind to myriad exciting ideas, including an unlikely marriage between fire and water.

Firstly, I must express my sincerest gratitude to the careful guidance, patient listening, and merciless editing of my supervisor, Dr. Jason Gerhard. I cannot begin to articulate how he has supported and enriched this work. It is probably most succinct to say that it simply would not have happened without his encouragement, inexhaustible creativity, and astounding thoroughness. His optimism and open-mindedness have fostered the most inventive research meetings that I have come to treasure as a bi-weekly highlight. I would also like to thank my co-supervisor, Dr. Gavin Grant, for his approachability, invaluable input, and practical perspective.

I greatly thank Paolo and Rory for introducing me to the thrilling, and sometimes improvisational, world of smouldering experimentation. Their infectious enthusiasm hooked me from day one. I also acknowledge Randy and Gary from Greenway, who made the biosolids acquisition exceptionally painless. I am in enormous debt to Shereen, who shared with me an exciting Christmas holiday in the lab. I could not have finished without her.

Important thanks to my great friends in RESTORE who I have shared many laughs with over the years. In particular, I would like to thank Ian, Chris P., and Chris K. for being such honest and heartening mentors and showing me that grad school is as much about pushing science as it is about having fun to release the frustration formed when science pushes back.

I would like to especially thank Becca for her terrific manuscript edits, delicious and bountiful dinners, and her endless positivity.

Finally, I would like to *not* thank my left scaphoid for being weak and inconveniently fracturing during the middle of the experimental work. That was a bummer.

Dedication

For my parents

Table of Contents

Chapter 4

Conclusions and Recommendations

Appendices

List of Tables

List of Figures

Chapter 1

Introduction

1.1 Problem Overview

In London, UK, 1842, the negative impacts of untreated wastewater on the surrounding population was explicitly addressed in Chadwick et al. (1843), a document which is credited for starting the first major campaign for wastewater treatment in Great Britain (Hamlin, 1998). Today, robust municipal wastewater treatment remains crucial in maintaining public health and protecting environmental quality. However, it persists as a major global challenge due to the expensive and complex treatment processes required to address evolving wastewater risks (Shannon et al., 2008). In the United States, wastewater treatment plants (WWTPs) are some of the most energy intensive public operations and, in combination with drinking water services, consume 30 – 40% of the total energy used by municipalities (U.S. EPA, 2014). Typically 50% of the operating and capital costs within WWTPs are dedicated to managing the solid by-product, biosolids. (U.S. EPA, 1994; Droste, 1997; Khiari et al., 2004). Compared to liquid stream treatment in WWTPs, biosolids management technology has advanced slower and there are limited options for disposal (or end use) (Metcalf and Eddy, 2003). In Canada, 90% of biosolids are either incinerated or land applied for agricultural purposes (Apedaile, 2001). These methods are both expensive in terms of transportation, energy input, and labour (Werther and Ogada, 1999; Wang et al., 2008; Roy et al., 2011). Land application is also subject to limitations and uncertain risks, largely stemming from contaminants of

emerging concern (U.S. EPA, 1995; Hale et al., 2001; Ternes et al., 2004; Venkatesan and Halden, 2014).

Self-sustaining smouldering combustion of organic wastes has been proven in the laboratory as a treatment option for hazardous liquid contaminants (e.g., creosote, coal tar, crude oil, trichloroethylene) and human faeces with moisture content as high as 70% (wet mass basis) (Pironi et al., 2009; Switzer et al., 2009; Pironi et al., 2011; Salman et al., 2015; Yermán et al., 2015). Smouldering combustion is driven by flameless exothermic oxidation reactions where the surface of the fuel is directly attacked by the oxidizer at temperatures typically between 500 – 700°C (Ohlemiller, 1985; Rein, 2009). By mixing the organic waste within an inert porous matrix (e.g., quartz sand), a self-sustaining smouldering reaction can be initiated and propagated via a forced airflow supply, destroying the organic waste (i.e., the fuel) (Pironi et al., 2009). In this mixture configuration, smouldering is an energy efficient solution for mass destruction as a self-sustaining reaction is achievable with a relatively small, one time input of energy (Switzer et al., 2009). The mixture's high heat capacity mitigates heat losses away from the reaction, while the rigid structure promotes airflow, and the large fraction of exposed organic waste surface area promotes surface reactions (Pironi et al., 2009). This also provides a robust method for the destruction of low calorific and/or high moisture content organic wastes, such as human faeces, which would otherwise require continuous energy input to thermally degrade via alternative means (e.g., incineration) (Yermán et al., 2015). These characteristics of smouldering combustion suggest it may be a low energy, cost-effective, on-site treatment alternative for WWTP biosolids. This hypothesis has never been tested.

1.2 Research Objectives

The objective of this work is to explore the technical and economic potential of utilizing smouldering combustion as a novel disposal technique for WWTP biosolids. To achieve this, a lab scale experimental study was completed to explore the limits for smouldering biosolids under self-sustaining conditions by varying biosolids moisture content, sand content, and air flux. Biosolids obtained from a local municipal WWTP were smouldered using established experimental procedures and data analyses techniques to identify these limits, and to characterize the smouldering propagation across experiments. Upon understanding the smouldering limitations, a preliminary economic analysis was conducted to estimate the payback period and potential cost savings from replacing an existing biosolids disposal method with an (in development) commercial smouldering combustion system.

1.3 Thesis Outline

This thesis is written in an integrated article format in accordance with the guidelines and regulations stipulated by the Faculty of Graduate Studies at the University of Western Ontario. Each chapter in the thesis is described below.

Chapter 2 is a review of the relevant literature and presents an overview of the wastewater treatment process with focus on biosolids processing and disposal, and economic considerations surrounding the WWTP industry. Also, an introduction to smouldering combustion is presented, where literature discussing the influence moisture has on smouldering propagation is highlighted. An overview of smouldering for mass destruction of hazardous liquids and human faeces is also presented.

Chapter 3 presents the full results from the lab scale experimental study exploring the smouldering limits with biosolids and a summary of the economic analysis. This chapter is written in a manuscript format for future submission to a peer reviewed journal.

Chapter 4 summarizes the research conducted in this work and presents conclusions as well as recommendations for future work.

Appendix A presents additional biosolids properties to supplement Chapter 3.

Appendix B presents a brief literature review on the boiling and evaporation within porous media.

Appendix C presents a comparison between virgin and re-wetted biosolids.

Appendix D presents emissions measurements from select experiments.

Appendix E presents data from an additional failure condition not discussed in Chapter 3.

Appendix F presents justification regarding mass loss assumptions.

Appendix G presents all remaining temperature, mass loss, and mass loss rate data.

1.4 References

Apedaile, E. (2001). A perspective on biosolids management. *The Canadian Journal of Infectious Diseases, 12*(4), 202.

Chadwick, E., Great Britain Home Office, & Great Britain Poor Law Commissioners. (1843). *Report on the Sanitary Conditions of the Labouring Population of Great Britain: A Supplementary Report on the Results of a Special Inquiry Into the Practice of Interment in Towns. Made at the Request of Her Majesty's Principal Secretary of State for the Home Department*: W. Clowes and Sons.

Droste, R. L. (1997). *Theory and Practice of Water and Wastewater Treatment*. New York, NY: Wiley.

Hale, R. C., La Guardia, M. J., Harvey, E. P., Gaylor, M. O., Mainor, T. M., & Duff, W. H. (2001). Flame retardants: Persistent pollutants in land-applied sludges. *Nature, 412*(6843), 140-141.

Hamlin, C. (1998). *Public Health and Social Justice in the Age of Chadwick: Britain, 1800-1854*: Cambridge University Press.

Khiari, B., Marias, F., Zagrouba, F., & Vaxelaire, J. (2004). Analytical study of the pyrolysis process in a wastewater treatment pilot station. *Desalination, 167*, 39-47.

Metcalf and Eddy. (2003). *Wastewater Engineering: Treatment and Reuse* (4th ed.). New York, NY: McGraw-Hill.

Ohlemiller, T. J. (1985). Modeling of smoldering combustion propagation. *Progress in energy and combustion science, 11*(4), 277-310.

Pironi, P., Switzer, C., Gerhard, J. I., Rein, G., & Torero, J. L. (2011). Self-sustaining smoldering combustion for NAPL remediation: laboratory evaluation of process sensitivity to key parameters. *Environmental Science & Technology, 45*(7), 2980-2986.

Pironi, P., Switzer, C., Rein, G., Fuentes, A., Gerhard, J. I., & Torero, J. L. (2009). *Small-scale forward smouldering experiments for remediation of coal tar in inert media* (Vol. 32): Elsevier.

Rein, G. (2009). Smouldering combustion phenomena in science and technology. *International Review of Chemical Engineering, 1*, 3-18.

Roy, M. M., Dutta, A., Corscadden, K., Havard, P., & Dickie, L. (2011). Review of biosolids management options and co-incineration of a biosolid-derived fuel. *Waste management, 31*(11), 2228-2235.

Salman, M., Gerhard, J. I., Major, D. W., Pironi, P., & Hadden, R. (2015). Remediation of trichloroethylene-contaminated soils by star technology using vegetable oil smoldering. *Journal of Hazardous Materials, 285*, 346-355.

Shannon, M. A., Bohn, P. W., Elimelech, M., Georgiadis, J. G., Mariñas, B. J., & Mayes, A. M. (2008). Science and technology for water purification in the coming decades. *Nature, 452*(7185), 301-310.

Switzer, C., Pironi, P., Gerhard, J., Rein, G., & Torero, J. (2009). Self-sustaining smoldering combustion: a novel remediation process for non-aqueous-phase liquids in porous media. *Environmental Science & Technology, 43*(15), 5871-5877.

Ternes, T. A., Joss, A., & Siegrist, H. (2004). Peer reviewed: scrutinizing pharmaceuticals and personal care products in wastewater treatment. *Environmental Science & Technology, 38*(20), 392A-399A.

U.S. EPA. (1994). *A Plain English Guide to the EPA Part 503 Biosolids Rule*: U. S. Environmental Protection Agency.

U.S. EPA. (1995). Part 503 Implementation Guidance (Office of Water, Trans.): U.S. Environmental Protection Agency.

U.S. EPA. (2014). Water: Sustainable Infrastructure. *Energy Effeciency for Water and Wastewater Facilities.* Retrieved February 16, 2015, from http://water.epa.gov/infrastructure/sustain/sustainable_infrastructure.cfm

Venkatesan, A. K., & Halden, R. U. (2014). Wastewater treatment plants as chemical observatories to forecast ecological and human health risks of manmade chemicals. *Scientific Reports, 4*.

Wang, H., Brown, S. L., Magesan, G. N., Slade, A. H., Quintern, M., Clinton, P. W., & Payn, T. W. (2008). Technological options for the management of biosolids. *Environmental Science and Pollution Research-International, 15*(4), 308-317.

Werther, J., & Ogada, T. (1999). Sewage sludge combustion. *Progress in energy and combustion science, 25*(1), 55-116.

Yermán, L., Hadden, R. M., Carrascal, J., Fabris, I., Cormier, D., Torero, J. L., Gerhard, J. I., Krajcovic, M., Pironi, P., & Cheng, Y.-L. (2015). Smouldering combustion as a treatment technology for faeces: Exploring the parameter space. *Fuel, 147*, 108-116.

Chapter 2

Literature Review

2.1 Introduction

Wastewater treatment plants (WWTPs) remove contaminants from sewage, allowing treated water to be safely discharged to the environment (Metcalf and Eddy, 2003). The major by-product of the treatment process is a sludge, which undergoes separate processing and the result is termed biosolids (U.S. EPA, 1994). Typically, the majority of WWTP costs are dedicated to managing biosolids, making it the most expensive component of the WWTP process (Droste, 1997; Metcalf and Eddy, 2003; Khiari et al., 2004). Currently, the major biosolids disposal (or end use) methods in Canada are incineration, land application for agricultural purposes, and landfilling (Apedaile, 2001). All of these methods are expensive (high energy input, person-hours, transportation distance) (Werther and Ogada, 1999; Wang et al., 2008; Bellur et al., 2009). In addition, land application is controversial and subject to restrictions and uncertain risks stemming from contaminants of emerging concern (U.S. EPA, 1995; Hale et al., 2001; Giger et al., 2003; Ternes et al., 2004; Bolong et al., 2009; Venkatesan and Halden, 2014).

Smouldering combustion of organic wastes is a novel soil remediation method that has proven effective for a wide range of hazardous organic liquid contaminants and human faeces mixed within an inert porous medium (e.g., natural soil or homogeneous quartz sand) (Switzer et al., 2009; Pironi et al., 2011; Switzer et al., 2014; Salman et al., 2015; Yermán et al., 2015). This method operates by igniting and propagating smouldering combustion via forced airflow through the porous medium, effectively destroying the

contaminant within its pore space (Pironi et al., 2009). Originally pursued as a soil remediation technology for contaminated industrial sites, this method of employing smouldering combustion presents significant potential as a novel ex-situ waste management technology (Switzer et al., 2009; Switzer et al., 2014; Yermán et al., 2015). This chapter presents the relevant literature to provide justification and context regarding this technology's extension into the WWTP industry as a new potential disposal method for biosolids.

2.2 Wastewater Treatment

2.2.1 General Overview

Wastewater treatment broadly defines the process of treating a water supply via various chemical, physical, and biological processes to remove harmful constituents and mitigate risk to the community and surrounding environment (Metcalf and Eddy, 2003). Wastewater is a combination of liquid and suspended contaminants derived from various sources including: municipal, industrial, and commercial use. Due to municipal usage, wastewater generally possesses high biological and chemical oxygen demands (BOD and COD, respectively), elevated nitrogen and phosphorous concentrations, high pathogen counts, and high concentrations of suspended solids. If untreated, this wastewater may produce anaerobic conditions, accelerate eutrophication, disrupt natural sedimentation, and transmit communicable diseases in receiving bodies of water (Metcalf and Eddy, 2003). BOD and COD are metrics for quantifying the biodegradable organics within a water sample (e.g., proteins, carbohydrates, and fats) and are measured as the oxygen needed to oxidize all organics (Hach et al., 1997; Metcalf and Eddy, 2003). Total

nitrogen (organic and free ammonia) and phosphorous (organic and inorganic) are essential plant nutrients that promote excess algae growth in receiving water bodies, which accelerates eutrophication (Metcalf and Eddy, 2003). However, these nutrients are quite valuable as agricultural fertilizer and their recovery is becoming a priority in WWTPs, especially phosphorous (Wang et al., 2008; CEC, 2010; Cordell et al., 2011; Sartorius et al., 2012; Donatello and Cheeseman, 2013). Waterborne diseases pose a major threat to public health and wastewater may contain a broad spectrum of pathogens including: *Enterococcus faecalis*, *Escherichia coli*, *E. coli* O157:H7, *Salmonella* sp., etc. (Shannon et al., 2007). Depending on the wastewater's origin (i.e., industrial effluent), there may also be heavy metals concentrations that will persist and accumulate in the environment, posing a serious toxicity risk (McGrath et al., 1994; Kurniawan et al., 2006; Ahluwalia and Goyal, 2007). There is growing interest in the impact of contaminants of emerging concern (CECs) and the role WWTPs play in transporting these contaminants into the environment (Ternes et al., 2004; Venkatesan and Halden, 2014). Thousands of contaminants have been identified as CECs including pharmaceuticals, flame retardants, insecticides, surfactants, endocrine disruptors (e.g., hormones), and antimicrobials (Ternes et al., 2004; Pal et al., 2010; Venkatesan and Halden, 2014). Recent interest in CECs is largely attributed to the evolution of analytical instrumentation allowing the detection of trace CECs. Over the past twenty five years, liquid chromatography – tandem mass spectrometry has facilitated the detection of CECs in nanogram-per-litre (ng/L) quantities (Ternes et al., 2004). It is expected that CECs, even in such trace concentrations, present danger to the environment and human health due to their persistence, bioaccumulation potential, and toxicity (Venkatesan and Halden, 2014).

As the variety of contaminants is so wide, specific WWTP processes are required to target individual groups of contaminants. This necessitates a series of robust, compatible processes to completely address effluent risks.

2.2.2 Liquid Stream Treatments

Liquid stream treatments vary significantly across WWTPs as influent characteristics, plant site conditions, regulatory constraints, public participation, and regional norms differ drastically (Qasim, 1999). However, a typical treatment path summarized by Metcalf and Eddy (2003) includes: grit removal, primary clarification, biological processing, secondary clarification, and disinfection as illustrated in Figure 2.1.
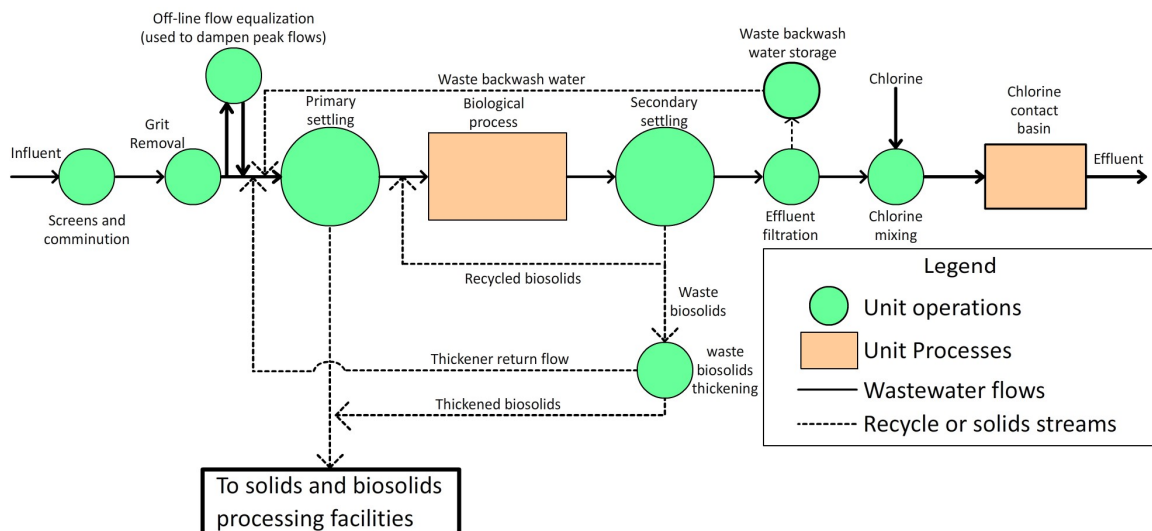
Figure 2.1: Basic process flow diagram of a typical wastewater treatment plant. (Adapted from Metcalf and Eddy (2003)).

Grit removal and primary clarification remove large, settleable particulates that may interfere with downstream processes while lowering the solids loading, BOD, nitrogen and phosphorous (nutrient) concentrations, and pathogen counts of the wastewater. Biological processing, such as digesters facilitating the growth of either aerobic or

anaerobic microorganisms, utilizes the organic content from the wastewater as a substrate to lower the effluent BOD and nutrient concentration. Secondary clarification settles low density suspended solids that may have flocculated during previous processing, and microorganisms from the biological processing. Secondary clarification further reduces suspended solids, BOD, nutrient concentrations, and pathogen counts. Final pathogen reduction is typically completed via disinfection, usually with chlorine addition (Qasim, 1999). Many more additional processes can be employed, including: additional clarification, nitrification, de-nitrification, attached growth digesters, coagulation, single/two-stage lime precipitation, ammonia stripping, ion exchange, filtration, carbon adsorption, reverse osmosis, electro-dialysis, etc. Qasim (1999) and Metcalf and Eddy (2003) present examples of combinations of these processes, suggesting the flexibility WWTP designers have in choosing an appropriate treatment path. In addition to these liquid treatments, significant effort is spent on managing the major by-product from WWTPs, biosolids.

2.2.3 Biosolids Introduction

A combination of particulate solids from the wastewater influent and/or biomass produced during the biological processing are settled during primary, secondary, and any additional clarification as sludge and sludge management persists as one of the greatest challenges in WWTPs (Droste, 1997; Tyagi and Lo, 2013). This sludge generally contains 0.25 – 12% solids by mass following clarification, where >70% of the solids are volatile (Metcalf and Eddy, 2003). The volatile solids are mostly composed of organic matter, which is measured as the dry mass lost after ignition at 550°C (U.S. EPA, 2001). A range of sludge physical and chemical properties are available from Metcalf and Eddy

(2003) and U.S. EPA (1979); and proximate, ultimate, and ash composition analyses are available for two samples of sludge from Cui et al. (2006). Ogada and Werther (1996) compared proximate and ultimate analyses between WWTP sludge and low grade coals, suggesting both had similar energy contents but sludge contained significantly more volatiles available for flaming combustion (further discussion is available in Appendix A). Following primary clarification, the (primary) sludge is usually transported to additional processing. Following secondary clarification downstream of biological processing, a portion of the (activated) sludge is recycled as return-activated sludge (RAS). As RAS contains useful microorganisms, it is re-routed upstream to raise the microorganism concentration and improve the biological processing efficiency (Scuras et al., 2001). The waste portion of this stream, or waste-activated sludge (WAS), is often combined with the primary sludge during additional processing steps. The final material is termed biosolids (U.S. EPA, 1994; Wang et al., 2008). For generalization in this text, the final sludge for disposal is referred to as *biosolids*, and all sludge processing leading towards biosolids production is termed *biosolids processing*.

2.2.4 Biosolids Processing

Depending on the intended disposal, the sludge undergoes various kinds of biosolids processing steps, including: preliminary, thickening, stabilization, conditioning, and dewatering (see Figure 2.2). Figure 2.2 only highlights the most popular biosolids processing steps, where Oleszkiewicz and Mavinic (2002) presented a more complete set of examples. The primary goal for biosolids processing is to lower the moisture content (MC) (raise the solids content) by removing water, thereby drastically reducing the total volume (Qasim, 1999). The resulting biosolids are easier to manage in terms of

transporting and handling, more valuable for land application due to the increased nutrient concentration, and easier to incinerate due to increased volatiles concentration (Werther and Ogada, 1999; Wang et al., 2008). Major processing costs are associated with removing the high fraction of absorbed water (i.e., interstitial, bound, and surface water), which necessitates multiple processing steps (Vesilind and Martel, 1990; Bellur et al., 2009).
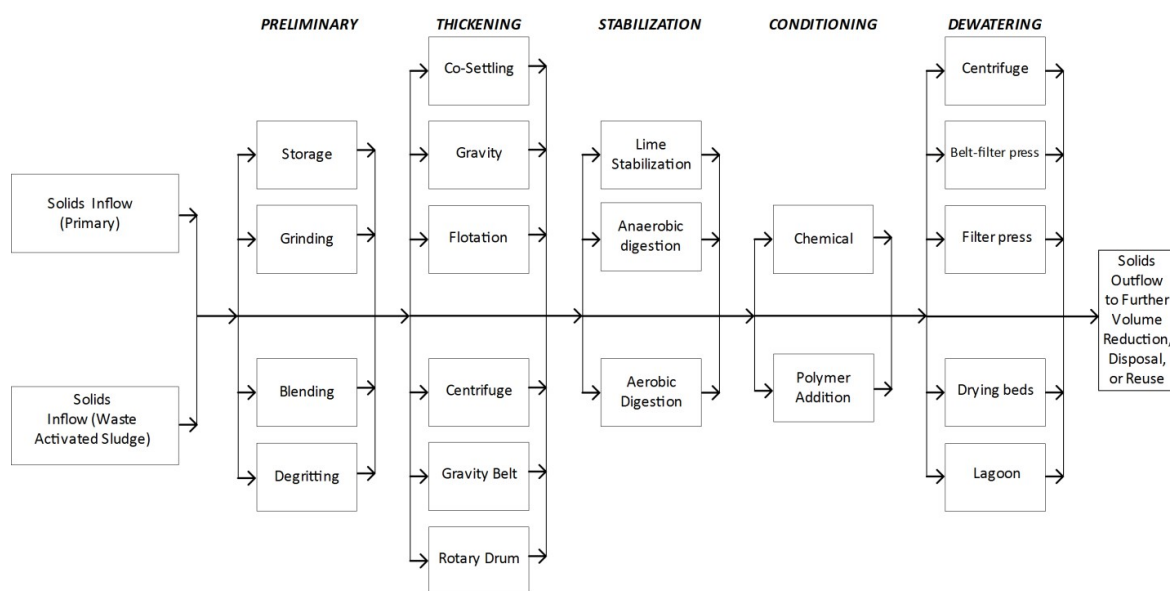
Figure 2.2: Basic process flow diagram of a typical biosolids processing path (adapted from Metcalf and Eddy (2003)).

Preliminary processing (e.g., storage, grinding, blending, degritting, etc.) is employed to prepare the biosolids for subsequent processing but does not significantly decrease MC (Droste, 1997; Qasim, 1999). Similarly, conditioning (e.g., polymer addition) is mainly used to improve the sludge's dewaterability (Christensen et al., 1993; Metcalf and Eddy, 2003). Thickening (e.g., co-settling, gravity, flotation, centrifuge, gravity belt, rotary drum, etc.) removes liquid from the sludge to improve downstream processing and disposal (Takács et al., 1991; Metcalf and Eddy, 2003). Dewatering (e.g., centrifuge, belt-

filter press, drying beds, lagoons, etc.) lowers sludge MC and is similar to thickening, however, it typically follows thickening and conditioning (Spinosa et al., 2001). Stabilization (e.g., lime stabilization, aerobic digestion, anaerobic digestion, etc.) generally lowers the pathogen count and improves the aesthetic qualities (e.g., smell) of the biosolids (Spinosa et al., 2001). Stabilization also lowers the volatile solids content of the sludge, thus lowering the total volume, and is required prior to land application to mitigate pathogen loading (U.S. EPA, 1995; Metcalf and Eddy, 2003).

Following a biosolids processing path, it is important to note the changing MC. After following a robust processing path biosolids MC may drop from 99% to 50% (wet mass basis) (Metcalf and Eddy, 2003). It is also interesting to highlight the influence that both liquid and solid stream processes have on the dry higher heating value of the sludge (HHV_d^s). The HHV_d^s is defined as the potential chemical energy within the sludge released through complete combustion, typically measured via bomb calorimetry (Washburn, 1933; Boundy et al., 2011). Given that the carbon from volatile solids is consumed as a substrate by microorganisms in biological processing, the increase in biological processing corresponds with a decline in volatile solids. For anaerobic digestion, Lipták (1974) presented an approximation to predict decline in volatile solids:

$$V_d = 13.7 \ln(SRT_{des}) + 18.9 \tag{1}$$

Here, V_d is the volatile solids fraction reduction (%) and SRT_{des} is the time of digestion (5 to 20 days). For example, the HHV_d^s range drops from $23 - 29$ kJ/g to $9 - 14$ kJ/g (dry mass basis) between primary to anaerobically digested sludge (WEF, 1988). In addition, certain stabilization and conditioning steps may change the HHV_d^s, such as lime

stabilization (lower it) and polymer addition (raise it) (Metcalf and Eddy, 2003).

Following information from Droste (1997) and Metcalf and Eddy (2003), Figure 2.3

summarizes popular biosolids processing steps and their associated impact on the HHV_d^s,

solids content, and sludge lower heating value (LHV^s). The LHV^s was estimated by

Boundy et al. (2011):

$$LHV^s = [(1 - MC)xHHV_d^s] - [MCxL_v]$$ (2)

where $MC(\%)$ is the sludge MC and $L_v\left(\frac{kJ}{g}\right)$ is the latent heat of vaporization of water,

2.447 kJ/g at 25°C.

Solids Content (%)
Dry Higher Heating Value (kJ/g)
Lower Heating Value (kJ/g)

PRELIMINARY

Solids Inflow (Fixed Film Waste Sludge) 3.0-10ᵃ% 16-23ᵃ kJ/g		
0.0ᵃ kJ/g		

Solids Inflow (Primary) 5.0-8.0% 23-29ᵃ kJ/g
0.0ᵃ kJ/g

Solids Inflow (Waste Activated Sludge) 0.5-2.0ᵃ% 20-23ᵃ kJ/g
0.0ᵃ kJ/g

Storage
Grinding
Blending
Degritting

THICKENING

Co-Settling 2.0-15ᵇ%
0.0-2.1ᵇ kJ/g

Gravity 4.0-10ᵃ%
0.0-0.5ᵃ kJ/g

Flotation 3.0-6.0ᵃ%
0.0ᵃ kJ/g

Centrifuge 3.0-6.0ᵃ%
0.0ᵃ kJ/g

Gravity Belt 9.0-12ᵃ%
0.0-1.1ᵃ kJ/g

Rotary Drum 3.0-6.0ᵃ%
0.0ᵃ kJ/g

STABILIZATION

Lime Stabilization

Anaerobic digestion 6.0-12ᵃ% 9.0-14ᵃ kJ/g
0.0ᵃ kJ/g

Aerobic Digestion 1.0-2.0ᵃ% 20-23ᵃ kJ/g
0.0-2.2ᵃ kJ/g

CONDITIONING

14-18ᵃ kJ/g
0.0-7.7ᵃ kJ/g

Chemical *Note**

Other *Note**

DEWATERING

Centrifuge 10-30ᵃ%
0.0-6.8ᵃ kJ/g

Belt-filter press 15-30ᵃ%
0.0-6.8ᵇ kJ/g

Filter press 20-50ᵇ%
0.0-13ᵃ kJ/g

Drying beds 20-25ᵇ%
0.0-5.2ᵇ kJ/g

Lagoon 25-30ᵃ%
0.0-6.8ᵃ kJ/g

Solids Outflow to Further Volume Reduction, Disposal, or Reuse

Figure 2.3: Biosolids moisture content, lower heating value, and dry higher heating value changes throughout typical biosolids processing steps superimposed on a process flow diagram adapted from Metcalf and Eddy (2003). All values are from Metcalf and Eddy (2003)ᵃ or Droste (1997)ᵇ. Shaded boxes represent a process step, or process category, that impacts the dry sludge higher heating value. Note*: The impact that conditioning has on solids (%) is accounted for in the high end points of subsequent dewatered values.

Problematic sludge properties (e.g., thixotropic viscosity and large fraction of absorbed water) and its variability (due many factors including: plant conditions, seasonality, weather conditions, inflow variations, etc.) creates a considerable challenge in designing, operating, and maintaining robust biosolids processing (Vesilind and Martel, 1990; Spinosa et al., 2001; Wang et al., 2008). In combination with the large volumes produced, overall biosolids management is a complex task for WWTPs and the degree of processing is often optimized against the disposal costs (Ogada and Werther, 1996; Qasim, 1999).

2.2.5 Biosolids Disposal Methods

Biosolids disposal methods do not aim to produce a resource (e.g., incineration, landfill) while end use methods utilize the end product biosolids as a resource (e.g., land application, composting). However, there can be some overlap between these categories, for example: some incineration methods (e.g., co-combustion) may be used for energy production, ash resulting from incineration can be used in a variety of construction applications or as a phosphorous source, and the utilization of biosolids as landfill cover can be viewed as a resource application (Werther and Ogada, 1999; Wang et al., 2008; Donatello and Cheeseman, 2013). For generalization in this text, all disposal/end use methods are simply referred to as *disposal methods*. In regards to popular Canadian biosolids disposal methods, in 2001 47% were incinerated, 43% were land applied, and 4% were landfilled (Apedaile, 2001). Across North America, land application and incineration are preferred as they both represent strong potential for meeting future demands (Werther and Ogada, 1999; Wang et al., 2008; Roy et al., 2011).

Land application implies the use of stabilized biosolids as a fertilizer for agricultural purposes (U.S. EPA, 1995). Some benefits of land application include: improved soil water retention, aggregate stability, and slow releasing nutrients, which is otherwise achieved by chemical manufactured fertilizer or malodorous livestock manure (U.S. EPA, 2000e; Singh and Agrawal, 2008). Land application is identified as the most effective way to completely utilize the organic carbon and nutrients within biosolids and is encouraged where the land is available, the biosolids are of adequate quality, and it is socially acceptable (Wang et al., 2008; CEC, 2010). However, stabilization, transportation, and handling can be expensive and there are strict heavy metal, pathogen loading, and use regulations (U.S. EPA, 1995; 2000e; Singh and Agrawal, 2008). In addition, there is a growing concern about the role of land application in facilitating a pathway for CECs to environmental receptors (Hale et al., 2001; Ternes et al., 2004; Venkatesan and Halden, 2014). Some CECs may adsorb onto the biosolids at even greater concentrations than is observed in liquid stream effluents and these CECs may enter water bodies via run-off or enter crops via plant uptake (Ternes et al., 2004). Venkatesan and Halden (2014) identified 123 different CECs in samples of biosolids in the United States (U.S.), which represented between 0.040 – 0 .15% (dry mass basis) of the of the biosolids. Lastly, the crop risk may be increased following improper storage and application of biosolids, which can lead to pathogen re-growth or recolonization, and increased plant uptake of toxic heavy metals, respectively (Zaleski et al., 2005; Singh and Agrawal, 2008). These risks need to be evaluated against the benefits land application provides and caution is given against full dependence on land application, as regulations

to mitigate these risks may change suddenly and require biosolids producers to adapt (Wang et al., 2008).

Incineration is the processes of thermally degrading biosolids via flaming combustion of the released biosolids volatiles at temperatures near 800°C (fluidized bed incinerators) or 500°C (multiple hearth incinerators) (Ogada and Werther, 1996; U.S. EPA, 2003b). Generally, fluidized bed incinerators are accepted as the more efficient option and present the strongest economic potential (Werther and Ogada, 1999; Dangtran et al., 2000). Incineration is an attractive technology for meeting future demands due to its low space footprint, significant waste volume reduction, and potential for energy recovery (Werther and Ogada, 1999; Roy et al., 2011). Furthermore, the resulting inert ash can be used for multiple construction applications including cement, brick filler, or subbase material for road construction; or treated as a source of phosphorous (U.S. EPA, 2003b; Donatello and Cheeseman, 2013). Major concerns surrounding incineration are largely associated with the emissions, notably the strict requirements regarding the production of particulates, NO_x, SO_x, and CO (U.S. EPA, 2003b). However, as emissions management technology has improved greatly over recent years, contemporary scrubbers alleviate much of the risk (Werther and Ogada, 1999).

While incineration can be an economic option, there are major costs associated with dewatering the biosolids to $85 - 65\%$ MC (wet mass basis) and the use of supplemental fuel for ignition and continuous addition to sustain incineration (Metcalf and Eddy, 2003; Murakami et al., 2009; U.S. EPA, 2003b). Given that biosolids combustion follows the drying of the water and release of volatile components (i.e., endothermic processes), significant water needs to be evaporated/boiled from the biosolids prior to combustion

(Cui et al., 2006). Depending on the biosolids energy content, biosolids with MC greater than 70% typically require a continuous addition of supplemental fuel to balance against the heat sink from boiling/evaporating water. Conversely, biosolids with MC less than 70% may be able to incinerate in a self-sustaining manner (i.e., without the continuous addition of supplemental fuel). Furthermore, in comparison to other disposals/end uses like land application or landfilling, incineration requires significant capital, which can be a major deterrent in constructing new incinerators (Wang et al., 2008).

Across WWTPs, biosolids processing and disposal method combinations vary as greatly as liquid stream process combinations (King and Painter, 1986). However, a consistency between WWTPs is the high cost to manage biosolids, where nearly 50% of a WWTP's capital and operating costs are dedicated to processing biosolids (Khiari et al., 2004).

2.2.6 Economic Considerations

Municipal wastewater treatment is an energy intensive and operationally demanding public operation that requires enormous capital and elaborate infrastructure (Shannon et al., 2008). In the U.S., municipal WWTPs and drinking water services account for $3 - 4\%$ of all energy consumption and $30 - 40\%$ of total energy consumed by municipalities, costing \$4 billion/year (U.S. EPA, 2014). The scenario is quite similar in Canada, as both countries experience similar per capita water usage in comparable economic environments and social norms. Canadians on average pay \$0.31/litre of water and use 343 litres/person with a gross domestic product (GDP) of \$44 500/person; Americans on average pay $\$0.4 - 0.8$/litre of water and use 382 litres/person with a GDP of \$54 800/person (Environment Canada, 2013a; CIA, 2014). Furthermore, as much of North

America's WWTP infrastructure approaches the end of its design life, an estimated $298 billion and $39 billion is required in the U.S. and Canada, respectively, to repair and upgrade WWTP infrastructure to good working condition (Félio et al., 2012; ASCE, 2013). These costs represent 1.7% and 2.6% of the U.S. and Canadian 2014 GDP, respectively. It is important to note that these costs do not consider upgrades due to evolving regulations that could result from emerging contaminants.

This presents a significant financial burden for North American municipalities, which are already in debt. A 2007 survey conducted collaboratively by The Federation for Canadian Municipalities and McGill University found that Canada's municipal deficit was $123 billion, where all water supply systems (i.e., drinking water, wastewater, and storm water) constituted 25% of the deficit (Mirza S, 2007). Optimistically, the resulting benefits from improved WWTP infrastructure are expected to greatly outweigh these costs. Environment Canada (2013b) estimated that $5.5 billion is required for Canadian WWTPs over the next 54 years to meet established regulations ($3 billion for capital, $1.7 billion for operation and maintenance, and $0.75 billion for reporting and monitoring). These costs were anticipated to provide $16.5 billion in benefits estimated from numerous projections including increased land value, greater recreational use of water bodies, increased commercial fishing, and reduced water supply costs (Environment Canada, 2013b). In addition, these costs are probably conservative as many environmental and social benefits are extremely difficult to quantify and are often undervalued (Hanley et al., 1998). In another sense, poor WWTP infrastructure could cause some insidious environmental damage, where the ramifications from such damage is not fully understood or even conceived in most cost-benefit analyses (Abdalla et al.,

1992). The above information considers WWTP infrastructure holistically to present justification for the advancement of WWTP technology. It is equally worthwhile to identify the operations that are currently driving the high costs. As previously mentioned, the highest costs in WWTPs are associated with biosolids management.

Following technical documents on biosolids management from the U.S. Environmental Protection Agency (U.S. EPA), operating and capital cost ranges for popular biosolids processing and disposal methods have been compiled in Figure 2.4 (U.S. EPA, 2000a; 2000b; 2000c; 2000d; 2000e; 2000f; 2000g; 2002; 2003a; 2003b; 2003c; 2006a; 2006b). It is important to caution that these approximations may not fully represent current technology as the technical documents were published from 2000 to 2006, with some cost information dating as far back as 1987 (U.S. EPA, 2000b). However, this information is assumed sufficient to understand the relative cost differences within biosolids management. All values have been converted to $2014 USD following historical U.S. inflation rates from The World Bank (2015). It is interesting to highlight the high variability in capital and operating/maintenance costs. For example, gravity thickening capital costs vary between $275 000 and $4.40 million, and alkaline stabilization operation and maintenance costs vary from $59 and $471/dry ton of sludge processed (U.S. EPA, 2000f). Comparing new biosolids management technologies' expected costs with these current costs presents the opportunity to explore the economic feasibility and identify what kind of WWTPs the new technologies may best fit into, from a financial perspective.
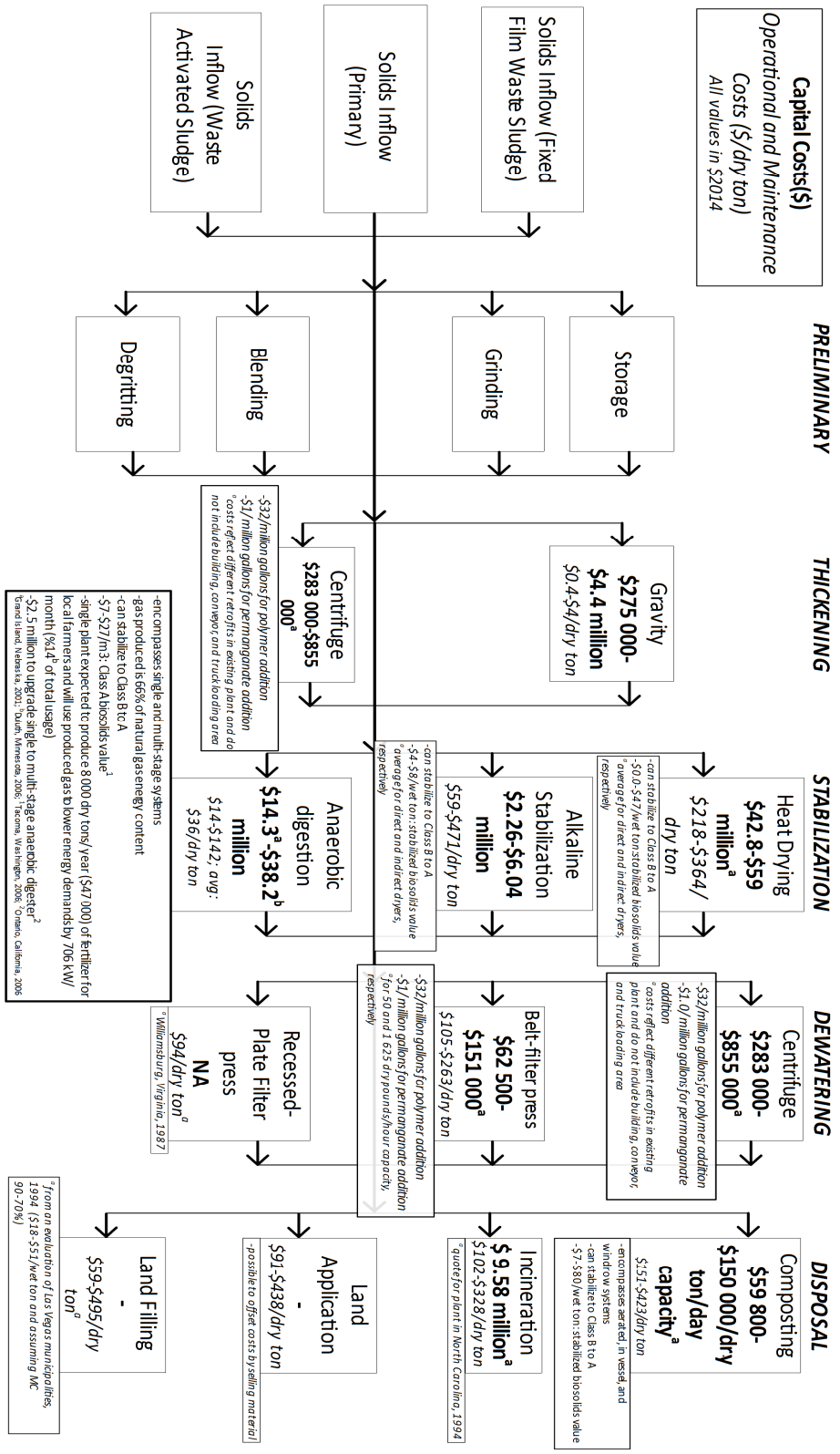
Figure 2.4: Typical biosolids processing steps' cost ranges superimposed on a process flow diagram adapted from Metcalf and Eddy (2003) and all costs are from U.S. EPA technical documents and represent an overview of the wastewater treatment industry from 2000-2006, unless otherwise stated. All historic values have been converted to present value ($2014) following standard U.S. inflation. Note*: available conditioning costs are noted in details.

Capital Costs($)
Operational and Maintenance
Costs ($/dry ton)
All values in $2014

Solids Inflow (Fixed Film Waste Sludge)

Solids Inflow (Primary)

Solids Inflow (Waste Activated Sludge)

PRELIMINARY

Storage

Grinding

Blending

Degritting

THICKENING

Gravity
$275 000-
$4.4 million
$0.4-$4/dry ton

Centrifuge
$283 000-$855 000[a]

-$32/million gallons for polymer addition
-$1/million gallons for permanganate addition
[a] costs reflect different retrofits in existing plant and do not include building, conveyor, and truck loading area

STABILIZATION

Heat Drying
$42.8-$59 million[a]
$218-$364/dry ton

-can stabilize to Class B to A
-$0.05-$47/wet ton stabilized biosolids value
[a] average for direct and indirect dryers, respectively

Alkaline Stabilization
$2.26-$6.04 million
$59-$471/dry ton

-can stabilize to Class B to A
-$4-$8/wet ton stabilized biosolids value
[a] average for direct and indirect dryers, respectively

Anaerobic digestion
$14.3-$38.2[b] million
$14-$142; avg: $36/dry ton

-encompasses single and multi-stage systems
-gas produced is 66% of natural gas energy content
-can stabilize to Class B to A
-$7-$27/m3: Class A biosolids value[1]
-single plant expected to produce 8000 dry tons/year ($47000) of fertilizer for local farmers and will use produced gas to lower energy demands by 706 kW/month (%14[b] of total usage)
[a] Williamsburg, Virginia, 1987
[b] $2.5 million to upgrade single to multi-stage anaerobic digester[2]

DEWATERING

Centrifuge
$283 000-$855 000[a]

-$32/million gallons for polymer addition
-$1/million gallons for permanganate addition
[a] costs reflect different retrofits in existing plant and do not include building, conveyor, and truck loading area

Belt-filter press
$62 500-$151 000[a]
$105-$263/dry ton

-$32/million gallons for polymer addition
-$1/million gallons for permanganate addition
[a] for 50 and 1 625 dry pounds/hour capacity, respectively

Recessed-Plate Filter press
NA
$94/dry ton[a]

DISPOSAL

Composting
$59 800-$150 000/dry ton/day capacity[a]
$151-$423/dry ton

-encompasses aerated, in vessel, and windrow systems
-can stabilize to Class B to A
-$7-$80/wet ton: stabilized biosolids value
[a] quote for plant in North Carolina, 1994

Incineration
$ 9.58 million[a]
$102-$328/dry ton

[a] quote for plant in North Carolina, 1994

Land Application
-
$91-$438/dry ton

-possible to offset costs by selling material

Land Filling
-
$59-$495/dry ton[a]

[a] from an evaluation of Las Vegas municipalities, 1994 ($18-$55/wet ton and assuming MC 90-70%)

[1]Grand Island, Nebraska, 2001; [2]Duth, Minnesota, 2006; [3]Tacoma, Washington, 2006; [4]Ontario, California, 2006

2.3 Smouldering Combustion

2.3.1 Definition of Smouldering Combustion

Smouldering is a flameless form of combustion driven by exothermic, heterogeneous oxidation reactions in which an oxidizer, typically oxygen within air, directly attacks the surface of a solid or liquid phase fuel (Ohlemiller, 1985; Switzer et al., 2009). Very generally, the rate of oxidation must overcome the heat losses for smouldering to be self-sustaining (Ohlemiller, 1985). Self-sustaining smouldering requires a porous fuel, or a fuel spread within a porous structure, to provide the required fuel surface area for oxidation and adequate oxidizer permeability (Pironi et al., 2009; Drysdale, 2011). An oxidizer supplied via convective and/or diffusive means is transported through the porous structure and diffuses directly into the surface of a condensed phase fuel (Ohlemiller, 1985). Smouldering may include a large number of elementary chemical reactions, including competing reactions, but the process can be generalized by considering the two most important reaction pathways (Ohlemiller, 1985; Rein, 2013):

Pyrolysis:

$$Fuel\ (solid) + Heat \rightarrow Pyrolysate\ (gas) + Char(solid) + Ash(solid) \qquad (3)$$

Char Oxidation:

$$Char(solid) + O_2 \rightarrow Heat + CO_2 + H_2O + Ash(solid) + Other\ Compounds \qquad (4)$$
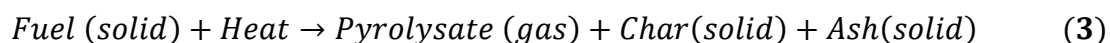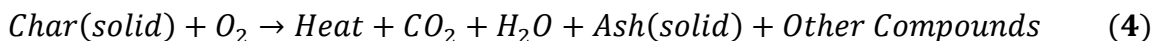
Pyrolysis is the thermal degradation of a fuel into smaller volatile molecules in response to heat and in the absence of oxidation (Sinha et al., 2000). In smouldering, pyrolysis is limited by the heat evolved from char oxidation and produces carbon rich material (char) and pyrolysate gas (Sinha et al., 2000; Rein, 2013). Char oxidation, the principal heat

source that drives smouldering (Ohlemiller et al., 2008), is a heterogeneous gas-solid oxidation reaction between carbon in the char, produced from pyrolysis, and the oxygen in the air (Ohlemiller et al., 2008; Tillman, 2012). Char oxidation is limited by the diffusion of oxygen into the surface of the char and produces heat, water vapour, carbon dioxide, ash, and other by-products (i.e., incomplete combustion products including: carbon monoxide, volatile organic compounds (VOCs), hydrocarbons, polyaromatic hydrocarbons (PAHs), and particulate matter) (Tillman, 2012; Rein, 2013).

Compared to flaming combustion, which is a homogeneous gas phase combustion surrounding a fuel that favours the oxidation of pyrolysate as opposed to char, smouldering produces much lower peak temperatures and heat of reactions (Rein, 2009; 2013). Flaming is a more complete combustion, where a complete combustion is a chemical reaction where certain elements of a fuel completely combine with oxygen, releasing energy in the form of heat (Ganesan, 1994). For example, when hydrocarbons undergo complete combustion in oxygen they will exclusively produce water vapour and carbon dioxide. Smouldering's characteristics result the formation of more incomplete combustion products and much slower propagation, roughly two orders of magnitude slower than flaming (Rein, 2009). Given that smouldering operates within a well insulated porous medium, heat energy is efficiently transferred from the oxidation zone to unburned fuel in the pyrolysis and preheating zones (Ohlemiller et al., 2008). In comparison to flaming, smouldering is much less susceptible to heat losses and quenching, the suppression of chemical processes driving combustion (Hadden and Rein, 2009; Yermán et al., 2015).

As smouldering propagation is controlled by the oxygen supply and heat losses, the combustion can vary greatly with an increased oxygen supply, affecting the products, peak temperature, and propagation velocity (Ohlemiller, 1985; Rein et al., 2006). Reflecting this, two major conclusions from an early analytical model describing one-dimensional, adiabatic, steady smouldering by Dosanjh et al. (1987) were: 1) The smouldering peak temperatures for a given fuel were only dependant on the initial oxygen mass flux and increased logarithmically with increasing oxygen mass flux. 2) The smouldering propagation velocity was linearly dependant on the oxygen mass flux, and also increased with increasing oxygen concentration.

Smouldering propagation can be idealized in two distinct one-dimensional scenarios: forward or reverse (opposed) smouldering, which defines the reaction and oxidizer propagate in the same or opposite directions, respectively (see Figure 2.5) (Ohlemiller and Lucca, 1983). Forward smouldering is often considered a more complete combustion than reverse smouldering (Ohlemiller, 1985; Schult et al., 1996; Rein, 2009). Upwards and downward smouldering denote if the reaction propagates against or with the direction of gravity, respectively (Drysdale, 2011). In upwards forward smouldering, buoyant forces from the hot combustion gases promote heat transfer ahead of the reaction, resulting in faster propagation compared to downward forward smouldering (Torero and Fernandez-Pello, 1996; Drysdale, 2011). Forced smouldering implies an external pressure gradient drives the oxidizer into the reaction zone, where the oxidizer movement in natural smouldering only results from the reaction, natural convection, and diffusion (He and Behrendt, 2009).
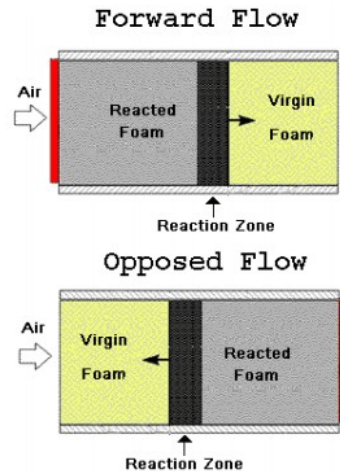
Figure 2.5: Conceptual diagram outlining the airflow and reaction propagation directions for forward and opposed smouldering (Rein, 2009).

2.3.2 Forward Smoldering Propagation

Forward smouldering combustion can be characterized by four zones: preheating, pyrolysis, oxidation, and cooling. A very common example of forward smouldering is cigarette burning, as illustrated in Figure 2.6.
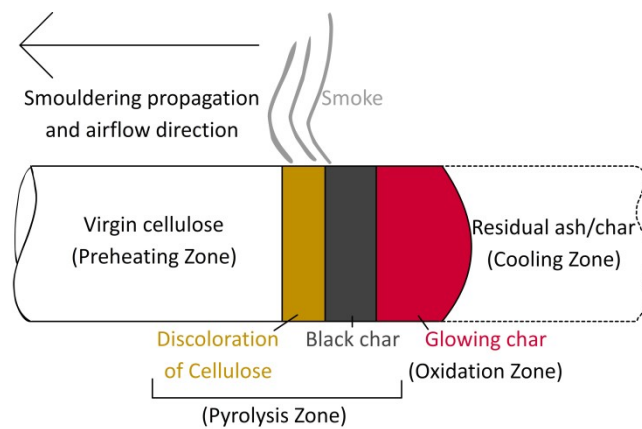
Figure 2.6: Steady forward smouldering along a cigarette illustrating key smouldering zones (adapted from Moussa et al. (1977)).

These zones may propagate at varying rates and dynamic thicknesses in response to heat losses and oxygen supply (Ohlemiller and Lucca, 1983; Rein et al., 2009; Hadden et al., 2013). For generalization in this text, the leading edge of these zones is simply called the *smouldering front.* The preheating zone boils/evaporates moisture ahead of the pyrolysis and oxidation zones and the pyrolysis zone thermally degrades the fuel in the absence of combustion. The preheating and pyrolysis zones are endothermic and are limited by the heat energy evolved from the oxidation zone (Ohlemiller, 1985; Rein, 2009). The oxidation zone is dominated by exothermic reactions where the condensed phased fuel, either virgin or char from pyrolysis, is directly destroyed by the oxidizer. The released heat energy is transported ahead to the preheating and pyrolysis via conduction, radiation, and convection (Ohlemiller et al., 2008; Switzer et al., 2014). The trailing cooling zone is where smouldering has ceased and the remaining material, largely inert, cools to ambient temperature (Rein, 2009). Torero and Fernandez-Pello (1996) presented temperature histories and temperature profiles at various times from forced forward smouldering in polyurethane foam. From this temperature data, the key smouldering zones were delineated using the temperature plateaus and peaks. The governing heat transfer mechanisms were identified at multiple airflow rates, where convection was considered secondary at airflow velocities <1.0 mm/s. At these low air flows, heat transfer was dominated by radiation, justified by the slow smouldering propagation and poor thermal conductivity of polyurethane foam (Torero and Fernandez-Pello, 1996). Torero and Fernandez-Pello (1996) found that forward smouldering quenching limits and peak temperatures were governed by complex interactions between oxygen supply, fuel thermal properties, and convective heat transfer ahead out of the oxidation zone.

In theory, forced forward smouldering propagation can be limited by either oxygen supply rate or reaction kinetics, where the transition between these limiting conditions is expected to occur at high air flows (Schult et al., 1996; Leach et al., 2000; Ohlemiller et al., 2008). Though nearly all examples of smouldering in the literature are oxygen limited, from modelling efforts, Schult et al. (1996) showed that the kinetically controlled propagation could be characterized by a significant fraction of trailing char. This was due to rapid cooling from the incoming gas resulting in incomplete combustion (Schult et al., 1996). Similar to that presented by Dosanjh et al. (1987), Torero et al. (1993) developed a simplified heat transfer based expression to estimate the forced forward propagation velocity:

$$u_{sml} = \frac{Y_{O_{2,a}} \rho_g u_g Q_{sml} - \dot{Q}''_{loss}(A_L/A_c)}{[(1-\varphi)\rho_s c_{p,s} + \varphi \rho_g c_{p,g}](T_S - T_a) - (1-\varphi)\rho_s Q_P + Y_{O_{2,a}} \rho_g Q_{sml}} \qquad (5)$$

where, u_{sml} and u_g (mm/s) are the velocities of the smouldering propagation and forced airflow, respectively, $Y_{O_{2,a}}$ (m^3/m^3) is the volume fraction of oxygen in the air, ρ_g and ρ_s (kg/m^3) are the densities of the air and solid, respectively, Q_{sml} and Q_P (kJ/kg) are the heats of smouldering and pyrolysis, respectively, $\dot{Q}''_{loss}(A_L/A_c)$ (W/m^2) is the radial heat loss, φ (m^3/m^3) is the porosity of the solid, $c_{p,g}$ and $c_{p,s}$ (kJ/kgK) are the specific heat capacities of the air and solid, respectively, T_S and T_a (K) is the peak smouldering temperature and ambient temperature, respectively. This assumes two-step pyrolysis and combined oxidative and char reactions far from quenching, where the oxidation and pyrolysis fronts move at the same velocity. Torero and Fernandez-Pello (1996) found this

expression correlated well with forced upwards and downward forward smouldering in polyurethane foam with air flow velocities between 0.0 to 4.1 mm/s and 1.7 to 4.1 mm/s, respectively. This validated that the observed forward smouldering propagation was controlled by the heat released and absorbed by oxidation and pyrolysis reactions, respectively. Bar-Ilan et al. (2004) conducted preliminary experiments that validated this expression in a microgravity environment using polyurethane foam with forced air flow velocities from 2.0 to 6.0 mm/s. However, it was acknowledged that buoyancy and char oxidation effects were not accounted for. Consequently, this expression only qualitatively described upwards forward smouldering experiments under the same conditions in normal gravity.

Significant work has also been completed using a free-stream of air flowing over a smouldering sample. Ohlemiller (1990) and Palmer (1957) found that the forward smouldering propagation velocity in cellulosic powder and dust indefinitely increased with increasing airflow rate. Ohlemiller (1990) observed flaming at a free-stream air velocity >2.5 m/s over a sample of cellulose undergoing forward smouldering. Sato and Sega (1989) detailed more complicated behaviour where a maximum smoulder propagation velocity of $8.0x10^{-3}$ cm/s was reached at a free-stream air velocity of 3.25 m/s over cellulosic powder. At a free-stream air velocity greater than 6.00 m/s, heat losses away from the smouldering front and instability in the front structure led to quenching. Pironi et al. (2009) conducted forced forward smouldering experiments using coal tar within coarse sand and appeared to approach a similar maximum propagation velocity at an inlet air flux of 15 cm/s. However, as these experiments used forced air through the

porous medium, as opposed to free flow above the porous medium, quenching resulting from high air flux may be significantly different and was never observed.

2.3.3 Effects of Moisture on Smouldering Propagation

Due to smouldering's resilience to quenching, self-sustaining smouldering is possible in fuels with low effective calorific values and/or high MC (Yermán et al., 2015). However, beyond some MC limitation, the heat losses from evaporating/boiling water out of wet fuels will shift the energy balance and quench the reaction. In addition, the redistribution of water ahead of a propagating smouldering front due to condensation in cooler zones may accumulate and limit the extent of propagation (Ohlemiller, 1985).

Hadden and Rein (2009) approximated the water required to quench a coal smouldering fire based on the thermal properties of coal and water. This approximation yielded results on the same order of magnitude as the actual water required to extinguish laboratory scale coal smouldering fires:

$$m_w = \frac{m_c c_{p,c} \Delta T_c}{c_{p,w}(100 - T_w) + \lambda'} \tag{6}$$

Here, m_c and m_w (kg) are the masses of coal and water, respectively, $c_{p,c}$ and $c_{p,w}$ (kJ/kgK) are the specific heat capacities of coal and water, respectively, ΔT_c (K) is difference between average smouldering and extinguished temperatures, λ' (kJ/kg) is latent heat of vaporization of water, and T_w (K) is the initial water temperature.

From a wildfire context, there are numerous studies exploring smouldering limitations in wet peat. Frandsen (1987) and Rein et al. (2008) explored the effects of inorganic and

moisture content on smouldering ignition of peat, and Prat et al. (2014) explored the smouldering propagation velocity in response to increasing MC. Frandsen (1987) detailed the impact that moisture and inorganic contents had on self-sustaining smouldering of peat moss between 0 to 1 moisture/organic ratio and 0 to 5 inorganic/organic ratio. It was found that the moisture/organic ratio limit that permitted self-sustaining smouldering linearly declined with increasing inorganic/organic ratio. This was expected to result from decreasing the energy per unit volume of mixture and producing less favourable thermodynamic conditions that promoted heat losses. A comparison between smouldering Douglas-fir duff and peat moss suggested that the heat production rate, the product of the mass loss rate ratio and heat of combustion ratio between the fuels, explained the shifted smoulder boundary. The Douglas-fir experienced lower smouldering limits and a lower heat production rate. The scatter in the experimental results was expected to mainly result from heterogeneous moisture distribution within the peat samples, which was partly due to a condensate zone formed ahead of the smouldering front. Following the experimental work of Frandsen (1987) and Frandsen (1997), Rein et al. (2008) used an ignition protocol roughly equivalent to the heating from a flaming stump, 100W for 30 min, and found that MC governed the smouldering ignition in peat with 8% inorganic content (dry mass basis). The critical MC for smouldering ignition was 55±2% (wet mass basis). Prat et al. (2014) found a dramatic drop in smouldering propagation velocity in peat with MC above 25% (dry mass basis).

Reversibly condensable compounds are driven ahead of the smouldering front by convection and/or diffusion and condense in cooler regions ahead of the preheating zone, which produces a heat sink (condensate zone) that grows as the smoulder front progresses

(Ohlemiller, 1985). These compounds may be in the fuel (e.g., water) and transition into the gas phase via boiling/evaporation, or are produced during oxidation and/or pyrolysis. This condensate zone is also referred to as the "sweat zone" (Uggla, 1974) and the net heat sink across this condensation zone is equal to the rate of sensible enthalpy accumulation (DeRis, 1970). Further insight into the boiling/evaporation and condensation within porous media and suggestions regarding the modelling of these linked phenomena are provided in Appendix B.

2.3.4 Applications of Smouldering

Only 2% of all combustion research was focused on smouldering in 2009 (Rein, 2009), where this research largely focused on residential fires, wildfires, emissions hazards, long term coal seam fires, and aerospace safety (Quintiere et al., 1982; Kaufman et al., 2002; Bar-Ilan et al., 2004; Kuenzer et al., 2007; Rein, 2009; 2013). Similarly, the literature related to smouldering biosolids, or materials similar to biosolids, is almost entirely limited to understanding the self-heating and fire hazards associated with their storage (Chirag et al., 2011; Della Zassa et al., 2013; He et al., 2014). Recently, there are a few studies related to engineering applications of smouldering combustion including: remediation of contaminated soils, production of biochar for carbon storage, enhanced oil extraction, in-situ coal gasification, and smouldering human faeces for sanitation purposes (Akkutlu and Yortsos, 2003; Renner, 2007; Blinderman et al., 2008; Rein, 2009; Switzer et al., 2009; Yermán et al., 2015).

In comparison to flaming, smouldering presents some interesting advantages for application: (1) Lower heat fluxes required to initiate smouldering reactions (Ohlemiller

et al., 2008; Rein, 2009); (2) Minimal atmospheric heat losses (Drysdale, 2011); and (3) As smouldering is slow and oxygen diffusion limited, smouldering combustion experiences comparable time scales between combustion and heat transfer. This promotes efficient heat transfer to unburned fuel and provides greater resistance to quenching (Ohlemiller, 1985; Howell et al., 1996; Ohlemiller et al., 2008; Switzer et al., 2009; Switzer et al., 2014; Yermán et al., 2015). These advantages suggest there is strong potential in utilizing smouldering for a variety of engineering applications and, in particular, there is growing interest in pursuing smouldering as a low-energy waste management technique (Yermán et al., 2015).

2.4 Smouldering as a Waste Management Technique

2.4.1 Introduction

Self-sustaining Treatment for Active Remediation (STAR) is a patented technology that employs smouldering combustion to destroy liquid hydrocarbons and was originally developed as an in-situ soil remediation technique (Switzer et al., 2009). As the organic contaminant (i.e., the fuel) is spread within a porous and largely inert soil medium, a smouldering reaction can be ignited and propagated to effectively clean the soil (see Figure 2.7) (Pironi et al., 2009).

Figure 2.7: Coarse grain sand (a) without coal tar, (b) with coal tar, (c) after STAR remediation (Pironi et al., 2009).

The porous medium increases the fuel surface area for reaction, provides porosity to permit air (oxidizer) flow, and supports the efficient storage, transfer, and recycling of the released reaction energy. A key advantage is that this configuration facilitates a self-sustaining reaction, meaning no additional energy input is required after ignition (Switzer et al., 2009). Smouldering in STAR typically reaches temperatures between $500 - 800°C$ for many minutes in one location resulting in upwards of 99% consumption of fuel, effectively producing clean soil (Pironi et al., 2011).

STAR was first intended for recalcitrant, dense non-aqueous phase liquids (DNAPLs), such as coal tar (Switzer et al., 2009). Recently, STAR has shown potential for treating more volatile DNAPLS mixed with fatty oils through a combination of volatilization and combustion (e.g., Trichloroethylene mixed with vegetable oil or emulsified vegetable oil) (Salman et al., 2015). Pironi et al. (2011) demonstrated resilience to quenching in experiments using coarse grain sand in a 15 cm tall column with 25% of pore space occupied by coal tar and up to 75% of pore space occupied by water. Though peak temperatures and propagation velocities dropped with increasing water contents, a self-

sustaining reaction was achieved in all cases, showing strong potential for the application of STAR below the ground water table. Sand grain size, which directly affects the pore size, and initial contaminant concentration were found to be the key parameters affecting the smoulder self-sustainability. Non-self-sustaining reactions resulted from average grain sizes greater than 10 mm and initial concentrations lower than 28 400 mg/kg for coal tar and 31 200 mg/kg for crude oil.

A phenomenological model was developed by MacPhee et al. (2012) to predict the smouldering propagation velocity and extent of soil remediation achieved during STAR application. The resultant two-dimensional "In Situ Smouldering Model" (ISSM) is a practical tool designed to simulate large scale engineered and natural environments. The ISSM couples a three-dimensional multiphase flow model (DNAPL3D) and a combustion front expansion model (based on Huygen's Principle) with an analytical expression for the forward smouldering velocity (from Pironi (2009) and similar to Equation 4) (Kueper and Frind, 1991; Torero et al., 1993; Richards and Bryce, 1995; Gerhard et al., 1998; Gerhard and Kueper, 2003a; 2003b; Grant et al., 2007; MacPhee et al., 2012). The ISSM has successfully predicted the one-dimensional and two-dimensional spreads and velocities of forward smouldering from lab scale smouldering experiments using coal tar within homogeneous coarse grain sand (MacPhee et al., 2012; Hasan et al., 2015).

Switzer et al. (2014) demonstrated the scalability of STAR over a series of experiments where the scale was increased 1000 fold from 0.003 to 3 m^3. The smouldering limits were found to increase with increasing scale due to lower heat losses from free surfaces. At the drum scale (0.3 m^3), an initial concentration of 12 000±4000 mg/kg mixed oil waste

(including waste from crude oil, petroleum refining, and some soil) achieved a self-sustaining smoulder. This initial concentration was less than half of the limiting concentration for coal tar or crude oil from lab experiments (0.003 m^3) (Pironi et al., 2011). Furthermore, propagation of the smouldering front in response to increasing air fluxes was consistent across scales, verifying that the controllability of the process via supplied air was maintained at larger scales. Additional work detailing the effectiveness of STAR in-situ was completed by Scholes (2013) and, following successful pilot trials, a field scale implementation of STAR is currently underway at a 38 acre site contaminated with coal tar in Newark, New Jersey.

2.4.2 Ex-situ Application

An extension to this technology is a patented and patent pending ex-situ application (STARx) that is commercialized by Savron (www.savronsolutions.com). STARx was originally developed for treating hazardous organic liquid wastes, similar to the STAR in-situ application (Pironi et al., 2011). The concept involves mixing these wastes within an inert porous medium (i.e., quartz sand) to form a fixed bed, facilitating the same conditions experienced in STAR. The controllability of this process, via airflow and selected properties of the porous medium, makes STARx an appropriate technology for materials with limited disposal options (Pironi et al., 2011; Switzer et al., 2014).

Recently, the application of smouldering in this configuration has extended to managing faeces, which have a much lower energy content and higher MC than previously studied wastes. Yermán et al. (2015) explored the self-sustainability of upwards forward smouldering using surrogate-human faeces mixed with sand as a function of faeces MC,

sand/faeces ratio (S/F), contaminant pack height, and airflow rate. The results were confirmed with an additional set of experiments using dog faeces. At a given scale, a boundary between self-sustaining (SS) and non-self-sustaining (NSS) smouldering depends on complex interactions between heat generation (e.g., fuel energy content, oxygen supply), heat retention (e.g., sand and fuel heat capacities) and heat loss (e.g., volatile compounds, water) and thus needs to be determined experimentally (Torero and Fernandez-Pello, 1996; Yermán et al., 2015). To identify the conditions that lead to SS smouldering, Yermán et al. (2015) mapped a parameter space over a fixed set of variables that identified the quenching limits. This study showed that, in a 98 cm tall and 16 cm diameter fixed bed using 108 g/min (5.7 cm/s) airflow, increasing the sand dilution from 3.25 to 4.25 g/g S/F linearly increased the limiting faeces MC that permitted a SS smoulder from 60 to 70% MC (wet mass basis). This result was hypothesized to be governed by the downward water migration into the smouldering front, where the S/F mixture's capacity for retaining condensed moisture increased with increasing S/F, thus decreasing the amount downward water migration and facilitating SS smouldering with higher MC faeces. Using a 50 cm tall pack and 65% faeces MC, the minimum air flux for SS smouldering was found to decrease from 5.8 cm/s to 0.74 cm/s when increasing the S/F from 2.75 to 3.75 g/g. This was due to increasing the fuel surface area available for oxygen diffusion in higher S/F systems. This means a lower oxygen gradient was needed from the pore space to the surface of the fuel to maintain a SS reaction and resulted in a lower minimum air flux (Leach et al., 2000; Yermán et al., 2015). For comparison, Pironi et al. (2011) found SS smouldering achievable in coal tar mixed with sand using an air flux at least 0.5 cm/s. As previously discussed in Section 2.3.3, the cooler porous medium

ahead of the smouldering front facilitates a condensation zone, which can limit the smouldering propagation (Ohlemiller, 1985). Indeed, accumulated condensation ahead of the smouldering zone, resulting from evaporated/boiled water and water produced during oxidation, was shown to limit the faeces MC for a SS reaction from 75 to 65% as the pack height increased from 20 to 98 cm (Yermán et al., 2015). This also agrees with Frandsen (1987), who recognized this redistribution of moisture can significantly affect the smouldering propagation and cause large moisture gradients that could quench the reaction. In summary, smouldering faeces was identified as a viable, controllable disposal technique, where a SS reaction was achieved at fuel MC higher than flaming combustion could permit.

2.5 Summary

Municipal wastewater treatment is an increasingly complex issue where managing the major by-product, biosolids, persists as the most expensive and challenging component (Droste, 1997; Shannon et al., 2008). With $298 and $39 billion expected in upgrading U.S. and Canadian WWTP infrastructure, respectively, there is strong incentive to pursue innovative, cost-effective, and energy efficient WWTP solutions (Félio et al., 2012; ASCE, 2013).

Smouldering combustion presents an interesting opportunity as a novel approach to biosolids management. Due to the efficient heat transfer to unburned fuel, self-sustaining smouldering is much more resilient to quenching than flaming combustion (Ohlemiller, 1985; Yermán et al., 2015). This means that low calorific and/or high moisture content fuels, such as biosolids, may be smouldered in an energy efficient and cost-effective

manner. STARx is a patented and patent pending technology that may be employed to achieve self-sustaining smouldering by intentionally mixing sand and biosolids to facilitate the necessary thermodynamic properties, fuel surface area, and permeability for air flow (Switzer et al., 2009).

The potential of WWTP biosolids to smoulder has never been studied. If they were susceptible to smouldering, key unknowns include: (1) What maximum moisture content could be smouldered, since this would dictate the degree of biosolids processing; (2) What minimum sand dilution would be required, as this would affect the mass destruction rate; (3) How would air flux impact the smouldering propagation, as this could be considered a key operator control; and (4) What would be the economic return for a full-scale smouldering system in a WWTP.

2.6 References

Abdalla, C. W., Roach, B. A., & Epp, D. J. (1992). Valuing environmental quality changes using averting expenditures: an application to groundwater contamination. *Land Economics*, 163-169.

Ahluwalia, S. S., & Goyal, D. (2007). Microbial and plant derived biomass for removal of heavy metals from wastewater. *Bioresource technology, 98*(12), 2243-2257.

Akkutlu, I. Y., & Yortsos, Y. C. (2003). The dynamics of in-situ combustion fronts in porous media. *Combustion and Flame, 134*(3), 229-247.

Apedaile, E. (2001). A perspective on biosolids management. *The Canadian Journal of Infectious Diseases, 12*(4), 202.

ASCE. (2013). America's Infrastructure Report Card for 2013. *Wastewater.* Retrieved June 6, 2015, from http://www.infrastructurereportcard.org/wastewater/

Bar-Ilan, A., Rein, G., Fernandez-Pello, A. C., Torero, J., & Urban, D. (2004). Forced forward smoldering experiments in microgravity. *Experimental thermal and fluid science, 28*(7), 743-751.

Bellur, S. R., Coronella, C. J., & Vásquez, V. R. (2009). Analysis of biosolids equilibrium moisture and drying. *Environmental progress & sustainable energy, 28*(2), 291-298.

Blinderman, M., Saulov, D. N., & Klimenko, A. Y. (2008). Forward and reverse combustion linking in underground coal gasification. *Energy, 33*(3), 446-454.

Bolong, N., Ismail, A., Salim, M. R., & Matsuura, T. (2009). A review of the effects of emerging contaminants in wastewater and options for their removal. *Desalination, 239*(1), 229-246.

Boundy, R., Diegel, S. W., Wright, L., & Davis, S. C. (2011). *Biomass Energy Data Book* (4th ed.). Oak Ridge, U.S.: U.S. Department of Energy, Energy Efficiency and Renewable Energy

CEC. (2010). Working Document on Sludge (Part III) (Vol. DG ENV.G.4/ETU/2008/0076r). Belgium: Commission of the European Communities Directorate-General Environment.

Chirag, K., Vijay, K., Raghavan, V., & Rangwala, A. (2011). Smoldering Combustion of Biomass Particles. *Journal of Applied Sciences, 11*(10), 1862-1866.

Christensen, J. R., Sørensen, P. B., Christensen, G. L., & Hansen, J. A. (1993). Mechanisms for overdosing in sludge conditioning. *Journal of Environmental Engineering, 119*(1), 159-171.

CIA. (2014). The World Factbook. *United States.* Retrieved June 10, 2015, from https://www.cia.gov/library/publications/resources/the-world-factbook/geos/us.html

Cordell, D., Rosemarin, A., Schröder, J., & Smit, A. (2011). Towards global phosphorus security: A systems framework for phosphorus recovery and reuse options. *Chemosphere, 84*(6), 747-758.

Cui, H., Ninomiya, Y., Masui, M., Mizukoshi, H., Sakano, T., & Kanaoka, C. (2006). Fundamental behaviors in combustion of raw sewage sludge. *Energy & Fuels, 20*(1), 77-83.

Dangtran, K., Mullen, J. F., & Mayrose, D. T. (2000). A comparison of fluid bed and multiple hearth biosolids incineration. *Proceedings of the Water Environment Federation, 2000*(1), 368-384.

Della Zassa, M., Biasin, A., Zerlottin, M., Refosco, D., & Canu, P. (2013). Self-heating of dried industrial wastewater sludge: Lab-scale investigation of supporting conditions. *Waste management*.

DeRis, J. (1970). Duct fires. *Combustion Science and Technology, 2*(4), 239-258.

Donatello, S., & Cheeseman, C. R. (2013). Recycling and recovery routes for incinerated sewage sludge ash (ISSA): A review. *Waste management, 33*(11), 2328-2340.

Dosanjh, S. S., Pagni, P. J., & Fernandez-Pello, A. C. (1987). Forced cocurrent smoldering combustion. *Combustion and Flame, 68*(2), 131-142.

Droste, R. L. (1997). *Theory and Practice of Water and Wastewater Treatment*. New York, NY: John Wiley & Sons, Ltd.

Drysdale, D. (2011). Spontaneous Ignition within Solids and Smoldering Combustion *An introduction to fire dynamics* (pp. 512): John Wiley & Sons, Ltd.

Environment Canada. (2013a). Wise Water Use. *We take our water for granted.* Retrieved June 10, 2015, from https://www.ec.gc.ca/eau-water/default.asp?lang=En&n=F25C70EC-1

Environment Canada. (2013b). Wastewater Systems Effluent Regulations Reporting. *What are the benefits of the Regulations?* Retrieved June 10, 2015, from https://www.ec.gc.ca/eu-ww/default.asp?lang=En&n=0D689118-1

Félio, G., Ferreira, B., McNally, C., Robertshaw, R., Andres, R., Siu, K., Buda, M., Thompson, A., Lounis, Z., & CIRC. (2012). Canadian Infrastructure Report Card Volume 1: 2012 Municipal Roads and Water Systems (Vol. 1): The Canadian Infrastructure Report Card.

Frandsen, W. H. (1987). The influence of moisture and mineral soil on the combustion limits of smoldering forest duff. *Canadian Journal of Forest Research, 17*(12), 1540-1544.

Frandsen, W. H. (1997). Ignition probability of organic soils. *Canadian Journal of Forest Research, 27*(9), 1471-1477.

Ganesan, V. (2012). *Internal Combustion Engines* (4 ed.): McGraw-Hill.

Gerhard, J., & Kueper, B. (2003a). Capillary pressure characteristics necessary for simulating DNAPL infiltration, redistribution, and immobilization in saturated porous media. *Water Resources Research, 39*(8).

Gerhard, J., & Kueper, B. (2003b). Relative permeability characteristics necessary for simulating DNAPL infiltration, redistribution, and immobilization in saturated porous media. *Water Resources Research, 39*(8).

Gerhard, J. I., Kueper, B. H., & Hecox, G. R. (1998). The influence of waterflood design on the recovery of mobile DNAPLs. *Groundwater, 36*(2), 283-292.

Giger, W., Alder, A. C., Golet, E. M., Kohler, H.-P. E., McArdell, C. S., Molnar, E., Siegrist, H., & Suter, M. J. (2003). Occurrence and fate of antibiotics as trace contaminants in wastewaters, sewage sludges, and surface waters. *CHIMIA International Journal for Chemistry, 57*(9), 485-491.

Grant, G. P., Gerhard, J. I., & Kueper, B. H. (2007). Multidimensional validation of a numerical model for simulating a DNAPL release in heterogeneous porous media. *Journal of contaminant hydrology, 92*(1), 109-128.

Hach, C. C., Klein Jr, R. L., & Gibbs, C. R. (1997). Biochemical Oxygen Demand. *Tech. Monogr*(7).

Hadden, R., & Rein, G. (2009). *Ignition and suppression of smouldering coal fires in small-scale experiments.* Paper presented at the 6th Mediterranean Combustion Symposium, Ajaccio, Corsica, France, MCS.

Hadden, R. M., Rein, G., & Belcher, C. M. (2013). Study of the competing chemical reactions in the initiation and spread of smouldering combustion in peat. *Proceedings of the Combustion Institute, 34*(2), 2547-2553.

Hale, R. C., La Guardia, M. J., Harvey, E. P., Gaylor, M. O., Mainor, T. M., & Duff, W. H. (2001). Flame retardants: Persistent pollutants in land-applied sludges. *Nature, 412*(6843), 140-141.

Hanley, N., Wright, R. E., & Adamowicz, V. (1998). Using choice experiments to value the environment. *Environmental and Resource Economics, 11*(3-4), 413-428.

Hasan, T., Gerhard, J. I., Hadden, R., & Rein, G. (2015). Self-sustaining smouldering combustion of coal tar for the remediation of contaminated sand: Two-dimensional experiments and computational simulations. *Fuel, 150*, 288-297.

He, F., & Behrendt, F. (2009). Comparison of natural upward and downward smoldering using the volume reaction method. *Energy & Fuels, 23*(12), 5813-5820.

He, F., Yi, W., Li, Y., Zha, J., & Luo, B. (2014). Effects of fuel properties on the natural downward smoldering of piled biomass powder: Experimental investigation. *Biomass and Bioenergy, 67*, 288-296.

Howell, J., Hall, M., & Ellzey, J. (1996). Combustion of hydrocarbon fuels within porous inert media. *Progress in energy and combustion science, 22*(2), 121-145.

Kaufman, Y. J., Tanré, D., & Boucher, O. (2002). A satellite view of aerosols in the climate system. *Nature, 419*(6903), 215-223.

Khiari, B., Marias, F., Zagrouba, F., & Vaxelaire, J. (2004). Analytical study of the pyrolysis process in a wastewater treatment pilot station. *Desalination, 167*, 39-47.

King, E., & Painter, H. (1986). Inhibition of respiration of activated sludge: variability and reproducibility of results. *Toxicity Assessment, 1*(1), 27-39.

Kuenzer, C., Zhang, J., Tetzlaff, A., Van Dijk, P., Voigt, S., Mehl, H., & Wagner, W. (2007). Uncontrolled coal fires and their environmental impacts: Investigating two arid mining regions in north-central China. *Applied Geography, 27*(1), 42-62.

Kueper, B. H., & Frind, E. O. (1991). Two-phase flow in heterogeneous porous media: 1. Model development. *Water Resources Research, 27*(6), 1049-1057.

Kurniawan, T. A., Chan, G. Y., Lo, W.-H., & Babel, S. (2006). Physico–chemical treatment techniques for wastewater laden with heavy metals. *Chemical Engineering Journal, 118*(1), 83-98.

Leach, S. V., Rein, G., Ellzey, J., Ezekoye, O. A., & Torero, J. L. (2000). Kinetic and fuel property effects on forward smoldering combustion. *Combustion and Flame, 120*(3), 346-358.

Lipták, B. G. (1974). *Environmental Engineers' Handbook* (1st ed.). Radnor, PA: Chilton Book Company.

MacPhee, S. L., Gerhard, J. I., & Rein, G. (2012). A novel method for simulating smoldering propagation and its application to STAR (Self-sustaining Treatment for Active Remediation). *Environmental Modelling & Software, 31*, 84-98.

McGrath, S., Chang, A., Page, A., & Witter, E. (1994). Land application of sewage sludge: scientific perspectives of heavy metal loading limits in Europe and the United States. *Environmental Reviews, 2*(1), 108-118.

Metcalf and Eddy. (2003). *Wastewater Engineering: Treatment and Reuse* (4th ed.). New York, NY: McGraw-Hill.

Mirza S. (2007). Danger Ahead: The Coming Collapse of Canadia's Municipal Infrastructure , Federation for Canadian Municipalities - McGill University.

Moussa, N. A., Toong, T., & Garris, C. (1977). *Mechanism of smoldering of cellulosic materials* (Vol. 16): Elsevier.

Murakami, T., Suzuki, Y., Nagasawa, H., Yamamoto, T., Koseki, T., Hirose, H., & Okamoto, S. (2009). Combustion characteristics of sewage sludge in an incineration plant for energy recovery. *Fuel Processing Technology, 90*(6), 778-783.

Ogada, T., & Werther, J. (1996). Combustion characteristics of wet sludge in a fluidized bed: release and combustion of the volatiles. *Fuel, 75*(5), 617-626.

Ohlemiller, T., & Lucca, D. (1983). An experimental comparison of forward and reverse smolder propagation in permeable fuel beds. *Combustion and Flame, 54*(1), 131-147.

Ohlemiller, T. J. (1985). Modeling of smoldering combustion propagation. *Progress in energy and combustion science, 11*(4), 277-310.

Ohlemiller, T. J. (1990). Smoldering combustion propagation through a permeable horizontal fuel layer. *Combustion and Flame, 81*(3), 341-353.

Ohlemiller, T. J., DiNenno, P. J., National Fire Protection Association, & Society of Fire Protection Engineers. (2008). Smoldering Combustion *SFPE Handbook of Fire Protection Engineering* (pp. 2-200-210): National Fire Protection Association.

Oleszkiewicz, J., & Mavinic, D. S. (2002). Wastewater biosolids: an overview of processing, treatment, and management. *Journal of Environmental Engineering and Science, 1*(2), 75-88.

Pal, A., Gin, K. Y.-H., Lin, A. Y.-C., & Reinhard, M. (2010). Impacts of emerging organic contaminants on freshwater resources: review of recent occurrences, sources, fate and effects. *Science of the Total Environment, 408*(24), 6062-6069.

Palmer, K. (1957). Smouldering combustion in dusts and fibrous materials. *Combustion and Flame, 1*(2), 129-154.

Pironi, P. (2009). *Smouldering combustion of liquids in porous media for remediating NAPL-contaminated soils.* Ph. D. Thesis, University of Edinburgh: Edinburgh, Scotland, UK.

Pironi, P., Switzer, C., Gerhard, J. I., Rein, G., & Torero, J. L. (2011). Self-sustaining smoldering combustion for NAPL remediation: laboratory evaluation of process sensitivity to key parameters. *Environmental Science & Technology, 45*(7), 2980-2986.

Pironi, P., Switzer, C., Rein, G., Fuentes, A., Gerhard, J. I., & Torero, J. L. (2009). *Small-scale forward smouldering experiments for remediation of coal tar in inert media* (Vol. 32): Elsevier.

Prat, N., Belcher, C., Hadden, R., Rein, G., & Yearsley, J. (2014). A laboratory study of the effect of moisture content on the spread of smouldering peat fires. *FLAMMA, 5*(1), 35-38.

Qasim, S. R. (1999). *Wastewater treatment plants: planning, design and operation*: CRC Press.

Quintiere, J. G., Birky, M., Macdonald, F., & Smith, G. (1982). An analysis of smoldering fires in closed compartments and their hazard due to carbon monoxide. *Fire and Materials, 6*(3-4), 99-110.

Rein, G. (2009). Smouldering combustion phenomena in science and technology. *International Review of Chemical Engineering, 1*, 3-18.

Rein, G. (2013). Smouldering fires and natural fuels. *Fire Phenomena and the Earth System: An Interdisciplinary Guide to Fire Science*, 15-33.

Rein, G., Cleaver, N., Ashton, C., Pironi, P., & Torero, J. L. (2008). The severity of smouldering peat fires and damage to the forest soil. *Catena, 74*(3), 304-309.

Rein, G., Cohen, S., & Simeoni, A. (2009). Carbon emissions from smouldering peat in shallow and strong fronts. *Proceedings of the Combustion Institute, 32*(2), 2489-2496.

Rein, G., Lautenberger, C., Fernandez-Pello, A. C., Torero, J. L., & Urban, D. L. (2006). Application of genetic algorithms and thermogravimetry to determine the kinetics of polyurethane foam in smoldering combustion. *Combustion and Flame, 146*(1), 95-108.

Renner, R. (2007). Rethinking biochar. *Environmental Science & Technology, 41*(17), 5932-5933.

Richards, G. D., & Bryce, R. W. (1995). A computer algorithm for simulating the spread of wildland fire perimeters for heterogeneous fuel and meteorological conditions. *International Journal of Wildland Fire, 5*(2), 73-79.

Roy, M. M., Dutta, A., Corscadden, K., Havard, P., & Dickie, L. (2011). Review of biosolids management options and co-incineration of a biosolid-derived fuel. *Waste management, 31*(11), 2228-2235.

Salman, M., Gerhard, J. I., Major, D. W., Pironi, P., & Hadden, R. (2015). Remediation of trichloroethylene-contaminated soils by star technology using vegetable oil smoldering. *Journal of Hazardous Materials, 285*, 346-355.

Sartorius, C., von Horn, J., & Tettenborn, F. (2012). Phosphorus recovery from wastewater—Expert survey on present use and future potential. *Water Environment Research, 84*(4), 313-322.

Sato, K., & Sega, S. (1989). Smolder spread in a horizontal layer of cellulosic powder. *Fire Safety Science, 2*, 87-96.

Scholes, G. C. (2013). *Ignition Method Development and First Field Demonstration of In Situ Smouldering Remediation.* (M.E.Sc.), The University of Western Ontario, London, ON.

Schult, D., Matkowsky, B., Volpert, V., & Fernandez-Pello, A. (1996). Forced forward smolder combustion. *Combustion and Flame, 104*(1), 1-26.

Scuras, S. E., Jobbagy, A., & Grady, C. L. (2001). Optimization of activated sludge reactor configuration:: kinetic considerations. *Water Research, 35*(18), 4277-4284.

Shannon, K., Lee, D.-Y., Trevors, J., & Beaudette, L. (2007). Application of real-time quantitative PCR for the detection of selected bacterial pathogens during municipal wastewater treatment. *Science of the Total Environment, 382*(1), 121-129.

Shannon, M. A., Bohn, P. W., Elimelech, M., Georgiadis, J. G., Mariñas, B. J., & Mayes, A. M. (2008). Science and technology for water purification in the coming decades. *Nature, 452*(7185), 301-310.

Singh, R., & Agrawal, M. (2008). Potential benefits and risks of land application of sewage sludge. *Waste management, 28*(2), 347-358.

Sinha, S., Jhalani, A., Ravi, M., & Ray, A. (2000). Modelling of pyrolysis in wood: A review. *SESI Journal, 10*(1), 41-62.

Spinosa, Ludovico, Vesilind, & Aarne, P. (2001). *Sludge into biosolids: processing, disposal, utilization*: IWA publishing.

Switzer, C., Pironi, P., Gerhard, J., Rein, G., & Torero, J. (2009). Self-sustaining smoldering combustion: a novel remediation process for non-aqueous-phase liquids in porous media. *Environmental Science & Technology, 43*(15), 5871-5877.

Switzer, C., Pironi, P., Gerhard, J. I., Rein, G., & Torero, J. L. (2014). Volumetric scale-up of smouldering remediation of contaminated materials. *Journal of Hazardous Materials, 268*, 51-60.

Takács, I., Patry, G. G., & Nolasco, D. (1991). A dynamic model of the clarification-thickening process. *Water Research, 25*(10), 1263-1271.

Ternes, T. A., Joss, A., & Siegrist, H. (2004). Peer reviewed: scrutinizing pharmaceuticals and personal care products in wastewater treatment. *Environmental Science & Technology, 38*(20), 392A-399A.

The World Bank. (2015). *World Development Indicators* [Data file]. Retrieved from: http://data.worldbank.org/country/united-states

Tillman, D. (2012). *The Combustion of Solid Fuels and Wastes*: Academic Press.

Torero, J., & Fernandez-Pello, A. (1996). Forward smolder of polyurethane foam in a forced air flow. *Combustion and Flame, 106*(1), 89-109.

Torero, J., Fernandez-Pello, A., & Kitano, M. (1993). Opposed forced flow smoldering of polyurethane foam. *Combustion Science and Technology, 91*(1-3), 95-117.

Tyagi, V. K., & Lo, S.-L. (2013). Sludge: A waste or renewable source for energy and resources recovery? *Renewable and Sustainable Energy Reviews, 25*, 708-728.

U.S. EPA. (1979). Process Design Manual Sludge Treatmentand Disposal U.S. Environmental Protection Agency

U.S. EPA. (1994). *A Plain English Guide to the EPA Part 503 Biosolids Rule*: U. S. Environmental Protection Agency.

U.S. EPA. (1995). Part 503 Implementation Guidance (Office of Water, Trans.): U.S. Environmental Protection Agency.

U.S. EPA. (2000a). Centrifuge Thickening and Dewatering (Office of Water, Trans.) (Vol. EPA 832-F-00-053). Washington, D.C.: U.S. Environmental Protection Agency.

U.S. EPA. (2000b). Filter Press, Recessed Plate (Office of Water, Trans.) (Vol. EPA 832-F-00-058). Washington, D.C.: U.S. Environmental Protection Agency.

U.S. EPA. (2000c). In-Vessel Composting of Biosolids (Office of Water, Trans.) (Vol. EPA 832-F-00-061). Washington, D.C.: U.S. Environmental Protection Agency.

U.S. EPA. (2000d). Odor Control in Biosolids Management (Office of Water, Trans.) (Vol. EPA 832-F-00-067). Washington, D.C.: U.S. Environmental Protection Agency.

U.S. EPA. (2000e). Land Application of Biosolids (Office of Water, Trans.) (Vol. EPA 832-F-00-064). Washington, D.C.: U.S. Environmental Protection Agency.

U.S. EPA. (2000f). Alkaline Stabilization of Biosolids (Office of Water, Trans.) (Vol. EPA 832-F-00-052). Washington, D.C.: U.S. Environmental Protection Agency.

U.S. EPA. (2000g). Belt Filter Press (Office of Water, Trans.) (Vol. EPA 832-F-00-057). Washington, D.C.: U.S. Environmental Protection Agency.

U.S. EPA. (2001). Method 1684: Total, Fixed, and Volatile Solids in Water, Solids, and Biosolids (Office of Water, Office of Science and Technology & Engineering and Analysis Division, Trans.): U.S. Environmental Protection Agency.

U.S. EPA. (2002). Use of Composting for Biosolids Management (Office of Water, Trans.) (Vol. EPA 832-F-02-024). Washington, D.C.: U.S. Environmental Protection Agency.

U.S. EPA. (2003a). Gravity Thickening (Office of Water, Trans.) (Vol. EPA 832-F-03-022). Washington, D.C.: U.S. Environmental Protection Agency.

U.S. EPA. (2003b). Use of Incineration for Biosolids Management (Office of Water, Trans.) (Vol. EPA 832-F-03-013). Washington, D.C.: U.S. Environmental Protection Agency.

U.S. EPA. (2003c). Use of Landfilling for Biosolids Management (Office of Water, Trans.) (Vol. EPA 832-F-03-012). Washington, D.C.: U.S. Environmental Protection Agency.

U.S. EPA. (2006a). Heat Drying (Office of Water, Trans.) (Vol. EPA 832-F-06-029). Washington, D.C.: U.S. Environmental Protection Agency.

U.S. EPA. (2006b). Multi-Stage Anaerobic Digestion (Office of Water, Trans.) (Vol. EPA 832-F-06-031). Washington, D.C.: U.S. Environmental Protection Agency.

U.S. EPA. (2014). Water: Sustainable Infrastructure. *Energy Effeciency for Water and Wastewater Facilities*. Retrieved February 16, 2015, from http://water.epa.gov/infrastructure/sustain/sustainable_infrastructure.cfm

Uggla, E. (1974). *Fire ecology in Swedish forests.* Paper presented at the Tall Timbers Fire Ecology.

Venkatesan, A. K., & Halden, R. U. (2014). Wastewater treatment plants as chemical observatories to forecast ecological and human health risks of manmade chemicals. *Scientific Reports, 4*.

Vesilind, P. A., & Martel, C. J. (1990). Freezing of water and wastewater sludges. *Journal of Environmental Engineering, 116*(5), 854-862.

Wang, H., Brown, S. L., Magesan, G. N., Slade, A. H., Quintern, M., Clinton, P. W., & Payn, T. W. (2008). Technological options for the management of biosolids. *Environmental Science and Pollution Research-International, 15*(4), 308-317.

Wang, L. K., Shammas, N. K., & Hung, Y. T. (2008). *Biosolids engineering and management* (Vol. 7): Springer.

Washburn, E. W. (1933). Standard states for bomb calorimetry. *J. Res. Natl. Bur. Stand.(US), 10*, 525-558.

WEF. (1988). *Sludge Conditioning, Manual of Practice no. FD-14* Alexandria, VA: Water Environment Federation.

Werther, J., & Ogada, T. (1999). Sewage sludge combustion. *Progress in energy and combustion science, 25*(1), 55-116.

Yermán, L., Hadden, R. M., Carrascal, J., Fabris, I., Cormier, D., Torero, J. L., Gerhard, J. I., Krajcovic, M., Pironi, P., & Cheng, Y.-L. (2015). Smouldering combustion as a treatment technology for faeces: Exploring the parameter space. *Fuel, 147*, 108-116.

Zaleski, K. J., Josephson, K. L., Gerba, C. P., & Pepper, I. (2005). Survival, growth, and regrowth of enteric indicator and pathogenic bacteria in biosolids, compost, soil, and land applied biosolids. *Journal of residuals science and technology, 2*(1), 49-63.

Chapter 3

Self-sustaining Smouldering Combustion as a Novel Destruction Method for Biosolids

3.1 Introduction

Wastewater treatment plants (WWTPs) treat sewage via various chemical, physical, and biological processes to remove harmful constituents and mitigate risk to the community and surrounding environment (Metcalf and Eddy, 2003). Municipal WWTPs are energy intensive operations which, combined with drinking water services, account for $3 - 4\%$ of all energy consumption in the United States and $30 - 40\%$ of total energy consumed by municipalities, costing \$4 billion/year (U.S. EPA, 2014). Furthermore, as much of North America's WWTP infrastructure approaches the end of its design life, an estimated \$298 billion is required in the United States (and \$39 billion in Canada) to expand and upgrade WWTP infrastructure (Félio et al., 2012; ASCE, 2013). The major by-product from WWTPs is biosolids and approximately 50% of WWTPs capital and operating costs are dedicated to processing biosolids, making it the most expensive component of the WWTP process (Khiari et al., 2004).

Biosolids are defined as the separated solids from WWTPs that undergo additional treatment for beneficial end use (U.S. EPA, 1994). These separated solids, largely organic, are first settled out from the liquid stream either before treatment (primary sludge) or after biological processing (waste activated sludge). The resulting sludge contains $88.00 - 99.75\%$ moisture content (wet mass basis) (Droste, 1997; Metcalf and Eddy, 2003). This sludge undergoes various processing steps (e.g., dewatering, thickening, conditioning) to reduce its volume and improve aesthetic qualities for easier

management, or undergoes stabilization to permit safe land application (Droste, 1997). The major disposal (or end use) methods for biosolids in Canada include incineration, land application for agricultural purposes, and landfilling (Apedaile, 2001). All of these methods are expensive in that they require high energy input, many person-hours, and/or large transportation distances (Werther and Ogada, 1999; Wang et al., 2008; Bellur et al., 2009). In addition, land application is controversial and subject to restrictions and uncertain risks stemming from contaminants of emerging concern (U.S. EPA, 1995; Hale et al., 2001; Giger et al., 2003; Ternes et al., 2004; Bolong et al., 2009; Venkatesan and Halden, 2014). In general, managing biosolids is a major challenge for WWTPs and there is a strong need to provide novel alternatives (Tyagi and Lo, 2013).

This chapter explores, for the first time, the possibility of using smouldering combustion as a new method for biosolids management. STARx (Self-sustaining Treatment for Active Remediation applied ex-situ) refers to the commercial technology that uses smouldering combustion to destroy organic wastes; to date it has been shown to be promising for a variety of organic industrial liquid wastes including coal tar, crude oil, and mixed hydrocarbons (Switzer et al., 2009; Pironi et al., 2011; Switzer et al., 2014). As explained below, smouldering has the potential to treat organic wastes in an energy efficient and cost-effective manner.

3.1.1 Smouldering Combustion

Smouldering combustion is a flameless, heterogeneous (i.e., fuel and oxidant in different phases) oxidation reaction limited by the rate at which oxygen diffuses into the surface of a solid or liquid fuel (Ohlemiller, 1985; Switzer et al., 2009). Smouldering is self-

sustaining when, after a short and localized energy input for ignition, the reaction propagates using only the heat produced by the fuel's oxidation (Switzer et al., 2009). Self-sustained smouldering requires a porous material, which provides a high surface area for reaction and adequate permeability for air flow (Drysdale, 2011). The majority of smouldering research has been performed in the context of fire prevention, and thus has focused on solid fuels such as polyurethane foam or stored biomass under natural air flow (e.g., He and Behrendt (2009), Palmer (1957), Quintiere et al. (1982), Rein et al. (2006)). STARx accelerates the reaction by using forced air flow and, taking advantage of the buoyant hot combustion gases, utilizing upwards forward smouldering. In this configuration, the reaction propagation and oxidizer flow are both in the upward direction against gravity (Torero and Fernandez-Pello, 1996).

Upwards forward smouldering promotes efficient heat transfer ahead to unburned fuel, which extends the fuel's limits with respect to quenching (i.e., the suppression of chemical processes driving combustion) relative to those for flaming combustion (Ohlemiller, 1985; Howell et al., 1996; Hadden and Rein, 2009; Yermán et al., 2015). This means that smouldering is much less susceptible to extinction than flaming and can achieve a self-sustaining reaction using fuels with very low effective calorific values and/or significant moisture content (Hadden and Rein, 2009; Yermán et al., 2015). Several studies have explored the self-sustained smouldering of peat in the context of forest fires. Frandsen (1987) detailed the impact that moisture and inorganic contents had on self-sustaining smouldering of peat moss between 0 to 1 moisture/organic ratio and 0 to 5 inorganic/organic ratio. It was found that the moisture/organic ratio limit that permitted self-sustaining smouldering linearly declined with increasing inorganic/organic

ratio. Using an ignition protocol roughly equivalent to the heating from a flaming stump, 100W for 30 min, Rein et al. (2008) found the critical moisture content for smouldering ignition to be 55±2% (wet mass basis). Prat et al. (2014) found a dramatic drop in smouldering propagation velocity above 25% moisture content (dry mass basis).

3.1.2 Application of Smouldering for Waste Management

Intentional smouldering for mass destruction was first developed for remediation of soil contaminated by organic industrial liquid wastes (Pironi et al., 2009; Switzer et al., 2009; Pironi et al., 2011; Salman et al., 2015). In this case, the fuel (i.e., contaminant) occupies a fraction of the pore space of an inert porous medium (i.e., soil). STARx extends this concept to intentionally mixing liquid wastes, which may be recently produced by industrial operations or were historically disposed in lagoons, with sand to form a smoulderable mixture. In addition to providing increased surface area for reaction and permeability for air (oxidant) flow, the sand promotes the efficient storage, transfer, and recycling of the released reaction energy (Switzer et al., 2014). Smouldering of organic liquids in sand typically achieves peak temperatures between 500 – 800°C for many minutes in one location resulting in upwards of 99% consumption of fuel, effectively producing clean, sterile sand that can be reused (Switzer et al., 2009).

In examining the sensitivity of a smouldering reaction, of interest is the effect of a variable on peak temperatures and reaction propagation rates in the self-sustaining regime, and the boundary between self-sustaining and non-self-sustaining reactions. Pironi et al. (2011) studied the influence of the fraction of pore space occupied by water on the smouldering of coal tar in sand. Though increasing water content reduced the peak

temperature and propagation velocity, a self-sustaining reaction was achieved in all cases from 0.0 to 75% water-filled porosity and 25% coal tar-filled porosity. This demonstrated the ability of an exothermic smouldering reaction to propagate itself and, with the excess energy generated, to sustain a water boiling front ahead of the reaction. The propagation rate of the reaction (and thus the waste destruction rate) was shown to be linearly dependent on air injection rate, which is expected for an oxygen-limited reaction (Dosanjh et al., 1987; Schult et al., 1996; Pironi et al., 2009). Smouldering was also shown to be sensitive to sand grain size and initial contaminant concentration; the reaction was non-self-sustaining for sands with average grain sizes greater than 10 mm and initial coal tar concentration lower than 25 000 mg/kg. These specific numbers are expected to be a function of experimental scale, with larger grain sizes and lower initial concentrations likely self-sustaining at larger scales (Switzer et al., 2014). This is because self-sustainability depends on a positive energy balance (heat generation minus heat losses) and increased scale means less relative heat loss to the external boundary due to lower surface area/volume ratio (Switzer et al., 2014). At a given scale, a boundary between self-sustaining and non-self-sustaining smouldering behaviour depends on complex interactions between variables that affect heat generation (e.g., fuel energy content, oxygen supply), heat retention (e.g., sand and fuel heat capacities) and heat loss (e.g., volatile compounds, moisture content) and thus needs to be determined experimentally (Torero and Fernandez-Pello, 1996).

Smouldering research on materials similar to biosolids is largely limited to understanding the self-heating and fire hazards associated with their storage (e.g., Chirag et al. (2011), Della Zassa et al. (2013), He et al. (2014)). The exception is a study on smouldering

faeces for international development purposes by Yermán et al. (2015). That work explored the self-sustainability of upwards forward smouldering using surrogate-human faeces and dog faeces mixed with sand as a function of faeces moisture content, sand/faeces mass ratio, contaminant pack height, and airflow rate. This study showed that faeces with moisture content as high as 70% (wet mass basis) could achieve a self-sustaining smoulder in a 98 cm tall and 16 cm diameter fixed bed using 108 g/min airflow and a sand/faeces mass ratio of 4.25. The cool porous medium ahead of the reaction provides a condensation zone, which can be problematic for very wet fuels (Ohlemiller, 1985). Indeed, accumulated condensation ahead of the smouldering zone, resulting from evaporated/boiled water and water produced during oxidation, was shown to limit the pack height for a self-sustaining reaction as faeces moisture content increased (Yermán et al., 2015).

These findings suggest that self-sustaining smouldering may provide an attractive biosolids destruction option for WWTPs, as it may minimize energy input and biosolids processing (e.g., reducing the need for dewatering). Thirty experiments were completed to (i) demonstrate, for the first time, the potential for WWTP biosolids to be smouldered, (ii) map the parameter space in which biosolids will permit self-sustained smouldering, and (iii) understand the sensitivity of the reaction to system energy content and air flux, a key operator parameter. This work aims to provide basic design information for considering STARx as an alternative biosolids disposal option. A coarse economic analysis was also conducted to provide a preliminary evaluation of the potential payback period large WWTPs may find from replacing typical biosolids disposal (i.e., land application or incineration) with STARx.

3.2 Materials and Methodology

3.2.1 Experimental Setup and Procedure

Biosolids were obtained from Greenway Pollution Control Centre (Greenway) in London, Ontario, Canada. Greenway utilizes a typical wastewater treatment path, where primary clarification initially removes settleable solids (primary sludge). The waste activated sludge is settled out in secondary clarification following aerobic digestion, and is thickened in either dissolved air flotation units or rotating drum thickeners. The combined primary and waste activated sludge is dewatered via centrifugation with polymer addition, and the sampling point for all biosolids used in this study was located after this final processing step.

Biosolids initial moisture content (MC) and ash content, measured by EPA Method 1684 (U.S. EPA, 2001), and biosolids dry higher heating value $\left(HHV_d^b\right)$ $\left(\frac{kJ}{g}\right)$, measured using a bomb calorimeter, are summarized in Table 3.1 (see Appendix A for full results). The presented values represent the minimum and maximum average properties measured from four batches $(19 - 120$ L) gathered 10 months apart. Each value in the first row of Table 3.1 is an average of at least three measurements from a batch that were all within 10% of the average. Note that the ash content represents $(dry\ solids - volatile\ solids)$. Table 3.1 further demonstrates that the measured values compare well against values from literature. However, since the measured HHV_d^b range was slightly lower than typical, this suggests that the employed biosolids provided a conservative sample with respect to biosolids energy content (WEF, 1988; Metcalf and Eddy, 2003).

Table 3.1: Biosolids Key Properties

	Initial Moisture Content % (g_{water}/g_{total})	Ash Content % (g_{ash}/g_{dry})	Dry Higher Heating Value (kJ/g_{dry})
Measured on Greenway Samples	72.2, 79.9	18.6, 22.8	17.2, 18.1
Literature Comparison	70.0 –90.0[a]	17.8, 27.5[b]	23.0 – 29.0[c] 20.0 – 23.0[c]

[a] Biosolids moisture content range following dewatering via centrifugation (Metcalf and Eddy, 2003)
[b] Ash content range from two samples of raw sewage sludge (Cui et al., 2006)
[c] Primary (high range) and activated sludge (low range) higher heating value ranges (WEF, 1988; Metcalf and Eddy, 2003)

To preserve the biosolids between the time of collection and experimentation, the biosolids were dried to <1% MC and stored in a 5°C cold room. When preparing an experiment, the stored biosolids were manually crushed to a particle diameter near 1 cm and mechanically mixed (KSM7581MS, KitchenAid) with water to reach the desired biosolids MC. The biosolids re-wetted to the initial MC exhibited some qualitative differences from the virgin biosolids, such as less absorbed (i.e., interstitial, bound) water (Vesilind and Martel, 1990). This is likely due to irreversible changes in the biosolids particles' structures upon drying and rewetting (Vesilind and Martel, 1990). Several smouldering experiments were conducted with virgin biosolids to confirm that, despite any qualitative differences in the appearance of the fuel, the rewetted biosolids provided indistinguishable quantitative smouldering data as detailed in Section 3.3.2 (further details in Appendix C).

Column smouldering experiments followed established experimental procedures (Switzer et al., 2009; Pironi et al., 2011; Yermán et al., 2015), which are briefly reviewed here. Figure 3.1 illustrates the experimental setup and data collection equipment. A 60 cm tall and 15 cm diameter stainless steel column rested upon a base component that housed a

coiled resistive heater (450 W, 120 V, Watlow Ltd.) and an air injection manifold. Sixteen thermocouples (Type K, Omega Ltd.) inserted horizontally into the centre of the column at 3.5 cm intervals along the column height were employed to track temperatures. The heater was connected to a 120 V AC, single-phase variable power supply (STACO Energy Products) and the entire column was wrapped in insulation (5 cm thick mineral wool, McMaster Carr) as is typical in smouldering studies to mimic larger scale systems where external heat losses are less prevalent (Switzer et al., 2009). The apparatus rested on a mass balance (KCC150, Metler Toledo) to provide real time mass loss. The emissions from a select number of experiments (presented in Appendix D and noted in Table 3.2) were analyzed for volume fractions of carbon monoxide, carbon dioxide, and oxygen using a gas analyzer (MGA3000C, ADC). The mass balance, thermocouples, and gas analyzer were connected to a data logger (Multifunction Switch/Measure Unit 34980A, Agilent Technologies) and personal computer, which logged all readings every two seconds.

Clean sand was packed into the apparatus base until just covering the heater and air manifold. Coarse sand (Number 12, Bell & Mackenzie Co., mean grain diameter = 0.88 mm, coefficient of uniformity = 1.6) and biosolids, mechanically mixed in three batches, was packed in the column above the base to a height of 40 cm in 10 cm lifts. This was topped with 15 cm of clean sand. All experiments were subjected to a uniform ignition procedure with the heater on until the first thermocouple, 2 cm above the heating element, reached 200°C. Air injection was then initiated, achieved by a mass flow controller (FMA5400/5500 Series, Omega Ltd.) connected to laboratory compressed air. The heater was turned off after the first thermocouple reached its peak temperature, and

the subsequent combustion was sustained by the energy released by the biosolids during upwards forward smouldering. Excluding heater inefficiency, the resistance heater provided a constant heat flux of approximately 408 W (3.4 A X 120 V). The length of the preheating phase varied between 1 and 4 hours depending on the biosolids MC and sand/biosolids mass ratio (S/B). The air remained on until the reaction extinguished and the entire column cooled to ambient temperatures.
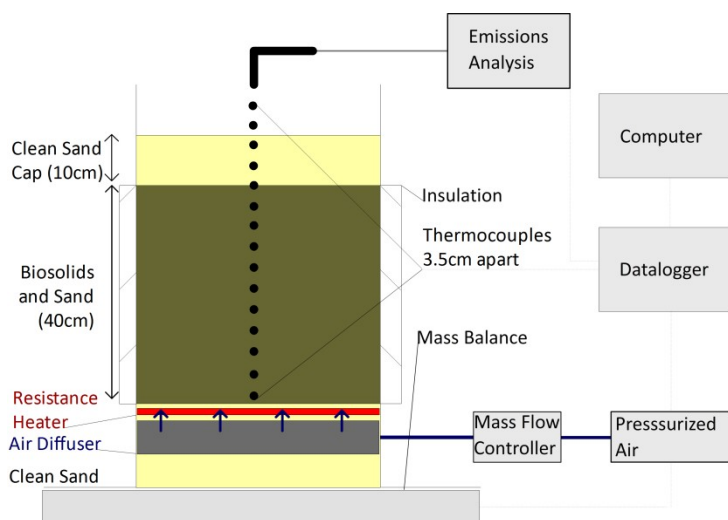
Figure 3.1: Illustration of the experimental set up.

Table 3.2 summarizes the twenty-three experiments (Experiments No. 0 to 23, excluding 10) performed to map the self-sustaining smouldering parameter space using biosolids with initial MCs ranging from 74 to 85% and S/Bs from 1.5 to 23 g/g. The focus was on the most economical condition for biosolids treatment, where the least processed (i.e., the wettest) biosolids can be destroyed at the maximum organic destruction rate (i.e., using the least amount of sand). All experiments were classified as self-sustaining (SS), non-self-sustaining (NSS), or borderline self-sustaining (BSS) (further defined in Section 3.3.1). These experiments also served to quantify the changes in key combustion metrics

(peak temperature, propagation velocity, and mass loss rate) within this parameter space. These experiments all used the same sand and an air flux of 3.3 cm/s (volume of air per unit cross-sectional area of column per time, i.e., Darcy flux). Seven experiments (Experiments No. 10 and 24 to 29) were performed to examine the sensitivity of the process to air fluxes between 1.6 and 8.1 cm/s for self-sustaining experiments with biosolids at both 73% and 79% MC and a non-self-sustaining experiment with 80% MC biosolids. In all cases, the reported combustion metrics were measured from the smouldering front passing through the middle 50% of the contaminant pack, between thermocouples (TCs) 3 and 9, as this region was unaffected by boundary effects (further discussed in Section 3.3.1). The smouldering front propagation velocities were calculated by averaging all local velocities (i.e., distance between successive thermocouples divided by time of arrival of the front), following the method of Pironi et al. (2009). A moving average of 2.7 and 1.7 min was applied to the mass loss data and the calculated mass loss rate, respectively, to reduce minor random noise in the mass balance data.

Additional experiments at very low S/Bs are excluded from Table 3.2 because they represent a failure condition that is expected to be unique to this experimental scale (see Appendix E).

Table 3.2: Input Parameters and Summarized Results for All Experiments

No.	Biosolids Moisture Content (%)		Biosolids Lower Heating Value (kJ/g)		Sand/Biosolids (g/g)		Effective System Lower Heating Value (kJ/g)	Pack Height (cm)	Darcy Air Flux (cm/s)	Self Sustaining?	Average Velocity[1] (cm/min) ±1.9%	Average Peak Temp[1] (°C) ±0.75%	Average Mass Loss Rate[1] (g/min) ±0.31%
	INPUT PARAMETERS										RESULTS		
	Initial	Final	Initial	Final	Initial	Final							
0[a]	74	73	3.0	4.5	4.5	4.7	0.52	40.5	3.3	SS	0.41	529	17
1[b]	74	-	2.8	4.5	4.5	-	0.51	34.5	3.3	SS	0.47	555	-
2	80	80	1.6	3.5	3.5	3.5	0.35	40.0	3.3	BSS	0.19	456	12
3	85	80	1.6	2.6	2.6	3.5	0.36	40.0	3.3	SS	0.21	481	13
4	74	74	2.9	4.5	4.5	4.6	0.51	40.0	3.3	SS	0.38	548	18
5	80	79	1.8	4.9	4.9	5.1	0.29	40.0	3.3	SS	0.27	470	10
6	85	83	0.9	5.2	5.2	5.8	0.13	40.0	3.3	NSS	-	-	-
7	74	72	3.2	23	23	25	0.12	40.0	3.3	NSS	-	-	-
8	74	72	3.2	9.9	9.9	11	0.28	40.0	3.3	SS	0.34	467	7
9[a]	80	80	1.6	2.6	2.6	2.6	0.44	37.0	3.3	NSS	-	-	-
10[a]	80	80	1.6	2.6	2.6	2.6	0.44	37.0	8.1	NSS	-	-	-
11	80	80	1.6	2.6	2.6	2.6	0.44	40.0	3.3	NSS	-	-	-
12	85	84	0.8	6.0	6.0	6.5	0.11	38.5	3.3	NSS	-	-	-
13	85	82	1.1	6.5	6.5	7.7	0.13	37.5	3.3	NSS	-	-	-
14	85	83	0.9	7.5	7.5	8.3	0.10	36.0	3.3	NSS	-	-	-
15	74	72	3.2	2.0	2.0	2.2	1.00	40.5	3.3	SS	0.38	612	23
16	74	71	3.5	1.5	1.5	1.7	1.30	39.0	3.3	SS	0.25	657	25
17	83	80	1.6	3.5	3.5	4.1	0.31	35.0	3.3	SS	0.20	456	9
18	83	82	1.1	3.0	3.0	3.1	0.27	35.0	3.3	NSS	-	-	-
19	77	75	2.6	2.0	2.0	2.2	0.82	40.5	3.3	SS	0.19	500	15
20	77	77	2.2	1.5	1.5	1.5	0.87	39.0	3.3	NSS	-	-	-
21	83	83	1.0	4.0	4.0	4.0	0.19	35.5	3.3	NSS	-	-	-
22	77	77	2.2	2.5	2.5	2.5	0.62	37.5	3.3	BSS	0.16	462	12
23	80	76	2.4	3.5	3.5	4.2	0.46	40.0	3.3	SS	0.27	499	12
24[c]	74	73	3.0	4.5	4.5	4.7	0.53	41.5	6.5	SS	0.62	569	25
25[c]	74	72	3.1	4.5	4.5	4.8	0.54	42.5	1.6	SS	0.23	481	11
26[c]	83	78	1.9	3.5	3.5	4.5	0.35	38.0	6.5	SS	0.45	495	17
27[c]	83	79	1.7	3.5	3.5	4.3	0.33	38.0	1.6	SS	0.18	391	6
28[c]	83	80	1.5	3.5	3.5	4.0	0.29	36.0	3.3	SS	0.28	482	12
29[c]	83	78	1.9	3.5	3.5	4.5	0.35	37.5	3.3	SS	0.26	441	10

[1] The error accounts for equipment uncertainty.

[a] Virgin biosolids were used for comparative purposes.

[b] No mass loss data is available, the amount of lost water from preheating is assumed negligible.

[c] Experiments are analyzed for carbon monoxide, carbon dioxide, and oxygen volume fractions.

The energy content of the biosolids is a function of MC. The biosolids lower heating value (LHV^b) $\left(\frac{kJ}{g}\right)$ was estimated (Boundy et al., 2011):

$$LHV^b = \left[(1 - MC)xHHV_d^b\right] - \left[MCxL_v\right] \qquad (1)$$

where MC (%) is the biosolids MC and L_v $\left(\frac{kJ}{g}\right)$ is the latent heat of vaporization of water, 2.447 kJ/g at 25°C. The equation demonstrates that as the MC of the fuel increases, the energy content linearly decreases. The *LHV* calculation assumes: (1) complete combustion (i.e., full oxidation of carbon compounds to carbon dioxide and water vapour) (Washburn, 1933), and (2) none of the energy lost during water evaporation/boiling is recovered (Boundy et al., 2011). Neither of these assumptions is true for smouldering; some incomplete combustion is expected (Ohlemiller, 1985; Yermán et al., 2015) and some heat recovery from steam is achieved. Therefore, these values are qualitative, presented to explain the relative change in energy content as biosolids MC changes.

The energy content of a unit mass of sand and biosolids mixture depends on the S/B in addition to the MC of the biosolids. The effective system lower heating value (LHV_e^s) is here estimated:

$$LHV_e^s = \frac{LHV^b}{\left[1 + \frac{S}{B}\right]} \qquad (2)$$

The equation reveals that as the amount of fuel dilution by sand increases, the effective energy content of the mixture linearly decreases. Note that LHV^b and LHV_e^s are bulk metrics considering each batch column experiment as a whole. However, it is

acknowledged that individual smouldering column experiments are dynamic systems in which local properties such as MC, S/B, and reaction and condensation zone thicknesses vary in space and in time. Nevertheless, LHV^b and LHV_e^s are considered suitable simple metrics for the purpose of categorizing the differences in the bulk, static energy balance between batches.

The 'initial' and 'final' values provided in Table 3.2 quantify the loss of moisture from the reaction zone prior to ignition during the preheating phase. There were two main sources of losses: (1) evaporation/boiling out of the column top, and (2) downwards water migration into the base of the apparatus and below the heater. These quantities were estimated with the mass loss data: the mass loss observed during preheating was assumed to be water boiling, while the mass remaining after the reaction reached the top of the column (TC13) was assumed to be water remaining below the heater due to early downwards mobilization. A mass balance analysis (Appendix F) indicates that these assumptions are robust and provide a conservative (i.e., low) estimate of the MC in the reaction zone as the front progresses. Table 3.2 reveals that overall the decrease in MC in the biosolids to be treated was $0 - 5\%$, with the higher values in the wettest biosolids/sand mixtures. It is noted that the mass of water below the heater could not be estimated by this method for the NSS and BSS experiments, so only evaporation/boiling was accounted for in those cases. In the Results and Discussion, all reported biosolids MC and S/B values are 'final' values (i.e., corrected for moisture changes occurring after packing) unless specified as 'initial'. In Table 3.2, every LHV^b and LHV_e^s is computed for 'final' conditions.

3.3 Results and Discussion

3.3.1 Definition of Self-sustaining and Non-Self-sustaining Experiments

Figures 3.2 and 3.3 illustrate the temperature profile and mass loss rate over time from a SS and NSS experiment, respectively. Figure 3.2 shows smouldering Experiment No. 4 (Table 3.2) with 74% MC biosolids mixed at 4.6 g/g S/B. Until 34 minutes, the data illustrates the boiling of water out of the 2 cm region closest to the heater (TC1). The boiling region lengthens until 90 minutes when the bottom 2 cm region dried and the temperature rose above 100°C; when it reached 200°C (162 min), the airflow was turned on. In this case, the water boiled during preheating did not leave the column but condensed in upper, cooler regions of the column; this is inferred from the negligible rate of mass loss during the preheating period. The forced airflow ignited the biosolids nearest to the heater, as seen in TC1's sharp increase to 657°C at 167 minutes, at which time the heater was turned off. The smouldering behaviour in Figure 3.2 is identified as SS due to (1) the consistent peak temperatures, here 548°C, as the smouldering front propagates the full length of the column, and (2) the steady rate of mass loss, here 18 g/min in the central portion of the column. This represents the first demonstration of the self-sustaining smouldering of WWTP biosolids.

Consistent boundary effects hold for all SS smouldering experiments. First, an atypically high peak temperature observed at TC1 (and corresponding high mass loss rate) due to excess energy supplied from the heater. Second, a declining mass loss rate as the front thickness shrinks as it approaches the top of the contaminant pack. Thus, only the data between TC3 and TC9 was considered when quantifying the combustion metrics for all

SS experiments. The minimal mass loss from boiling and water migration below the heater in this case, means that the 'final' MC is unchanged from 74% (see Table 3.2). The total mass loss indicated that 98% of the biosolids volatile solids and water within the system was removed over the experiment's duration. The remaining mass is primarily trapped condensed pyrolysate in the top sand cap, and char remaining in a thin layer around the inside wall of the column due to edge effects; it is not associated with remaining biosolids as the sand in the reaction zone was found to be completely clean and dry upon excavation (see Appendix F). The smouldering front propagation velocity was constant at 0.38 cm/min. TC12 and TC13 are in the clean sand cap and TC13 and TC14 are in the air above the column; their low temperatures during the smouldering phase show the extent of energy capture and recycling within the unburned fuel. After the biosolids are destroyed, TC12 and TC13 reveal the forward propagation of the heat wave and convective cooling of the clean, hot sand by forced air.

In contrast, Figure 3.3 illustrates a NSS reaction for Experiment No. 6 (Table 3.2) with 83% MC biosolids mixed at 5.8 g/g S/B. The preheating and ignition characteristics are similar to Figure 3.2. The subsequent declining peak temperatures of 465°C to 319°C from TC3 to TC9 reveals insufficient energy released relative to the heat losses; here the heat losses are considerably increased due to almost doubling the water/dry biosolids mass ratio relative to the SS 74% MC case discussed above. The mass loss rate correspondingly linearly declines from 9 – 5 g/min over this same region, providing additional evidence that the smouldering reaction is dying after ignition. Clearly, biosolids can be smouldered in a self-sustaining manner under some conditions and not others; this parameter space is mapped out in Section 3.3.5 below.
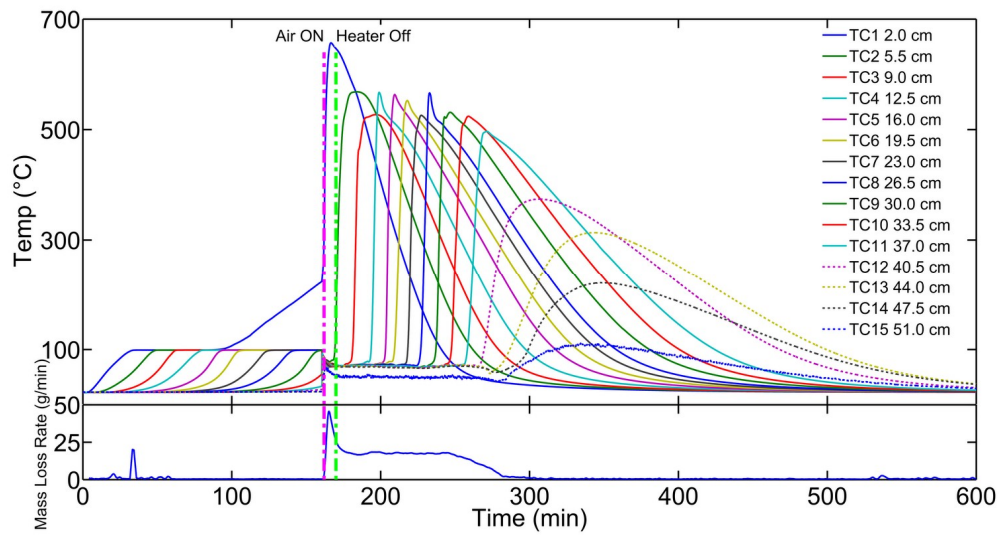
Figure 3.2: Temperature and mass loss rate for Experiment No. 4, a self-sustaining smouldering experiment with 74% moisture content re-wetted biosolids in a fixed bed at a 4.6 g/g sand/biosolids mass ratio. The solid lines represent thermocouples within the contaminant pack.
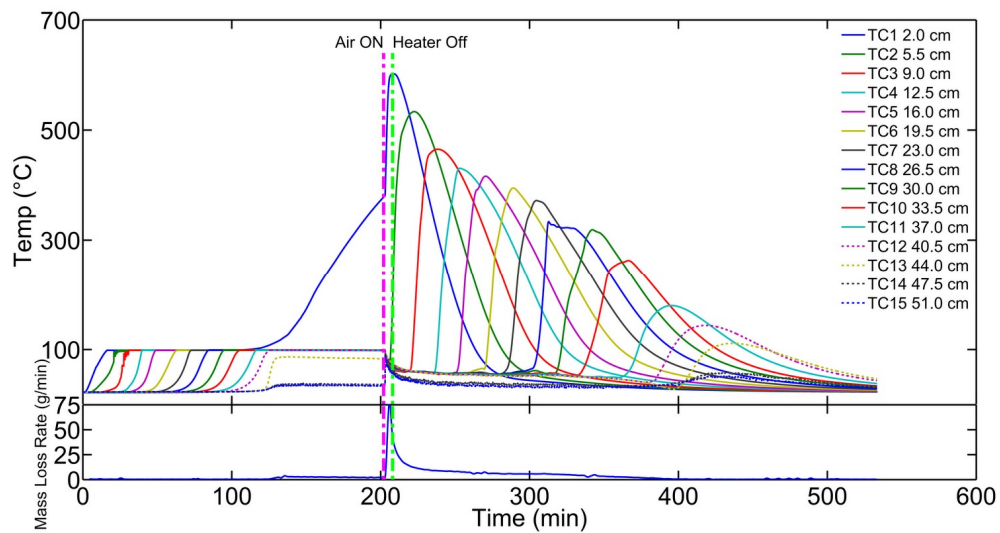
Figure 3.3: Temperature and mass loss rate for Experiment No. 6, a self-sustaining smouldering experiment with 83% moisture content re-wetted biosolids in a fixed bed at a 5.8 g/g sand/biosolids mass ratio. The solid lines represent thermocouples within the contaminant pack.

3.3.2 Comparison between Rewetted Biosolids and Virgin Biosolids

Comparing re-wetted to virgin biosolids experiments indicates that the employed method of re-wetting biosolids does not significantly affect the propagation of a SS reaction, as all of the combustion metrics differed less than 6% (see Experiments No. 0, 1, and 4 in Table 3.2; also see Appendix C for full results). However, when comparing conditions that result in NSS reactions, re-wetted biosolids led to more rapid quenching of the reaction than did virgin biosolids. This is expected to result from the increased downward migration of water towards the smouldering front; recall that re-wetted biosolids had a much higher fraction of free (i.e., mobile) water. Therefore, using re-wetted biosolids in place of virgin biosolids provides meaningful results that are nearly identical to those obtained from virgin biosolids, though re-wetted biosolids likely provide a conservative (i.e., lower MC) estimate of the smouldering quenching limits.

3.3.3 Repeatability of Self-sustaining Experiments

Table 3.3 presents six experiments that explored the repeatability for two SS scenarios: (1) 73% MC biosolids at 4.7 g/g S/B, which is far from the quenching limit, and (2) 79% MC biosolids at 4.4 g/g S/B, which is close to the quenching limit. As these S/Bs were quite similar, the differences between these scenarios are mainly attributed to the increased biosolids MC, which shifted the overall energy balance.

Table 3.3: Combustion Metrics' Variability Far From Quenching (73% Biosolids Moisture Content, 4.7 g/g Sand/Biosolids Mass Ratio) and Near Quenching (79% Biosolids Moisture Content, 4.4 g/g Sand/Biosolids Mass Ratio)

Experiment No.	Quenching Limit Proximity	Average Propagation Velocity (cm/min)	Average Peak Temperature (˚C)	Average Mass Loss Rate (g/min)
0[a]		0.41	529	17
1	Far	0.47	555	-
4		0.38	548	18
Average of 3 Repeats[1]		0.42±12%	544±2.8%	-
31		0.28	482	12
32	Near	0.26	441	10
18		0.20	456	8.6
Average of 3 Repeats[1]		0.25±19%	460±5.1%	10±19%

[a]Virgin biosolids were employed and, due to its strong similarity to the re-wetted biosolids results, it has been included as a repeat.
[1] The 95% confidence intervals between experiments were assumed normally distributed.

The small variability in key combustion metrics suggests the experimental methodology is reproducible. It is noted that the relative variability generally increased slightly with increasing biosolids MC. Overall, it can be concluded that results with greater than 20% change in average propagation velocity and average mass loss rate, and greater than 6% change in average peak temperature, are due to intentionally varied experimental parameters.

3.3.4 Smouldering Propagation Velocity Sensitivity to Air Flux

The smouldering combustion's sensitivity to varying air flux was explored as it can be considered a key operator control parameter for the mass destruction rate and will aid in full scale system design. Figure 3.4 presents the smouldering propagation velocity as a function of air flux far from the quenching limits (73% MC biosolids, 4.7 g/g S/B) and near the quenching limits (79% MC biosolids, 4.4 g/g S/B). The smouldering front

velocity in the 73% MC experiments increased from 0.23 to 0.62 cm/min (2.7 times increase) resulting from increasing the air flux from 1.6 to 6.5 cm/s (4.1 times increase). The 79% MC experiments exhibited slower front velocities from 0.18 to 0.45 cm/min (2.5 times increase) over the same increase in air flux. A linear relationship between the two agrees with smouldering of contaminated soil over a similar range of air fluxes at a comparable scale (Pironi et al., 2009). This suggests that the reaction is oxygen limited over the employed air flux range (Dosanjh et al., 1987; Schult et al., 1996).
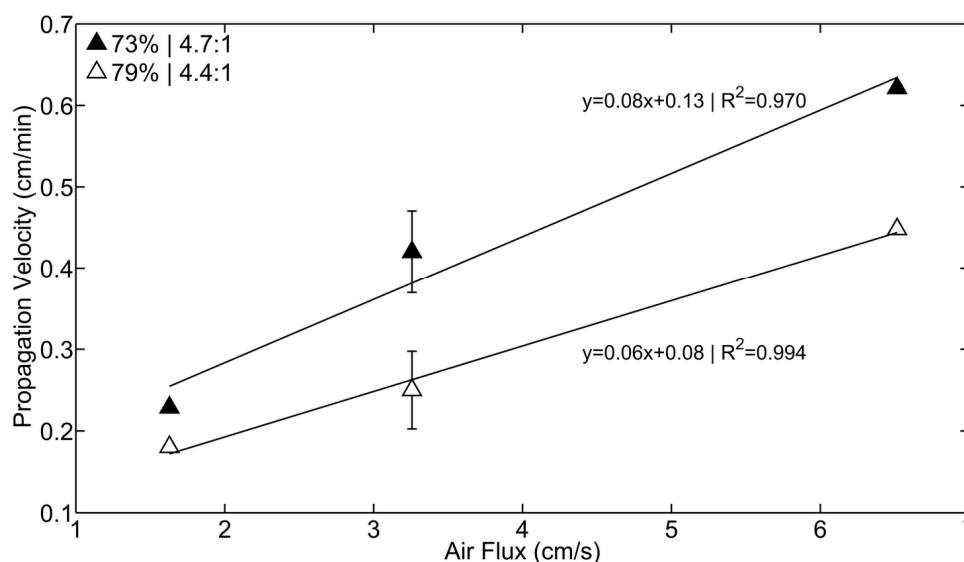
Figure 3.4: Average smouldering propagation velocity as a function of air flux for 73% moisture content biosolids in a fixed bed at a 4.7 g/g sand/biosolids mass ratio (black triangles) and for 79% moisture content biosolids in a fixed bed at a 4.4 g/g sand/biosolids mass ratio (white triangles). The error bars indicate the 95% confidence intervals from three repeat experiments.

3.3.5 Mapping the Self-sustaining Smouldering Parameter Space

Mapping the parameter space in which biosolids facilitate a SS smouldering reaction is important for determining the maximum destruction rate possible and minimum amount

of sludge pre-drying necessary. In Figure 3.5, the vertical axis plots biosolids MC while the horizontal axis considers S/B, as these represent two key system metrics to be optimized. The parameter space map distinguishes between SS (green, square symbols) and NSS (red, triangle symbols) experiments, with a black dashed line approximating the biosolids quenching limits at the column scale. Figure 3.5 reveals first that biosolids with a MC above 70% and up to 80% can be successfully smouldered in a SS manner. This is a novel, important result, the consequences of which are further discussed in subsequent sections. Second, it is important to acknowledge that biosolids cannot be smouldered in the absence of mixing with sand (i.e, S/B = 0). In that case, the re-wetted biosolids lack the key permeability and heat retention characteristics provided by the sand. Once sand is added, however, Figure 3.5 reveals that SS smouldering is possible over a wide range of S/B ratios and that the chosen S/B influences the biosolids MC that can be smouldered.

To aid analysis and discussion, the parameter space is divided into three regions. In Region I, where there is minimal dilution of the fuel with sand (S/B<3.5 g/g), a linear increase in the MC of the biosolids that can be smouldered is achieved with increasing S/B. Three likely reasons for this are: 1) higher S/B means less biosolids filling the sand pore space, which increases the surface area available for smouldering combustion; (2) increased permeability to air, which decreases the pressure drop across the column and decreases air pore velocities thus increasing the oxygen residence time through the reaction zone; and (3) increased effective heat capacity (sand plus biosolids) in the drying zone, which promotes heat retention and mitigates heat losses ahead of the smouldering front.

In Region II, where fuel dilution by sand is intermediate (3.5 g/g<S/B<11 g/g), a plateau at approximately 80% biosolids MC is observed above which SS smouldering is not possible regardless of further increases in the amount of sand (Figure 3.5). The LHV^b – which is constant for a given MC and independent of S/B (see Equation 1) – governs the SS/NSS divide in this region. The LHV^b above 80% MC is less than 1.6 kJ/g; for comparison purposes, the LHV of wood with 10 – 60% MC is 17 – 8.4 kJ/g, respectively, and for charcoal with 1 – 10% MC is 32 – 25 kJ/g, respectively (Quaak et al., 1999). It is expected that the heat losses in the system, primarily due to the large fraction of water when biosolids MC>80%, exceeds the energy produced during smouldering. However, Figure 3.5 reveals that SS smouldering is possible over a large range in this region for MC<80%, with S/B as high as 11 g/g.

Region III, characterized by high fuel dilution by sand (S/B>11 g/g), was explored with only two experiments – Experiments 7 and 8 (Table 3.2) – since it is far from the optimal region for commercial treatment of biosolids. For 72% MC biosolids, it was found that increasing the S/B from 11 to 25 g/g shifted from SS to NSS smouldering, corresponding to a drop in LHV_e^s from 0.28 to 0.12 kJ/g, respectively. The high S/B limit is likely governed by a minimum system energy content value in this range, which is probably a function of the heat losses at a given scale of experimentation (Switzer et al., 2014; Yermán et al., 2015). It is important to note that the LHV_e^s and LHV^b, which provide critical thresholds of SS smouldering in Regions II and III, are not alone able to predict the SS/NNS divide in Region I, as neither account for the complexity of interrelated factors discussed above that cause quenching when the dilution by sand is minimal.

Two BSS (borderline SS) experiments are included on the SS boundary in Region I. These experiments exhibited SS smouldering through 65% of the contaminant pack, but abruptly extinguished leaving un-burnt, wet biosolids above the corresponding height (See Appendix G). It is suspected that these BSS experiments were sensitive to moisture accumulation ahead of the smouldering front due to condensation as observed for smouldering of wet faeces in tall columns (Yermán et al., 2015). This means the lower part of the column was in the SS region but the MC conditions were changing in the upper part of the column so as to leave the SS region, leading to quenching. It is interesting to note the close proximity of SS and BSS Experiments No. 3 and 2, respectively. This suggests that due to experimental variability (e.g., column packing, water redistribution, preheating time, etc.) some slight perturbation on SS reactions near the quenching limits could result in poorly repeatable quenching behaviour.
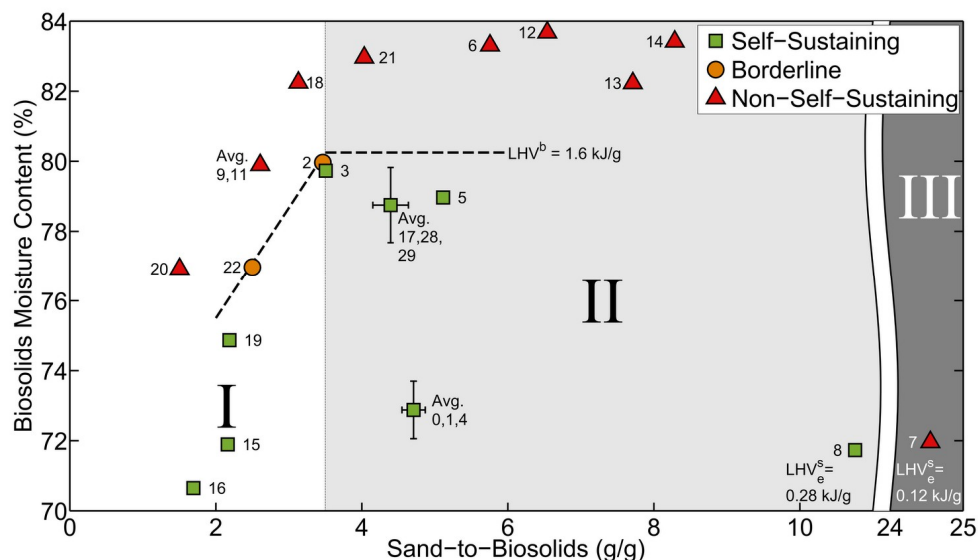
Figure 3.5: Parameter space illustrating the biosolids moisture content and sand/biosolids mass ratio combinations that facilitate self-sustained smouldering at a Darcy air flux of 3.3 cm/s. The error bars denote 95% confidence intervals obtained from three repeat experiments. All relevant experiments are numbered (see Table 3.2) and the three key self-sustaining regions (I, II, and III) are identified in darkening shades of gray for further discussion in the text. The biosolids lower heating value (LHV^b) defining the self-sustaining boundary in Region II is labelled, as well as the effective system heating values (LHV_e^s) for Experiments No. 8 and 7, which define the self-sustaining boundary in Region III.

A potential optimum for operating a biosolids smouldering system is observed at the intersection of the dashed black lines between Regions I and II in Figure 3.5: biosolids with a MC of 80% within a S/B of the mixture of 3.5 g/g (i.e., in the vicinity of Experiment No. 3). This is significant because such high MC biosolids would otherwise require (i) extensive processing (e.g., dewatering, thickening, pre-drying) or (ii) supplemental fuel for disposal in incinerators, and it is these costs that often dominate the disposal operating cost (Werther and Ogada, 1999).

It is noted that this optimal location in Figure 3.5, as well as the region boundaries identified in the figure, are not absolute. These limits are specific to the system variables employed (i.e., scale of experiment, sand grain size and distribution, airflow injection rate, biosolids properties). It is expected that the limits would shift in response to changing system variables. For example, it is known that larger scale systems are more energy efficient because the surface area-to-volume ratio of the reactor is reduced (Switzer et al., 2014). Thus a larger smouldering system may shift the boundary between Region I and II upwards and to the left, since reduced heat losses would allow wetter biosolids to smoulder for the same energy content. The most representative process limits and optimal system conditions should be determined at the pilot scale for a given application (biosolids, sand). Furthermore, it is noted that the boundary between Regions I and II represents both a theoretical and a practical limit on smouldering, since as MC is increased the energy balance is shifted further towards quenching and the boundary identifies where this balance tips. However, the boundary between Regions II and Region III is only a practical limit and not a theoretical limit; theoretically, there is no limit on how much sand dilution can occur since the energy dilution could be compensated for by other factors (e.g., increased airflow rate). Despite all these qualifications, we expect that the optimal location and boundary limits identified in Figure 3.5 are (a) conservative, because this small scale exhibits maximum heat losses, and (b) broadly representative of those expected for smouldering of biosolids; thus, overall it provides an important starting place to support further research and up-scaling.

3.3.6 Smouldering Robustness among Self-sustaining Experiments

Section 3.3.5 had separated all experiments into SS, BSS, and NSS cases; here we discuss the sensitivity of the robustness of the smouldering reaction amongst the SS experiments. This is explored by comparing the mass loss rate and average peak temperatures as a function of both LHV_e^s and air flux in Figures 3.6 and 3.7, respectively. The SS reactions that are most robust, or least sensitive to quenching, are expected to exhibit the highest average peak temperatures and highest mass loss rates (Yermán et al., 2015).
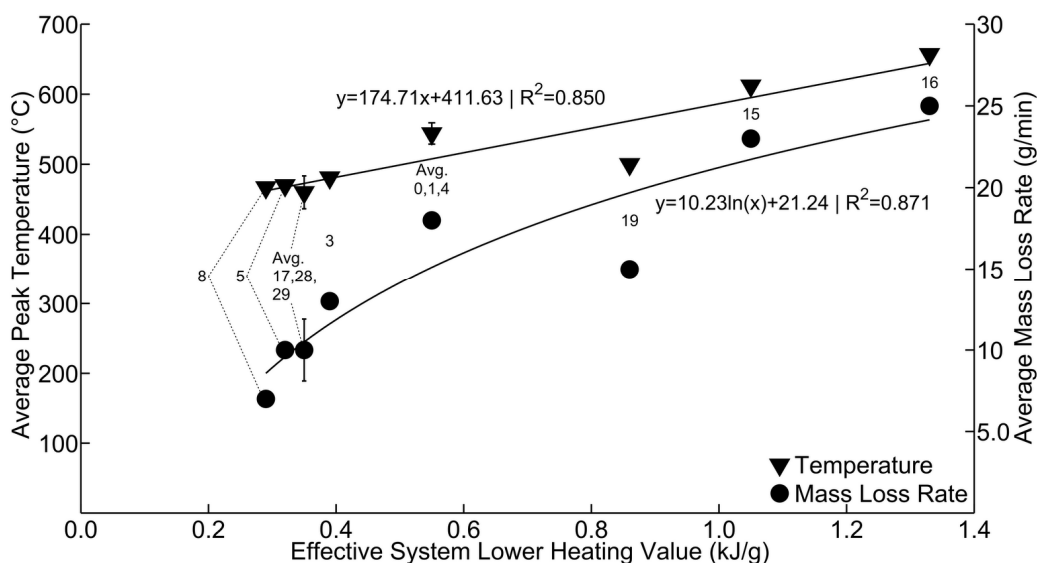
Figure 3.6: The average peak temperatures (downward triangles) and average mass loss rate (circles) from self-sustaining experiments versus effective system lower heating value. All experiments were completed with a Darcy air flux of 3.3 cm/s. The error bars indicate the 95% confidence intervals from three repeat experiments and all experiments are numbered (see Table 3.2) for further discussion in the text.
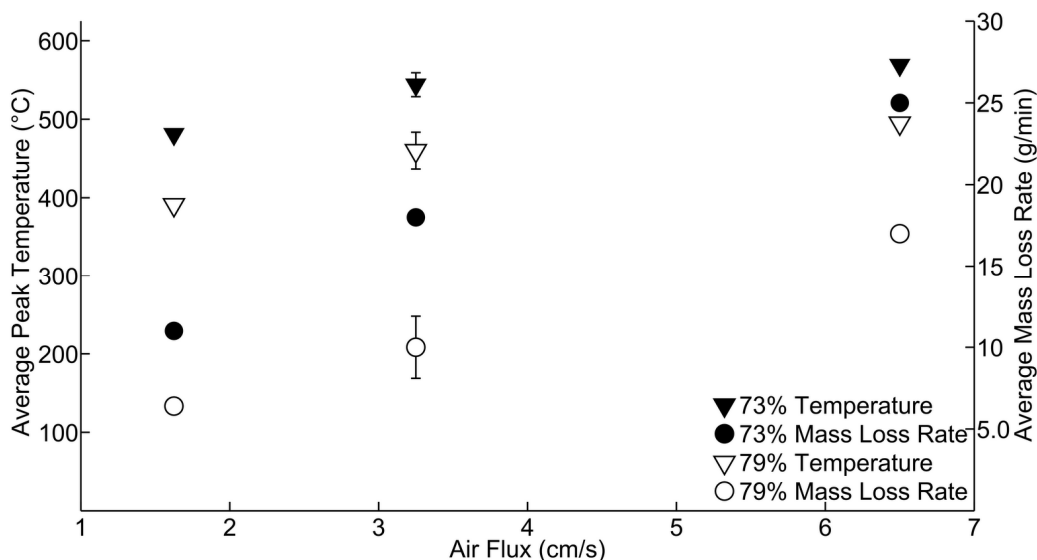
Figure 3.7: The average peak temperatures (downward triangles) and average mass loss rate (circles) from self-sustaining experiments far from the quenching limits (73% MC biosolids, 4.7 g/g S/B) (black) and near the quenching limits (79% MC biosolids, 4.4 g/g S/B) (white) resulting from increasing Darcy air flux. The error bars indicate the 95% confidence intervals from three repeat experiments.

Recall that LHV_e^s is a measure of the energy content of the fuel/sand mixture and depends on both biosolids MC and S/B. Figure 3.6 shows that increasing the LHV_e^s, by decreasing biosolids MC and/or decreasing S/B, linearly increased the average peak temperatures and logarithmically increased mass loss rates for SS experiments. This is due to excess energy driving hotter reactions that, in turn, support faster reaction kinetics. These trends are clearest amongst the SS experiments that lie furthest from the low S/B quenching limits, as defined in Figure 3.5 and Section 3.3.5 above (i.e., Experiments No. 0, 1, 4, 8, 15, and 16). The remaining SS experiments (i.e., Experiments No. 3, 5, 17, 19, 28, and 29) are near the low S/B quenching limits (i.e., near the black dashed lines from Region I and II in Figure 3.5) and exhibit some scatter around the trends in Figure 3.6. In

particular, Experiment No. 19 experienced a unique 'U' shaped peak temperature and mass loss rate profile as the smouldering robustness dropped considerably through the middle 30% of the contaminant pack, which lowered its average peak temperature and mass loss rate (see Appendix G). Overall, it is observed that within the SS set of experiments, there is considerable variability in smouldering metrics. Nearly a four-fold increase in biosolids mass destruction rate is possible, all other operational factors being equal, by maximizing the LHV_e^s of the biosolids/sand mixture.

In Figure 3.7, an increase in smouldering robustness as a function of air flux is observed for the two SS cases, one far from the quenching limits (Experiments No. 0, 1 ,4, 24, 25; Table 3.2) and one near the quenching limits (Experiments No. 17, 26, 27, 28, 29; Table 3.2). For the 73% MC experiments (far from the quenching limits), increasing the air flux from 1.6 to 6.5 cm/s increased the average mass loss rate and average peak temperature from 11 g/min and 481°C to 25 g/min and 569°C, respectively. For the 79% MC experiments (near the quenching limits), the same increase in air flux produced lower mass loss rates and average peak temperatures from 6.4 g/min and 391°C to 17 g/min and 495°C, respectively. The increase in robustness with air flux, especially the logarithmic increase in temperature, is largely due to the increase in the oxygen concentration in the bulk pore space in the reaction zone and associated increase in oxygen flux diffusing into the smouldering fuel surface (Dosanjh et al., 1987; Leach et al., 2000; Yermán et al., 2015). For both cases, the emissions' carbon monoxide/carbon dioxide volume ratio was found to decrease with increasing air flux, indicating a lower fraction of incomplete combustion and providing further evidence of increased robustness (for details see Appendix D) .

This raises the question of to what degree the SS/NSS distinctions identified in Figure 3.5 are a function of the fixed air flux of 3.3 cm/s used in those experiments. Increasing the air flux from 3.3 to 8.1 cm/s did not affect the NSS result in Experiments No. 9 and 10 (80% biosolids MC and 2.6 g/g S/B, Table 3.2) (see Appendix C). As these experiments were quite close to the low S/B quenching limits in Figure 3.5, it is concluded that increasing the air flux will likely not overcome the heat losses in many NSS smouldering cases limiting the ability to significantly stretch the SS parameter space towards the left (i.e., further into the more economical S/B region). Conversely, there is a minimum air flux required for SS smouldering, which, from the SS results in Figure 3.7, is lower than 1.6 cm/s for mixtures either near or far from the quenching limits identified in Figure 3.5. For comparison, Pironi et al. (2011) found SS smouldering achievable in coal tar and sand using an air flux at least 0.5 cm/s and Yermán et al. (2015) found the minimum air flux was a function of sand/faeces mass ratio (S/F), where a SS reaction was achieved with 0.74cm/s when the S/F was at least 3.75 g/g. The minimum air flux has not been explored in this study as it represents an uneconomical condition (i.e., minimum mass destruction rate from Figure 3.7).

This gradation in SS smouldering robustness has important implications when considering the applicability of smouldering as a practical process for WWTPs. Generally, biosolids experience temporal variability in properties due to plant conditions, seasonality, weather conditions, etc. (King and Painter, 1986). This variability is expected to shift the sand/biosolids mixture properties (i.e., LHV^b and LHV_e^s) with respect to the quenching limits. Regular monitoring of biosolids key properties (e.g., Table 3.1) would assist in (a) ensuring the system is in the SS region where it is sufficiently robust and can

withstand variations, and (b) balancing proximity to the quenching limits, where the system is most economical (minimum sand, maximum destruction rate). Manipulating the S/B or the amount of biosolids pre-drying would be cumbersome in response to property changes. Manipulating the air flux may be the most straightforward tool for increasing the smouldering's robustness near the quenching limits. However, the limits of this approach need to be fully understood (Sato and Sega, 1985). It is noted that the column scale is the most challenging for testing smouldering, since the surface area to volume ratio – and thus heat losses – are maximized (Switzer et al., 2014). This means the results presented are likely highly conservative relative to a full scale application. In other words, the SS/NSS boundary identified in Figure 3.5 may represent robust smouldering conditions at full scale application where heat losses are minimized. For these reasons, optimization of the system operation and boundaries of the parameter space for treatment at a WWTP should be done at the pilot or full field scale.

3.3.7 Economic Considerations

An economic analysis has been completed to estimate the expected payback period and cost savings for considering STARx as a biosolids treatment retrofit in an existing WWTP. 80% MC biosolids in a 3.5 g/g S/B fixed sand bed was assumed as the most economical condition for STARx, as identified in Section 3.3.5. Operating costs were assumed for a large WWTP similar to Greenway, a high capacity plant rated at 150 000 m^3/day influent that produced 45 dry tons/day of biosolids in 2013 (City of London, 2014). Cost savings associated with replacing either land application or incineration were considered, as these are the most popular disposal methods practiced in Canada (Apedaile, 2001).

Each biosolids disposal option requires a specific sequence of sludge processing steps, or 'processing path', to ensure the waste is in a suitable condition. The biosolids processing path assumed for land application, incineration, and STARx are summarized in Table 3.4 (see Chapter 2 for further discussion on the assumed paths). Land application requires some degree of sludge stabilization to achieve either Class A or Class B biosolids for safe use and, depending on the desired biosolids MC, may also require rigorous thickening and dewatering with polymer addition (U.S. EPA, 1995). Biosolids for incineration do not usually require stabilization but need dewatering and thickening (usually with polymer addition) to reach a final MC between 60 – 85% (U.S. EPA, 2003b). An economical processing path, following the anticipated changes in biosolids properties, was chosen for the biosolids to reach 80% MC biosolids with a LHV^b greater than 1.6 kJ/g, such that it is suitable for treatment by smouldering with the STARx process. This processing path only requires minimal biosolids dewatering and thickening, without polymer addition. Each step in a processing path has a range of reported costs, which depends on many factors including: local equipment, available infrastructure, prior processing, influent characteristics, and plant size (Metcalf and Eddy, 2003). For a given processing path, summing the lowest cost estimates for all steps provides a low-end estimate of the processing path cost, while summing the highest cost estimates provides a high-end processing path cost. Ranges also exist for estimates of the disposal costs per dry ton of biosolids, from which the highest and lowest reported values provide the end-points. Taken together, it is possible to define the envelope of expected costs, from the highest possible processing and disposal costs (high/high), through intermediate cases (high/low, low/high) to the lowest possible total cost for both steps (low/low). The range

of possibilities in combining processing/disposal endpoint costs to define the members of the sensitivity analysis presented below is summarized in Table 3.4.

The expected costs, both the low and the high ends of the reported ranges, for all biosolids processing steps and disposal options are summarized in Table 3.5; here all costs are independent of previous processing steps. These estimates of operating and capital costs were obtained primarily from United States Environmental Protection Agency technical documents (U.S. EPA, 2000a; 2000b; 2000c; 2000d; 2000e; 2000f; 2000g; 2002; 2003a; 2003b; 2003c; 2006a; 2006b). All costs acquired from older publications were converted to present value using standard US inflation (The World Bank, 2015). Chapter 2 presents a summary of these costs mapped onto a WWTP biosolids processing flow diagram. The STARx operating and capital cost estimates were provided by Savron, the company implementing the technology commercially (G. Grant, Personal Communication, January, 2015). An initial investment of $7.5 million is expected to implement STARx in a WWTP to handle a high biosolids loading and a conservative minimum acceptable rate of return of 15% was used to calculate all discounted payback periods. The capital associated with an incinerator or equipment for land application is neglected since this analysis only considers a WWTP retrofit.

Table 3.4: Processing Pathways and Cost End-Points for Considered Disposal Options

Disposal	Expected Processing Path	Processing Cost Range	Disposal Cost Range
Land Application	Thickening, Polymer Addition, Stabilization, and Dewatering	High / Low	High / Low
Incineration	Thickening, Polymer Addition, and Dewatering	High / Low	High / Low
STARx	Minimal Thickening and Dewatering	Low	Fixed

Table 3.5: Estimated Biosolids Processing and Disposal Cost Ranges

Processing	Disposal	Cost Range ($/dry ton of biosolids)	
	Low	High
Thickening	4.0	0.40
Dewatering	94	260
Polymer Addition	0.0	27.0
Stabilization	14	470
[1] Land Application	91	440
Incineration	100	330
STARx	307	

[1] Land Application costs may be offset up to $80 /wet ton by selling the material as fertilizer (U.S. EPA, 2002), but these savings were neglected due to infrequent practice

Figure 3.8 presents the potential cost savings and losses per day resulting from replacing incineration or land application at a plant with STARx. A sensitivity has been performed on the existing operating costs for each comparison, where high and low costs were assumed for each biosolids processing path and disposal option; the exception is STARx costs (i.e., capital, processing, and disposal) which remained fixed (see Table 3.4 for all cost range assumptions). The discounted payback periods on the initial STARx capital have been included for the profitable cases.

The results in Figure 3.8 suggest that in some cases it may be economical to replace existing disposal methods with STARx. In particular, replacing land application appeared profitable in all cases except where low land application costs and low biosolids processing costs exist. Otherwise, the estimated cost savings using SS smouldering varied from $5 000 to $30 000/ day. Furthermore, the analysis suggests that for large WWTPs experiencing high costs for both land application and biosolids processing, payback for implementing STARx might be on the order of 1 year. This is significant as it suggests STARx may be a profitable retrofit with a very short payback period for a wide spectrum

of WWTPs that currently practice land application. These high savings mainly result from removing sludge stabilization, which is generally quite expensive (Table 3.5).

Replacing incineration with STARx presents opportunity for savings in only one of the four cases: $8 000/day of savings with a discounted payback period of 3 years for a large WWTP currently experiencing high incineration costs with high biosolids processing costs. This suggests STARx may be a profitable retrofit for a much narrower spectrum of WWTPs that currently practice incineration.
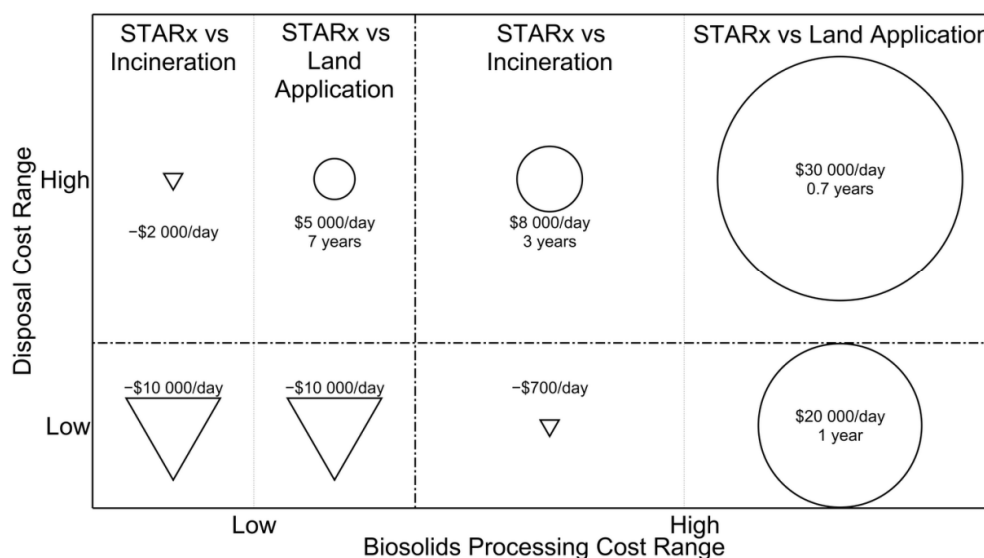
Figure 3.8: Summary of cost/benefit for replacing land application and incineration with STARx in a high capacity WWTP. The figure considers the four cases of whether existing processing and disposal costs are at the high or low end of estimated ranges in Table 3.5. Savings from implementing STARx are graphically represented with a circle, the size of which indicates the magnitude of savings, and the associated text quantifies the savings and discounted payback period on the investment. Losses from implementing STARx are graphically represented with a triangle, the size of which indicates the magnitude of losses, and the associated text quantifies the losses (negative savings).

This economic analysis represents only an initial approximation. Important factors not considered include: (1) Many WWTPs that employ incineration or land application are susceptible to high operating cost variability due to oil and gas price fluctuations. Many incinerators are energy intensive and require fuel for start-up or continuous operation, while land application costs fluctuate due to transportation costs (Wang et al., 2008; Bellur et al., 2009). As STARx employs a SS reaction requiring minimal energy input, its operating costs are much less influenced by fuel price fluctuations; (2) STARx is new and not yet in full scale operation for any waste treatment, therefore costs are only estimates, likely conservative, and are expected to decrease as the technology matures; (3) STARx shows a strong potential for heat energy recovery, either from hot sand or the emissions, which may further offset biosolids processing and operating costs (Yermán et al., 2015); (4) The emissions from smouldering biosolids have not been characterized so the emissions treatment system assumed in STARx's capital and operating cost estimates were taken from a STARx system designed to smoulder liquid hydrocarbon wastes. This assumption may affect the approximated costs either negatively or positively. WWTPs currently practicing incineration may be able to retrofit existing emissions management systems, which would lower STARx's capital cost. Alternatively, the incomplete gaseous products produced from smouldering biosolids may necessitate a more robust/expensive system than that assumed; (5) STARx's quenching limitations are expected to extend at larger scales, which means that higher biosolids MC or lower S/B could be employed. Currently, the analysis assumes an optimized set of conditions taken from column experiments, and these conditions are assumed robust enough to permit normal variation in daily/seasonal plant conditions; (6) The ash management resulting from STARx has

not been considered; this material needs to be characterized and assessed if there is any opportunity for offsetting costs (e.g., fertilizer potential from remaining nitrogen or phosphorous, potential for cement and other construction applications, etc.). Otherwise it will most likely require landfill disposal and increase operating costs (Donatello and Cheeseman, 2013); (7) The maintenance costs have not been fully considered. As there are no examples of full scale implementation of STARx, these costs are difficult to quantify. (8) No salvage or demolition costs were incorporated in the incineration cases.

3.4 Summary and Conclusions

Experimental results indicate that biosolids with MC as high as 80%, with a lower heating value greater than 1.6 kJ/kg, may be successfully smouldered in a self-sustaining manner. This is significant as WWTP disposal methods often require expensive dewatering, thickening, and conditioning processes to reduce the biosolids MC significantly below this value prior to disposal. The biosolids need to be mixed within a fixed sand bed, where sand/biosolids mass ratios from 1.7 to 11 g/g lead to self-sustaining smouldering, even with effective energy contents of the sand/biomass mixtures as low as 0.28 kJ/g. With a sand/biosolids mass ratio between 1.7 and 4 g/g, increasing biosolids MC from 73% to 80% was possible by linearly increasing the amount of diluting sand. Above a sand/biosolids ratio of 4 g/g, the upper biosolids MC limit for smouldering (80%) was independent of the amount of sand added. The exception was an upper limit on the amount of sand that can be added, with smouldering dying when the overall energy of the sand/fuel mixture was diluted to 0.12 kJ/g at a sand/biosolids mass ratio of 25 g/g. These limits are specific to the employed experimental system but are expected to be conservative and broadly representative.

The robustness of the self-sustaining smouldering reaction, as identified by peak temperatures and mass destruction rates, is lowest near the identified quenching limits. However, increasing the effective energy content of the sand/fuel mixtures (e.g., by lowering biosolids MC) and/or increasing the applied air flux both improve smouldering robustness. Increasing air flux also proportionally increased the smouldering front propagation velocity. As air flux can be easily varied by the system operator, this presents a means for controlling the mass destruction rate.

An economic analysis shows that there is significant potential for cost savings from replacing either incineration or land application disposal methods with STARx. The greatest potential was found with replacing land application in a large capacity WWTP that experiences high biosolids processing and land application costs. This resulted in an estimated payback period on the order of 1 year. The least potential was found for replacing incineration, which under the same biosolids processing cost assumptions and high incineration costs resulted in an estimated payback period of 7 years.

This work suggests that smouldering destruction presents significant potential as a new, low energy, on-site alternative method for biosolids management that may provide significant WWTP operating cost savings resulting from minimized biosolids processing and low-end disposal costs. This is a new, beneficial environmental application of smouldering in addition to destroying liquid industrial waste and faeces treatment for sanitation as previously reported. However, further study is required before it can be fully exploited. For example, exploration into the characteristics of the resulting ash, emissions analysis, and examining how smouldering is affected by scale of the reactor would be beneficial. Additional research into energy recovery (e.g. from the emissions, from the

hot sand) may provide additional value. Most of these issues would be best addressed in

the implentation of a pilot scale smouldering reactor operated on site at a WWTP.

3.5 References

Apedaile, E. (2001). A perspective on biosolids management. *The Canadian Journal of Infectious Diseases, 12*(4), 202.

ASCE. (2013). America's Infrastructure Report Card for 2013. *Wastewater.* Retrieved June 6, 2015, from http://www.infrastructurereportcard.org/wastewater/

Bellur, S. R., Coronella, C. J., & Vásquez, V. R. (2009). Analysis of biosolids equilibrium moisture and drying. *Environmental progress & sustainable energy, 28*(2), 291-298.

Bolong, N., Ismail, A., Salim, M. R., & Matsuura, T. (2009). A review of the effects of emerging contaminants in wastewater and options for their removal. *Desalination, 239*(1), 229-246.

Boundy, R., Diegel, S. W., Wright, L., & Davis, S. C. (2011). *Biomass Energy Data Book* (4th ed.). Oak Ridge, U.S.: U.S. Department of Energy, Energy Efficiency and Renewable Energy

Chirag, K., Vijay, K., Raghavan, V., & Rangwala, A. (2011). Smoldering Combustion of Biomass Particles. *Journal of Applied Sciences, 11*(10), 1862-1866.

Cui, H., Ninomiya, Y., Masui, M., Mizukoshi, H., Sakano, T., & Kanaoka, C. (2006). Fundamental behaviors in combustion of raw sewage sludge. *Energy & Fuels, 20*(1), 77-83.

Della Zassa, M., Biasin, A., Zerlottin, M., Refosco, D., & Canu, P. (2013). Self-heating of dried industrial wastewater sludge: Lab-scale investigation of supporting conditions. *Waste management*.

Donatello, S., & Cheeseman, C. R. (2013). Recycling and recovery routes for incinerated sewage sludge ash (ISSA): A review. *Waste management, 33*(11), 2328-2340.

Dosanjh, S. S., Pagni, P. J., & Fernandez-Pello, A. C. (1987). Forced cocurrent smoldering combustion. *Combustion and Flame, 68*(2), 131-142.

Droste, R. L. (1997). *Theory and Practice of Water and Wastewater Treatment*. New York, NY: John Wiley & Sons, Ltd.

Drysdale, D. (2011). Spontaneous Ignition within Solids and Smoldering Combustion *An introduction to fire dynamics* (pp. 512): John Wiley & Sons, Ltd.

Félio, G., Ferreira, B., McNally, C., Robertshaw, R., Andres, R., Siu, K., Buda, M., Thompson, A., Lounis, Z., & CIRC. (2012). Canadian Infrastructure Report Card Volume 1: 2012 Municipal Roads and Water Systems (Vol. 1): The Canadian Infrastructure Report Card.

Frandsen, W. H. (1987). The influence of moisture and mineral soil on the combustion limits of smoldering forest duff. *Canadian Journal of Forest Research, 17*(12), 1540-1544.

Giger, W., Alder, A. C., Golet, E. M., Kohler, H.-P. E., McArdell, C. S., Molnar, E., Siegrist, H., & Suter, M. J. (2003). Occurrence and fate of antibiotics as trace contaminants in wastewaters, sewage sludges, and surface waters. *CHIMIA International Journal for Chemistry, 57*(9), 485-491.

Hadden, R., & Rein, G. (2009). *Ignition and suppression of smouldering coal fires in small-scale experiments.* Paper presented at the 6th Mediterranean Combustion Symposium, Ajaccio, Corsica, France, MCS.

Hale, R. C., La Guardia, M. J., Harvey, E. P., Gaylor, M. O., Mainor, T. M., & Duff, W. H. (2001). Flame retardants: Persistent pollutants in land-applied sludges. *Nature, 412*(6843), 140-141.

He, F., & Behrendt, F. (2009). Comparison of natural upward and downward smoldering using the volume reaction method. *Energy & Fuels, 23*(12), 5813-5820.

He, F., Yi, W., Li, Y., Zha, J., & Luo, B. (2014). Effects of fuel properties on the natural downward smoldering of piled biomass powder: Experimental investigation. *Biomass and Bioenergy, 67*, 288-296.

Howell, J., Hall, M., & Ellzey, J. (1996). Combustion of hydrocarbon fuels within porous inert media. *Progress in energy and combustion science, 22*(2), 121-145.

Khiari, B., Marias, F., Zagrouba, F., & Vaxelaire, J. (2004). Analytical study of the pyrolysis process in a wastewater treatment pilot station. *Desalination, 167*, 39-47.

King, E., & Painter, H. (1986). Inhibition of respiration of activated sludge: variability and reproducibility of results. *Toxicity Assessment, 1*(1), 27-39.

Leach, S. V., Rein, G., Ellzey, J., Ezekoye, O. A., & Torero, J. L. (2000). Kinetic and fuel property effects on forward smoldering combustion. *Combustion and Flame, 120*(3), 346-358.

Metcalf and Eddy. (2003). *Wastewater Engineering: Treatment and Reuse* (4th ed.). New York, NY: McGraw-Hill.

Ohlemiller, T. J. (1985). Modeling of smoldering combustion propagation. *Progress in energy and combustion science, 11*(4), 277-310.

Palmer, K. (1957). Smouldering combustion in dusts and fibrous materials. *Combustion and Flame, 1*(2), 129-154.

Pironi, P., Switzer, C., Gerhard, J. I., Rein, G., & Torero, J. L. (2011). Self-sustaining smoldering combustion for NAPL remediation: laboratory evaluation of process sensitivity to key parameters. *Environmental Science & Technology, 45*(7), 2980-2986.

Pironi, P., Switzer, C., Rein, G., Fuentes, A., Gerhard, J. I., & Torero, J. L. (2009). *Small-scale forward smouldering experiments for remediation of coal tar in inert media* (Vol. 32): Elsevier.

Prat, N., Belcher, C., Hadden, R., Rein, G., & Yearsley, J. (2014). A laboratory study of the effect of moisture content on the spread of smouldering peat fires. *FLAMMA, 5*(1), 35-38.

Quaak, P., Knoef, H., & Stassen, H. E. (1999). *Energy from Biomass: A Review of Combustion and Gasification Technologies* (Vol. 23): World Bank Publications.

Quintiere, J. G., Birky, M., Macdonald, F., & Smith, G. (1982). An analysis of smoldering fires in closed compartments and their hazard due to carbon monoxide. *Fire and Materials, 6*(3-4), 99-110.

Rein, G., Cleaver, N., Ashton, C., Pironi, P., & Torero, J. L. (2008). The severity of smouldering peat fires and damage to the forest soil. *Catena, 74*(3), 304-309.

Rein, G., Lautenberger, C., Fernandez-Pello, A. C., Torero, J. L., & Urban, D. L. (2006). Application of genetic algorithms and thermogravimetry to determine the kinetics

of polyurethane foam in smoldering combustion. *Combustion and Flame, 146*(1), 95-108.

Salman, M., Gerhard, J. I., Major, D. W., Pironi, P., & Hadden, R. (2015). Remediation of trichloroethylene-contaminated soils by star technology using vegetable oil smoldering. *Journal of Hazardous Materials, 285*, 346-355.

Sato, K., & Sega, S. (1985). The mode of burning zone spread along cylindrical cellulosic material. *Journal of Fire Sciences, 3*(1), 26-34.

Schult, D., Matkowsky, B., Volpert, V., & Fernandez-Pello, A. (1996). Forced forward smolder combustion. *Combustion and Flame, 104*(1), 1-26.

Switzer, C., Pironi, P., Gerhard, J., Rein, G., & Torero, J. (2009). Self-sustaining smoldering combustion: a novel remediation process for non-aqueous-phase liquids in porous media. *Environmental Science & Technology, 43*(15), 5871-5877.

Switzer, C., Pironi, P., Gerhard, J. I., Rein, G., & Torero, J. L. (2014). Volumetric scale-up of smouldering remediation of contaminated materials. *Journal of Hazardous Materials, 268*, 51-60.

Ternes, T. A., Joss, A., & Siegrist, H. (2004). Peer reviewed: scrutinizing pharmaceuticals and personal care products in wastewater treatment. *Environmental Science & Technology, 38*(20), 392A-399A.

The World Bank. (2015). *World Development Indicators* [Data file]. Retrieved from: http://data.worldbank.org/country/united-states

Torero, J., & Fernandez-Pello, A. (1996). Forward smolder of polyurethane foam in a forced air flow. *Combustion and Flame, 106*(1), 89-109.

Tyagi, V. K., & Lo, S.-L. (2013). Sludge: A waste or renewable source for energy and resources recovery? *Renewable and Sustainable Energy Reviews, 25*, 708-728.

U.S. EPA. (1994). *A Plain English Guide to the EPA Part 503 Biosolids Rule*: U. S. Environmental Protection Agency.

U.S. EPA. (1995). Part 503 Implementation Guidance (Office of Water, Trans.): U.S. Environmental Protection Agency.

U.S. EPA. (2000a). Centrifuge Thickening and Dewatering (Office of Water, Trans.) (Vol. EPA 832-F-00-053). Washington, D.C.: U.S. Environmental Protection Agency.

U.S. EPA. (2000b). Filter Press, Recessed Plate (Office of Water, Trans.) (Vol. EPA 832-F-00-058). Washington, D.C.: U.S. Environmental Protection Agency.

U.S. EPA. (2000c). In-Vessel Composting of Biosolids (Office of Water, Trans.) (Vol. EPA 832-F-00-061). Washington, D.C.: U.S. Environmental Protection Agency.

U.S. EPA. (2000d). Odor Control in Biosolids Management (Office of Water, Trans.) (Vol. EPA 832-F-00-067). Washington, D.C.: U.S. Environmental Protection Agency.

U.S. EPA. (2000e). Land Application of Biosolids (Office of Water, Trans.) (Vol. EPA 832-F-00-064). Washington, D.C.: U.S. Environmental Protection Agency.

U.S. EPA. (2000f). Alkaline Stabilization of Biosolids (Office of Water, Trans.) (Vol. EPA 832-F-00-052). Washington, D.C.: U.S. Environmental Protection Agency.

U.S. EPA. (2000g). Belt Filter Press (Office of Water, Trans.) (Vol. EPA 832-F-00-057). Washington, D.C.: U.S. Environmental Protection Agency.

U.S. EPA. (2001). Method 1684: Total, Fixed, and Volatile Solids in Water, Solids, and Biosolids (Office of Water, Office of Science and Technology & Engineering and Analysis Division, Trans.): U.S. Environmental Protection Agency.

U.S. EPA. (2002). Use of Composting for Biosolids Management (Office of Water, Trans.) (Vol. EPA 832-F-02-024). Washington, D.C.: U.S. Environmental Protection Agency.

U.S. EPA. (2003a). Gravity Thickening (Office of Water, Trans.) (Vol. EPA 832-F-03-022). Washington, D.C.: U.S. Environmental Protection Agency.

U.S. EPA. (2003b). Use of Incineration for Biosolids Management (Office of Water, Trans.) (Vol. EPA 832-F-03-013). Washington, D.C.: U.S. Environmental Protection Agency.

U.S. EPA. (2003c). Use of Landfilling for Biosolids Management (Office of Water, Trans.) (Vol. EPA 832-F-03-012). Washington, D.C.: U.S. Environmental Protection Agency.

U.S. EPA. (2006a). Heat Drying (Office of Water, Trans.) (Vol. EPA 832-F-06-029). Washington, D.C.: U.S. Environmental Protection Agency.

U.S. EPA. (2006b). Multi-Stage Anaerobic Digestion (Office of Water, Trans.) (Vol. EPA 832-F-06-031). Washington, D.C.: U.S. Environmental Protection Agency.

U.S. EPA. (2014). Water: Sustainable Infrastructure. *Energy Effeciency for Water and Wastewater Facilities*. Retrieved February 16, 2015, from http://water.epa.gov/infrastructure/sustain/sustainable_infrastructure.cfm

Venkatesan, A. K., & Halden, R. U. (2014). Wastewater treatment plants as chemical observatories to forecast ecological and human health risks of manmade chemicals. *Scientific Reports, 4*.

Vesilind, P. A., & Martel, C. J. (1990). Freezing of water and wastewater sludges. *Journal of Environmental Engineering, 116*(5), 854-862.

Wang, H., Brown, S. L., Magesan, G. N., Slade, A. H., Quintern, M., Clinton, P. W., & Payn, T. W. (2008). Technological options for the management of biosolids. *Environmental Science and Pollution Research-International, 15*(4), 308-317.

Washburn, E. W. (1933). Standard states for bomb calorimetry. *J. Res. Natl. Bur. Stand.(US), 10*, 525-558.

WEF. (1988). *Sludge Conditioning, Manual of Practice no. FD-14* Alexandria, VA: Water Environment Federation.

Werther, J., & Ogada, T. (1999). Sewage sludge combustion. *Progress in energy and combustion science, 25*(1), 55-116.

Yermán, L., Hadden, R. M., Carrascal, J., Fabris, I., Cormier, D., Torero, J. L., Gerhard, J. I., Krajcovic, M., Pironi, P., & Cheng, Y.-L. (2015). Smouldering combustion as a treatment technology for faeces: Exploring the parameter space. *Fuel, 147*, 108-116.

Chapter 4

Conclusions and Recommendations

4.1 Conclusions

This thesis explored the potential in using self-sustaining (SS) smouldering as a new method for mass destruction of biosolids from a wastewater treatment plant (WWTP). A suite of lab scale column experiments varied biosolids moisture content (MC), sand/biosolids mass ratio (S/B), and air flux to determine the conditions that cause quenching, and to characterize SS reactions. These experiments were quantified in terms of mass loss rate, peak temperature, and propagation velocity, where a limited number of experiments also quantified the emissions' carbon monoxide/carbon dioxide volume ratio. Following these experimental results, optimal biosolids conditions were assumed for a hypothetical full scale implementation of a smouldering combustion system in a WWTP via Self-sustaining Treatment for Active Remediation applied ex-situ (STARx). The operating and capital costs for this application of STARx were estimated and compared against a range of existing WWTP costs in a rough economic analysis. This analysis approximated the potential payback period and cost savings for replacing an existing WWTP biosolids disposal with a STARx system.

Results suggest that:

- SS smouldering was achieved with biosolids having a MC as high as 80% and an associated lower heating value (LHV[b]) greater than 1.6 kJ/g.

- S/Bs between 1.7 and 11 g/g supported SS smouldering, where three distinct regions were identified that caused quenching. Region I (S/Bs lower than 3.5 g/g) was limited by a combination of reaction surface area, air permeability, and heat capacity of the drying front ahead of the smouldering front. Region II (S/Bs higher than 3.5 g/g and lower than 11 g/g) was limited by a LHV^b of 1.6 kJ/g. Region III (S/Bs higher than 11 g/g) was limited by the system energy content, which may be approximated using the effective system lower heating value (LHV_e^s), as quenching was observed from a LHV_e^s drop from 0.28 to 0.12 kJ/g. The LHV^b and LHV_e^s are bulk metrics used to explain changes in the static energy balance between differing S/B mixtures and do not account for dynamic changes in the systems. Furthermore, Regions I and II represent both theoretical and practical limits, where Region III is only a practical limit. These limits are broadly representative of smouldering in this configuration but are specific to the system variables (e.g., scale, sand grain size, airflow) and can be pushed, to a limited extent, in various directions by changing system variables.

- To maximize the biosolids destruction rate and minimize biosolids processing, a potential optimum condition for smouldering biosolids in a WWTP may be near 80% MC biosolids using a S/B of 3.5 g/g (i.e., smouldering the wettest biosolids with the least amount of sand).

- SS smouldering was most sensitive near the quenching limits. However, increasing the LHV_e^s and air flux increased the reaction robustness (i.e., increased the peak temperatures and associated mass loss rate), where the increasing air flux also linearly increased the propagation velocity. As air flux is an easily

manipulated parameter, it may be an appropriate means for controlling the smouldering sensitivity and mass destruction rate.

- There is potential for cost savings in replacing either land application or incineration with STARx in a large capacity WWTP. A sensitivity on the cost ranges suggested STARx was a profitable replacement for land application, except when replacing low cost land application that required low cost biosolids processing. Conversely, in regards to replacing incineration, STARx was only profitable when replacing high cost incineration that required high cost biosolids processing. The greatest savings potential was found when replacing high cost land application that required high biosolids processing costs, which resulted in a payback on the order of one year.

In summary, SS smouldering presents strong potential as a new, low energy, on-site alternative method for biosolids destruction, which may provide significant WWTP operating cost savings due to minimized biosolids processing and low-end disposal costs. In a broader context, this suggests the exciting usefulness smouldering may provide as a novel waste management technique for many other low calorific/high moisture content organic wastes.

4.2 Recommendations

As this study serves as an initial investigation in introducing SS smouldering as a new biosolids disposal technique in a WWTP, there are many intriguing avenues left for further research.

The following is recommended:

- Characterizing the emissions would be valuable prior to full scale implementation. As smouldering includes some incomplete combustion, the resulting emissions need to be characterized so that proper management is implemented.

- Characterizing the ash may reveal some additional value resulting from smouldering biosolids. For example, the ash may have suitable properties as a fertilizer due to the bioavailability of the phosphorous and possible presence of nitrogen, or value as a concrete additive for construction purposes. Alternatively, this ash will otherwise require disposal and increase operating costs.

- Additional research into energy recovery, either from the hot combustion gases or hot sand, would be very beneficial. For example, this may present a source of heat for partial drying for biosolids and decrease the operating costs.

- Finally, the effect of scale needs to be investigated. The quenching limits identified in this work are strongly influenced by the scale (e.g., significant heat losses out of the column boundaries). Increasing the scale may also increase the robustness of the reaction and shift the quenching limits. A pilot scale study would be most appropriate to investigate this.

Appendices

Appendix A: Supplemental Biosolids Property Measurements

In addition to biosolids ash content, moisture content (MC), and dry higher heating value (HHV_d^b), effective conductivity (K_e) and effective specific heat capacity (Cv_e) have been measured using a handheld thermal analyser (KD2 PRO, Decagon Devices) in Tables A1 to A4. Further details on experimental conditions are available in Table 3.2 (Chapter 3).

Table A1: Various Batches of Biosolids Key Properties

Batch Number[1,2]	Date batch Collected	Relevant Experiments No.	Moisture Content % (g_{water}/g_{total})	Ash Content % (g_{ash}/g_{dry})	Dry Higher Heating Value (HHV_d^b) (kJ/g_{dry})
1[a]	06/02/2014	2 to 8, 12 to18	73.2	18.8	17953
			73.0	18.4	18409
			73.0	18.6	18537
					19937
					17953
					18122
					17307
					16863
					18409
					18075
2[b]	04/06/2014	0,1	73.6	NA	17342
			73.9		16280
			73.8		18071
			74.1		
3	23/10/2014	9 to 11	79.8	NA	17134
			79.6		17205
			79.7		17188
			80.3		
4[c]	16/12/2014	19 to 32	71.9	22.7	NA
			72.0	22.8	
			71.9	22.8	
			71.9	22.9	
			73.0	22.6	
			72.4	22.9	
			72.5	22.8	

[1] All analyses were performed independent of one another and only correspond to the batch number.
[2] A "batch" refers to a large sample (19-120 L) of biosolids collected over the course of a 30 minute period at Greenway Pollution Control Centre.
[a] Multiple HHV_d^b were measured over the course of 20 days from the date of acquisition.
[b] Ash contents measured from Batch 1 were assumed for approximating the migration in self-sustaining
[c] No HHV_d^b was measured, as the range measured from Batches 1 to 4 is assumed representative of the

Table A2: Verification of Thermal Properties and Equipment Comparison

Material	KD2 PRO Sensor	Temp °C	K_e (effective conductivity) W/(m·K)	Cv_e (effective specific heat capacity) MJ/(m³·K)	Error %
Dry biosolids	SH-1	24.45	0.105	0.843	0.0007
Clean sand	SH-1	23.53	0.232	1.196	0.0022
Clean sand	SH-1	23.49	0.233	1.207	0.0021
Clean sand	SH-1	23.16	0.232	1.203	0.0022
Clean sand	SH-1	22.96	0.233	1.204	0.0021
Clean sand	SH-1	22.86	0.232	1.199	0.0021
Dry sand and biosolids	SH-1	23.01	0.217	0.818	0.0027
Dry sand and biosolids	SH-1	23.04	0.220	0.821	0.0027
Dry sand and biosolids	SH-1	22.98	0.220	0.821	0.0027
Dry sand and biosolids	SH-1	22.90	0.221	0.822	0.0027
Dry sand and biosolids	KS-1	22.47	0.188	NA	0.0016
Wet sand and biosolids	SH-1	19.83	1.142	1.690	0.0073
Wet sand and biosolids	SH-1	20.40	1.138	1.689	0.0075
Wet sand and biosolids	SH-1	20.71	1.133	1.686	0.0074
Wet sand and biosolids	SH-1	20.92	1.127	1.680	0.0073
Wet sand and biosolids	SH-1	21.06	1.124	1.677	0.0073
Wet sand and biosolids	KS-1	21.26	0.851	NA	0.0169
Wet sand and biosolids	KS-1	21.33	0.817	NA	0.0179
Wet sand and biosolids	KS-1	21.32	0.812	NA	0.0171

Table A3: Comparison between Measured Thermal Properties and Literature Values

Material Measured	Cv_e MJ/(m³·K)	K_e W/(m·K)	Cv_e from literature [MJ/m³·K]	K_e from literature [W/m·K]
Sand	1.2	0.23	1.2-1.4 (for 0.4-0.3 porosity, respectively)[1]	0.30 (dry sand)[2]
biosolids (dry)	0.84	0.1	2 (assuming wet (75% MC), density =1g/cm3)[3] 0.69-3.1 (dry to 75% MC)[4]	0.30-0.35[5]
biosolids (75% MC)	NA	NA		0.50-0.62 [extrapolated][5]
biosolids (dry) and sand *following Experiment No. 4 conditions*	0.82	0.22	>1.2 (assuming fixed porosity of 0.4)[1,4]	NA
Biosolids (75% MC) and sand *following Experiment No. 4 conditions*	1.7	1.1	1.8 (assuming 75% filled pore space from 0.4)[1,3]	NA

[1](Koorevaar et al., 1983), [2](Oke, 2002), [3](Kim and Parker, 2008), [4](Moffet, 1997), [5](Dewil et al., 2007)

Table A4: Effective Specific Heat Capacity for Multiple Experiments

Experiment No. Initial Conditions	Sand/Biosolids (g/g)	Biosolids Moisture Content (%)	Cv_e MJ/(m³·K)
1	4.5	74	1.557
2	3.5	80	1.859
3	2.6	85	2.217
4	4.5	74	1.557
5	4.9	80	1.704
6	5.2	83	1.575
7	23	74	1.210
8	9.9	74	1.293

Thermogravimetric analysis (SDT Q600, TA instruments) was conducted on dry and 75% MC biosolids in Figures A1 and A2, respectively.
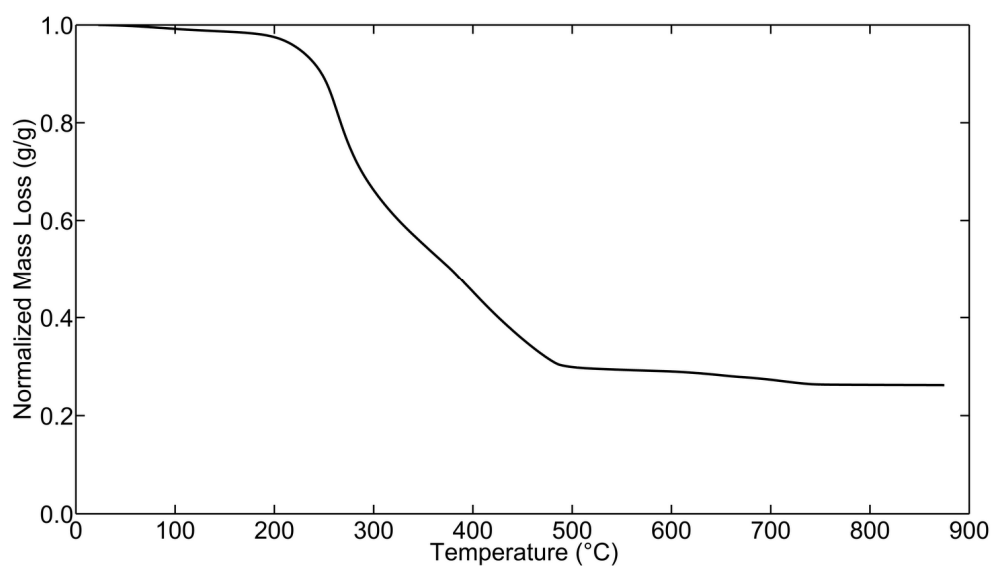

Figure A1: Thermogravimetric data using dry biosolids (>1% MC) in air at 50K/min.
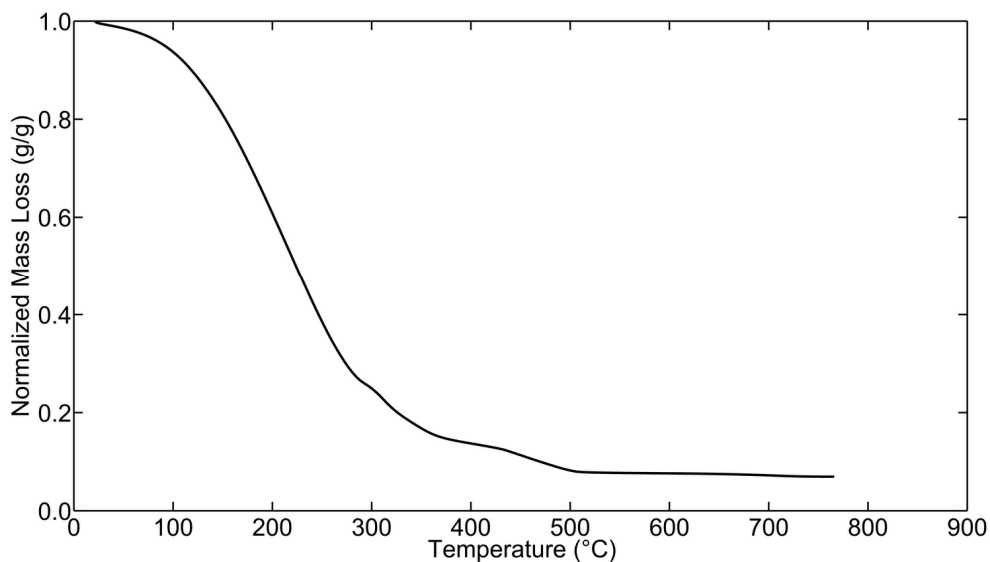
Figure A2: Thermogravimetric data using wet biosolids (74% MC) in air at 80K/min.

References

Dewil, R., Appels, L., & Baeyens, J. (2007). *Improving the heat transfer properties of waste activated sludge by advanced oxidation processes.* Paper presented at the Proceedings of European Congress of Chemical Engineering (ECCE-6), Copenhagen.

Kim, Y., & Parker, W. (2008). A technical and economic evaluation of the pyrolysis of sewage sludge for the production of bio-oil. *Bioresource technology, 99*(5), 1409-1416.

Koorevaar, P., Menelik, G., & Dirksen, C. (1983). *Elements of Soil Physics*: Elsevier Science.

Moffet, C. A. (1997). *Quantity and Quality of Runoff from Two Biosolids-amended Chihuahuan Desert Grassland Soils*: Texas Tech University.

Oke, T. R. (2002). *Boundary Layer Climates*: Taylor & Francis.

Appendix B: Phase Change within Porous Media: A Brief Review

There is a considerable body of research dedicated to observing the movement of moisture via phase change within porous media and its effect on heat transfer mechanisms. Much of the liquid-gas phase change research is separated into either boiling and evaporation applications or condensation applications.

Boiling and Evaporation

Bejan (2004) described the coupling between mass and heat transfer required to quantify the effect of evaporation. The drying rate is related to the vapour pressure and a connection is drawn between heat transfer and drying rates, assuming that the surface of the drying material is saturated:

$$\frac{dW}{dt} = -h_m A(P_s - P_a) \tag{1}$$

$$\frac{dQ}{dt} = hA(T_a - T_s) \tag{2}$$

$$\frac{dW}{dt}L = -\frac{dQ}{dt} \tag{3}$$

$$\frac{dW}{dt} = -\frac{hA}{L}(T_a - T_s) \tag{4}$$

Here, dW/dt is the drying rate, h_m is the moisture transfer coefficient, A is the drying surface area, P_s and P_a are the vapour pressures at the surface and in the atmosphere, respectively, T_s and T_a are the temperatures on the surface and in the atmosphere, respectively, dQ/dt is the heating rate, h is the convective heat transfer coefficient, and L is the latent heat of evaporation.

Moise and Tudose (1998) expanded upon this connection between heat transfer and drying rate to develop the "plug flow and external transfer" model for packed bed of granular materials. Bejan (2013) discussed the heat transfer during nucleate boiling, where nucleate boiling defines the first stage in the boiling process where the temperature difference between T_{sat} and $T_{boiling}$ is $5.0 - 30°C$ (Incropera, 2011). It is suggested that approximating the heat transfer coefficient here is most reliably executed using the correlation presented by Rohsenow (1951):

$$T_w - T_{sat} = \frac{h_{fg}}{c_{P,l}} Pr_l^S C_{sf} \left[\frac{q''_w}{\mu_l h_{fg}} \left(\frac{\sigma}{g(\rho_l - \rho_v)} \right)^{\frac{1}{2}} \right]^{\frac{1}{3}} \tag{5}$$

where all fluid properties are at the saturated temperature, h_{fg} is the heat transfer coefficient during nucleate boiling, T_w and T_{sat} are the wall and saturated temperatures, respectively, $C_{P,l}$ is the liquid specific heat capacity, Pr_l^S is the Prandtl number of the liquid phase, q''_w is the heat transferred to drive the phase change, μ_l is the liquid phase viscosity, σ is the liquid/gas interfacial surface tension, g is gravity and $\rho_l - \rho_v$ is the density difference between the two phases, and C_{sf} is a calibration coefficient and depends on the nature of the heating surface-liquid combination.

Nield and Bejan (2006) summarized a wide body of research regarding the differences between evaporation and boiling driving phase change. Within this summary, an important effect is the boiling process driving convective heat transfer within a porous medium. This phenomenon is mapped by Ramesh and Torrance (1990) as a function of Raleigh Number (Ra) and the dimensionless heat flux at the wall boundary (Q_b) and was found to be predominantly observed in highly conductive systems. Najjari and Ben

Nasrallah (2002) expanded upon this with a numerical study on the boiling with mixed convection in a vertical porous layer. Ruffino and DiMarzo (2004) suggested a simplified approach in describing the impact that evaporative cooling has on a heated surface by using a single heat sink term. This was developed for predicting the effectiveness of fire sprinklers in cooling a hot surface and the heat sink term is presented:

$$\rho_s c_s V_s \frac{dT_s^w}{dt} = hS\left(T_g^w - T_s^w\right) - \rho_l U A \beta \kappa \Delta h \tag{6}$$

where C_s is the specific heat of the sprinkler link, V_s is the volume of the sprinkler link, ρ_s is the density of the sprinkler link, $T_g^w - T_s^w$ is the difference between the gas phase and the wetted sprinkler link temperature, h is the convective heat transfer coefficient, S is the sprinkler link surface area, ρ_l is the liquid density, U is the gas velocity, A is the sprinkler link area orthogonal to airflow, β is the water volumetric fraction, κ is the collection efficiency, and Δh is the latent heat of vaporization.

Condensation

Vafai and Sarkar (1986, 1987) observed the condensation within a porous medium and its effects on heat transfer using a 1 dimensional numerical model. Sözen and Vafai (1990) explored the thermal charging of a packed bed via forced convection of a condensing gas undergoing phase change. The model had assumed thermal non-equilibrium with the vapour and water constituting the fluid phase, and the heat transfer due to the changing fluid phase was proportional to the mass transfer of the vapour to liquid. Al-Nimr and Alkam (1997) also considered a similar mass and heat transfer relation. However, the

mass transfer was a function of T_{sat} and T_s, opposed to vapour pressures, and the method was employed to predict a condensed film's thickness:

$$h_{fg} \frac{d\dot{m}}{dx} = bq_s'' = b \frac{k_{f,eff}(T_{sat} - T_s)}{\delta} \tag{7}$$

Here, $d\dot{m}/dx$ is the mass flow rate along the vertical wall, h_{fg} is the latent heat of condensation, b is the liquid film width, $k_{f,eff}$ is the effective thermal conductivity through the liquid region, q''_s is the surface heat flux, $T_{sat} - T_s$ is the difference between the surface and saturated temperature, and δ is the liquid film thickness.

Practical Approach to Evaporating and Condensation within Porous Media

Packed bed dryers and condensers for food drying, evaporative cooling, air striping, and distillation purposes are major drivers for research surrounding moisture movement and its impact on heat transfer in porous media (Bejan, 2004; Li et al., 2006; Hemis et al., 2011). In particular, it is interesting to contrast the approach that ElGamal et al. (2013) employed against Alnaimat et al. (2011). ElGamal et al. (2013) observed the drying of grains of rice and had established a local thermal non-equilibrium model within the COMSOL environment describing the moisture movement between the solid grains of rice to the gas phase. The model's governing equations were greatly simplified and functions of the relative humidity (H) and rice grain moisture content (M). In addition, validated empirical coefficients dependant on airflow rate for the heat transfer and mass transfer coefficients were employed. Alnaimat et al. (2011) took more classical and rigorous approach to develop a local thermal non-equilibrium model for evaporation and condensation. Here, the heat transfer from evaporation was proportional to the mass

transfer term and dependant on the saturation pressure P_{sat}. An interesting assumption in this model was the constant water saturation term in the evaporation model as it was assumed that the evaporated mass was instantly replaced by trickling liquid into the packed bed. Additionally, the COMSOL literature has also provided significant insight into this problem and suggests solved problems to account for evaporation/boiling and condensation within its environment (Guides; Multiphysics, 2012). In particular, a solved example describing a method to account for property changes and the heat of fusion during the melting of a rod of ice to water provided a very interesting approach to solving phase change problems (COMSOL Multiphysics, 2012). This is completed via simulating the ice as a porous structure where the porosity is filled with water and undergoes $0 \leq \theta \leq 1$ during phase change. Thermodynamic properties such as k_{eff}, C_{peff}, and ρ_{eff} are proportionally affected by this change as they are solved using the volume averaging between the solid and liquid phases. The heat of fusion is accounted for via a step function H(T) from 0 – 1 that is centered on T_{melt} (0°C) and the $\frac{dH}{dT}$ is used to describe the pulse of the phase change (see Figure B1). This method presents a very simple and abbreviated option for modelling phase change as a function of temperature without simultaneously modelling mass transfer, as the function H(T) accounts for the change. Though this approach has only been validated for ice-water, where the aforementioned properties do not undergo drastic differences, it is worthwhile to consider its utility as a straightforward approach to modelling liquid-gas phase change.
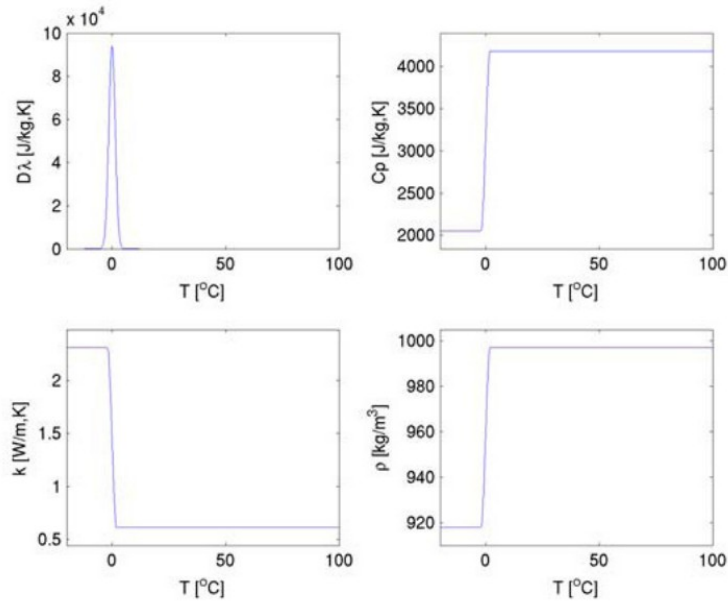
Figure B1: Ice thermodynamic property changes upon melting (COMSOL, 2012).

References

Al-Nimr, M., & Alkam, M. (1997). Film condensation on a vertical plate imbedded in a porous medium. *Applied Energy, 56*(1), 47-57.

Alnaimat, F., Klausner, J. F., & Mei, R. (2011). Transient analysis of direct contact evaporation and condensation within packed beds. *International Journal of Heat and Mass Transfer, 54*(15), 3381-3393.

Bejan, A. (2004). *Porous and complex flow structures in modern technologies*: Springer.

ElGamal, R., Ronsse, F., & Pieters, J. (2013). *Modeling deep-bed grain drying using Comsol Multiphysics*. Paper presented at the COMSOL Conference 2013.

Guides, C. U. Heat Transfer Module. *COMSOL Multiphysics, 3*.

Hemis, M., Singh, C., Jayas, D., & Bettahar, A. (2011). Simulation of coupled heat and mass transfer in granular porous media: application to the drying of wheat. *Drying Technology, 29*(11), 1267-1272.

Incropera, F. P. (2011). *Fundamentals of heat and mass transfer*: John Wiley & Sons.

Li, Y., Klausner, J. F., Mei, R., & Knight, J. (2006). Direct contact condensation in packed beds. *International Journal of Heat and Mass Transfer, 49*(25), 4751-4761.

Moise, A., & Tudose, R. Z. (1998). Air isothermal flow through packed beds. *Experimental thermal and fluid science, 18*(2), 134-141.

Multiphysics, C. (2012). COMSOL Multiphysics User Guide (Version 4.3 a). *COMSOL, AB*.

Najjari, M., & Ben Nasrallah, S. (2002). Numerical study of boiling with mixed convection in a vertical porous layer. *International Journal of Thermal Sciences, 41*(10), 913-925.

Nield, D. A., & Bejan, A. (2006). *Convection in porous media*: springer.

Ramesh, P., & Torrance, K. (1990). Numerical algorithm for problems involving boiling and natural convection in porous materials. *Numerical Heat Transfer, 17*(1), 1-24.

Rohsenow, W. M. (1951). A method of correlating heat transfer data for surface boiling of liquids: Cambridge, Mass.: MIT Division of Industrial Cooporation,[1951].

Ruffino, P., & DiMarzo, M. (2004). The simulation of fire sprinklers thermal response in presence of water droplets. *Fire safety journal, 39*(8), 721-736.

Sözen, M., & Vafai, K. (1990). Analysis of the non-thermal equilibrium condensing flow of a gas through a packed bed. *International Journal of Heat and Mass Transfer, 33*(6), 1247-1261.

Vafai, K., & Sarkar, S. (1986). Condensation effects in a fibrous insulation slab. *Journal of heat transfer, 108*(3), 667-675.

Vafai, K., & Sarkar, S. (1987). Heat and mass transfer in partial enclosures. *Journal of thermophysics and heat transfer, 1*(3), 253-259.

Appendix C: Re-wetted and Virgin Biosolids Comparison

Virgin vs. Rewetted for Self-sustaining Experiments

Figure C1 presents photos contrasting the visual difference between re-wetted and virgin biosolids. Two main differences are the lower fraction of free water (Vesilind and Martel, 1990) and the presence of porosity within the virgin biosolids, where the free water fraction greatly increases and the porosity is completely lost upon re-wetting. Figures C2 and C3 illustrate the temperature, mass loss, and mass loss rate profiles from self-sustaining (SS) smouldering experiments using virgin and re-wetted biosolids, respectively, initially at 74% moisture content (MC) and 4.5 g/g sand/biosolids mass ratio (S/B). Note, that due to preheating and packing process, the biosolids MC and S/B upon ignition vary slightly (see Table 3.2, Chapter 3). For SS experiments, the smouldering propagation is nearly identical between re-wetted and virgin biosolids, suggesting that this method of re-wetting provides analogous results to those expected from using virgin biosolids under the same MC and S/B conditions (see Table C1).

Figure C1: Visual comparison between (1) virgin biosolids resting on top of clean sand and (2) re-wetted biosolids.
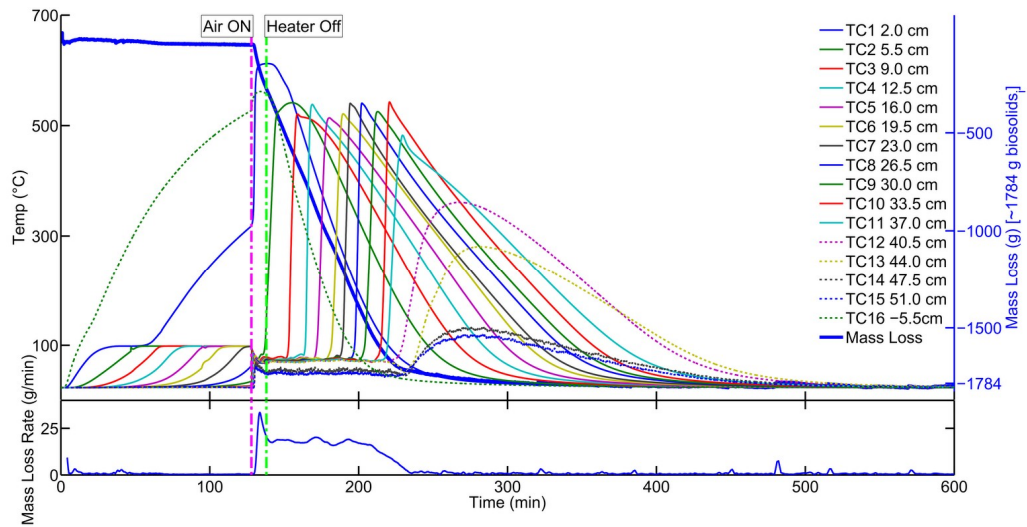
Figure C2: Temperature, mass loss, and mass loss rate profiles for Experiment No. 0, a self-sustaining smouldering experiment with 73% moisture content virgin biosolids in a fixed bed at a 4.7 g/g sand/biosolids mass ratio and an air flux of 3.3 cm/s. The solid lines represent thermocouples within the contaminant pack. The top second y axis (blue) shows the initial volatile solids and water mass in the column, 1784 g.
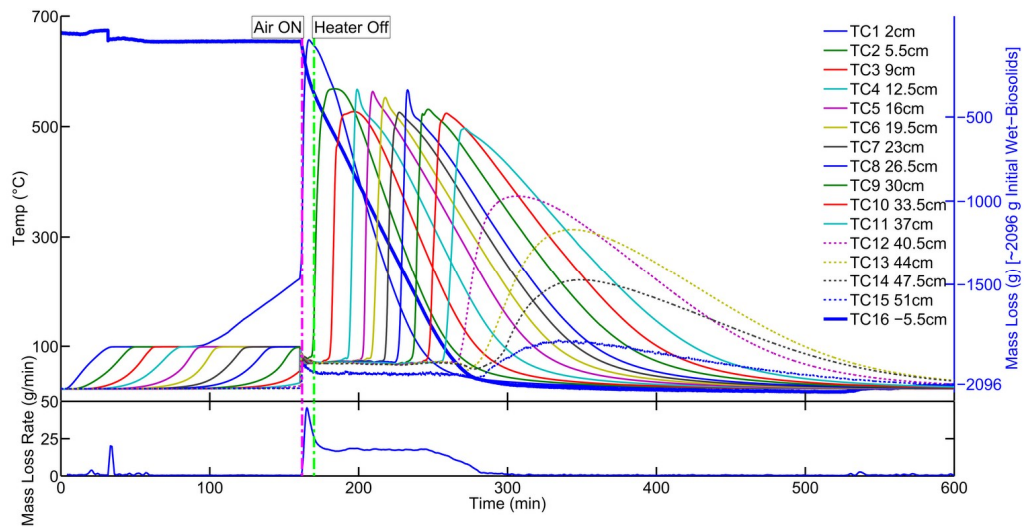

Figure C3: Temperature, mass loss, and mass loss rate profiles for Experiment No. 4, a self-sustaining smouldering experiment with 74% moisture content virgin biosolids in a fixed bed at a 4.6 g/g sand/biosolids mass ratio and an air flux of 3.3 cm/s. The solid lines represent thermocouples within the contaminant pack. The top second y axis (blue) shows the initial volatile solids and water mass in the column, 2096 g.

Table C1: Combustion Metric Comparison between Virgin and Re-Wetted Biosolids

Experiment No.	Virgin or Re-wetted?	Average Propagation Velocity (cm/min)	Average Peak Temperature (˚C)	Average Mass Loss Rate (g/min)
0	Virgin	0.41±25%	529±1.9%	17±0.47%
1	Re-wetted	0.47±9.3%	555±2.2%	-
4	Re-wetted	0.38±14%	548±3.2%	18±0.19%

Virgin vs. Rewetted for Non-Self-sustaining Experiments

Figures C4 and C5 illustrate the temperature, mass loss, and mass loss rate profiles from non-self-sustaining (NSS) smouldering experiments using virgin and re-wetted biosolids, respectively, at 80% moisture content (MC) and 2.6 g/g sand/biosolids mass ratio (S/B). For NSS experiments, the peak temperature and mass loss rate declines are similar between re-wetted and virgin biosolids. However, extinction appears to occur slowest with the virgin biosolids in Figure C5. This is expected to be due to the two main differences identified in Figure C1: (1) the lower fraction of free water caused less water to flow down into the oncoming smouldering front and (2) the presence of biosolids porosity provided greater surface area for reaction and higher air permeability. In support of (1), Figure C4 represents a very short, almost non-discernible temperature plateau just below 100°C at 19 – 20 min at TC16 (-5.5 cm below the heater, see Appendix G for experimental set-up), where Figure C5 has a long temperature plateau at 24 min in TC16 that lasts for 32 minutes. This temperature plateau is due to the water boiling out of this initially dry region, which had migrated down approximately 6 cm from the contaminant pack. As Figure C5 has a much longer temperature plateau than Figure C4, it shows that much more water had migrated downward in this experiment. In summary, this suggests

that using re-wetted biosolids in place of virgin biosolids provides a low estimate of the

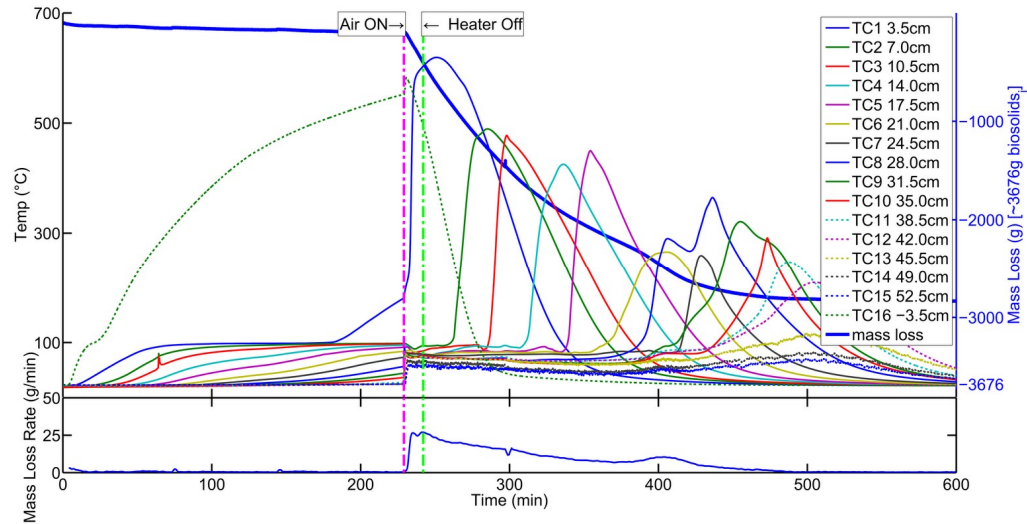quenching limits, as virgin biosolids appear to be more resilient to quenching.

Figure C4: Temperature, mass loss, and mass loss rate profiles for Experiment No. 9, a non-self-sustaining smouldering experiment with 80% moisture content virgin biosolids in a fixed bed at a 2.6 g/g sand/biosolids mass ratio and an air flux of 3.3 cm/s. The solid lines represent thermocouples within the contaminant pack. The top second y axis (blue) shows the initial volatile solids and water mass in the column, 3676 g.
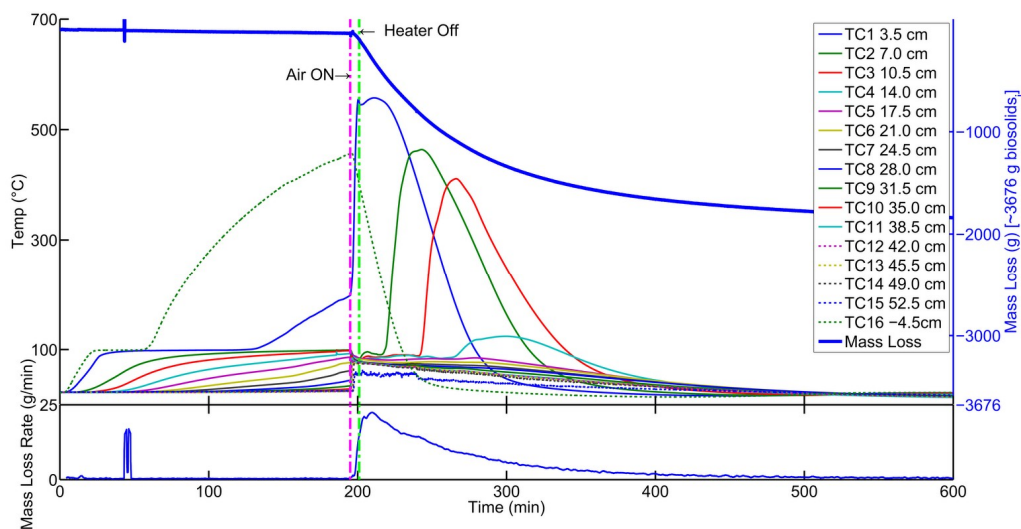
Figure C5: Temperature, mass loss, and mass loss rate profiles for Experiment No. 11, a non-self-sustaining smouldering experiment with 80% moisture content re-wetted biosolids in a fixed bed at a 2.6 g/g sand/biosolids mass ratio and an air flux of 3.3 cm/s. The solid lines represent thermocouples within the contaminant pack. The sum of the masses of volatile solids and water added into the column is noted as the lower boundary on the top second y axis (blue), 3676 g. The disturbance in the mass data at 43 minutes is due to rearranging equipment.

Virgin Non-Self-sustaining Experiment Response to Increased Air Flux

Figure C6 illustrates the temperature, mass loss, and mass loss rate profiles for Experiment No. 10, 80% MC virgin biosolids in a S/B of 2.6 g/g with an air flux of 8.1 cm/s (i.e., the same biosolids MC and S/B as Figure C4, but with a 2.5 times increase in air flux). As Experiment No. 9 in Figure C4 was very near to the quenching limits defined in Chapter 3 (Figure 3.5), it offered an ideal condition to identify if increasing air flux would produce a SS reaction that was otherwise NSS. However, Figure C6 appears to extinguish quicker than Figure C4. This is expected to result from the increased air flux promoting heat transfer away from the smouldering front, opposed to overcoming the heat losses with the increased the oxygen supply (Sato and Sega, 1985). This suggests that increasing the air flux will not significantly extend the smouldering quenching limits

and may actually promote heat transfer away from smouldering front for experiments just beyond the quenching limits.
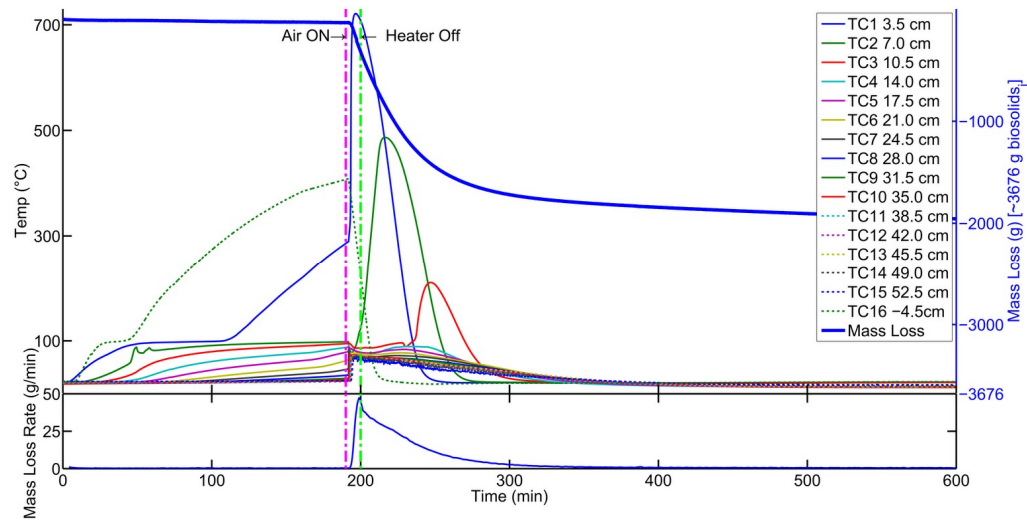

Figure C6: Temperature, mass loss, and mass loss rate profiles for Experiment No. 10, a non-self-sustaining smouldering experiment with 80% moisture content virgin biosolids in a fixed bed at a 2.6 g/g sand/biosolids mass ratio and an air flux of 8.1 cm/s. The solid lines represent thermocouples within the contaminant pack. The top second y axis (blue) shows the initial volatile solids and water mass in the column, 3676 g.

References

Sato, K., & Sega, S. (1985). The mode of burning zone spread along cylindrical cellulosic material. *Journal of Fire Sciences, 3*(1), 26-34.

Vesilind, P. A., & Martel, C. J. (1990). Freezing of water and wastewater sludges. *Journal of Environmental Engineering, 116*(5), 854-862.

Appendix D: Emissions Measurements from Select Experiments

Experiments No. 24 to 29 had measured emissions (i.e., volume % of carbon dioxide (CO_2), carbon monoxide (CO), and oxygen (O_2)) and their profiles are presented in Figures D1 to D6, respectively (details in Experimental Set up and Procedure in Chapter 3). The $CO+CO_2+O_2$ is presented to suggest the % of oxidized emissions that are not accounted for, possibly nitrous oxide (N_2O) (Barton and Atwater, 2002). Table D1 presents the CO/CO_2 results, measured during combustion, where the ascending trend in Experiments No. 24 to 25 and 26 to 27 agrees with the decreasing smouldering robustness discussed in the Results and Discussion section in Chapter 3. There is a lag in the data when the emissions respond to the forced airflow due to the time it took for the emissions to travel through the sampling line. It is important to note that Figures D5 and D6 had used a new batch of drying material to condense potentially damaging constituents within the emissions prior to analysis (98% calcium sulphate and 2% cobalt chloride, Drierite). It is suspected that this new match of material may have tampered the emissions measured in Figures D5 and D6, resulting in a very unsteady $CO+CO_2+O_2$. This has not been explored in detail and Figures D5 and D6 should be viewed cautiously; they are primarily presented to suggest a possible failure in emissions analysis.
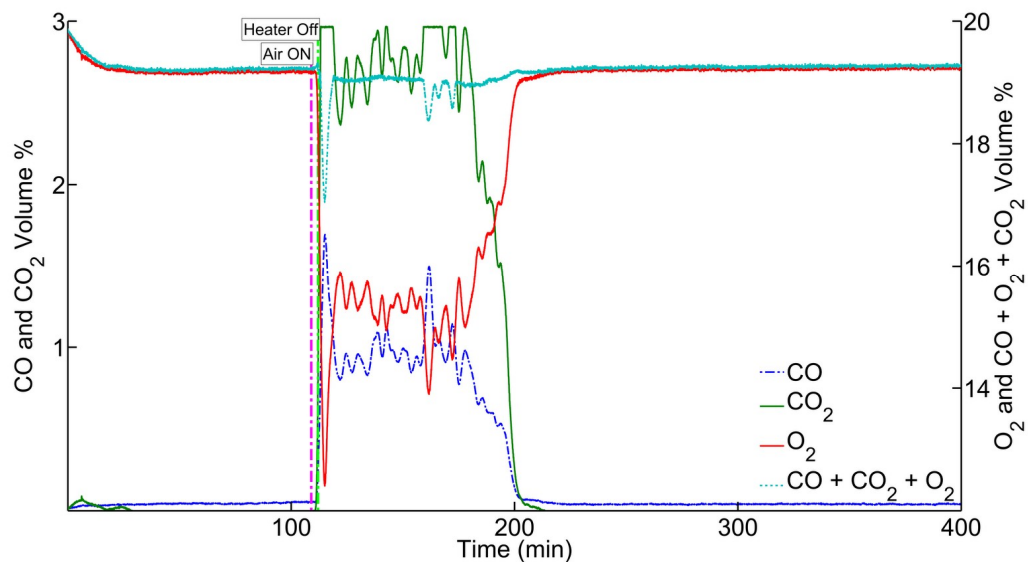
Figure D1: The carbon dioxide (CO$_2$) (solid green), carbon monoxide (CO) (dashed blue), and oxygen (O$_2$) (solid red) volume % for Experiment No. 24. The upper CO$_2$ detection was limited to 3%, which cut off peaks and resulted in the false drops in CO+CO$_2$+O$_2$ (dotted light blue).
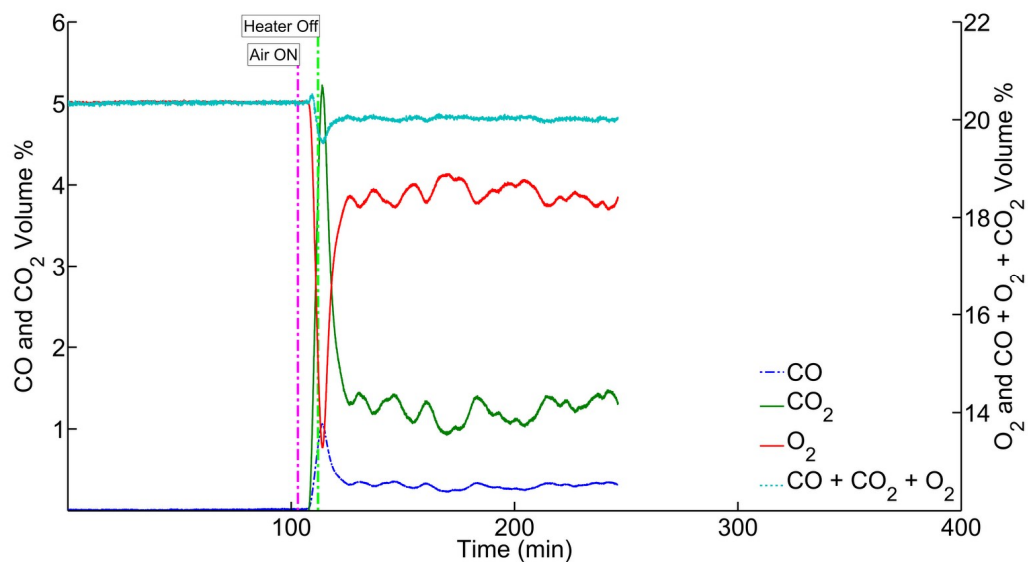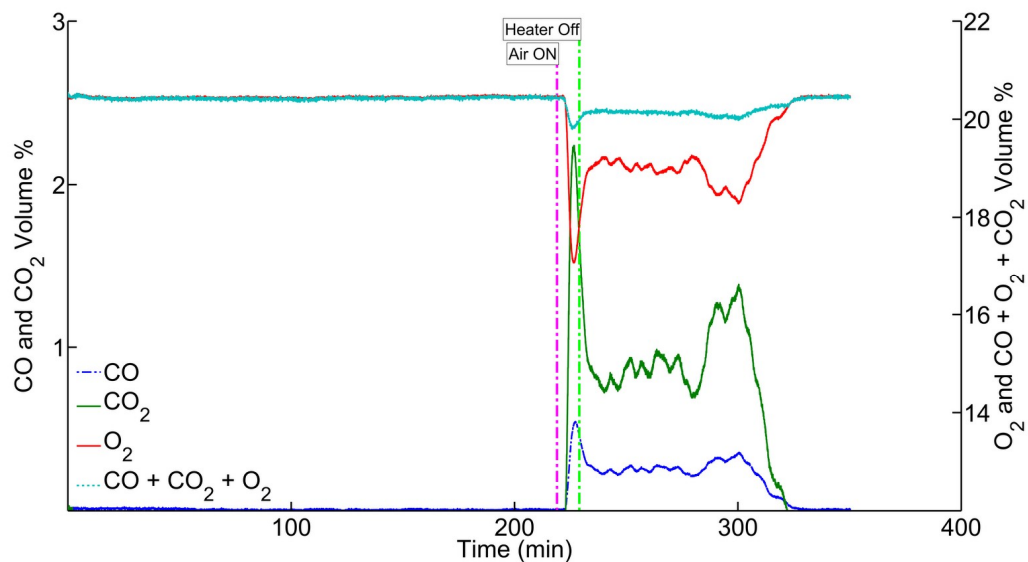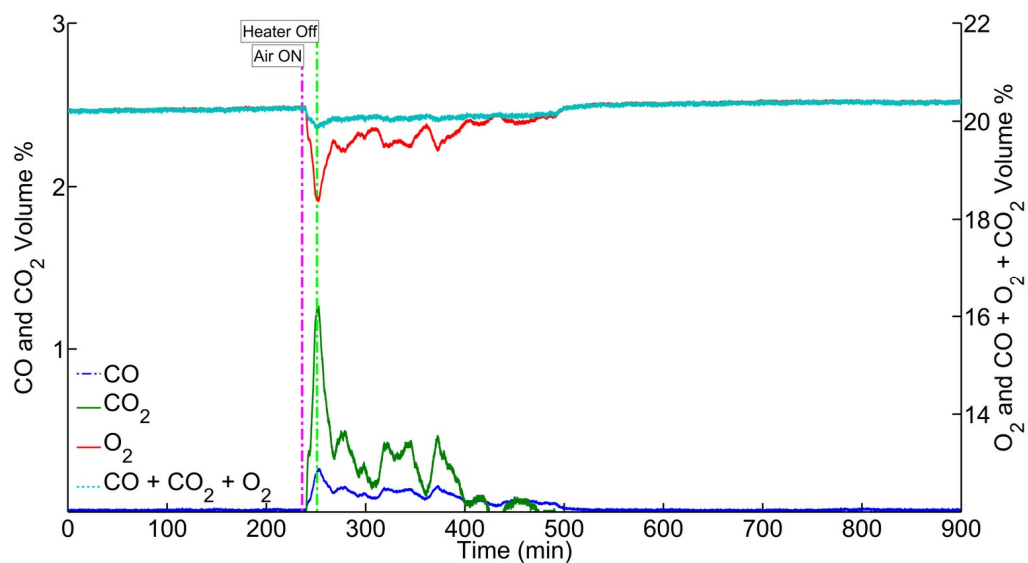

Figure D2: The carbon dioxide (CO$_2$) (solid green), carbon monoxide (CO) (dashed blue), oxygen (O$_2$) (solid red), and CO+CO$_2$+O$_2$ (dotted light blue) volume % for Experiment No. 25.

Figure D3: The carbon dioxide (CO₂) (solid green), carbon monoxide (CO) (dashed blue), oxygen (O₂) (solid red), and CO+CO₂+O₂ (dotted light blue) volume % for Experiment No. 26.

Figure D4: The carbon dioxide (CO₂) (solid green), carbon monoxide (CO) (dashed blue), oxygen (O₂) (solid red), and CO+CO₂+O₂ (dotted light blue) volume % for Experiment No. 27.
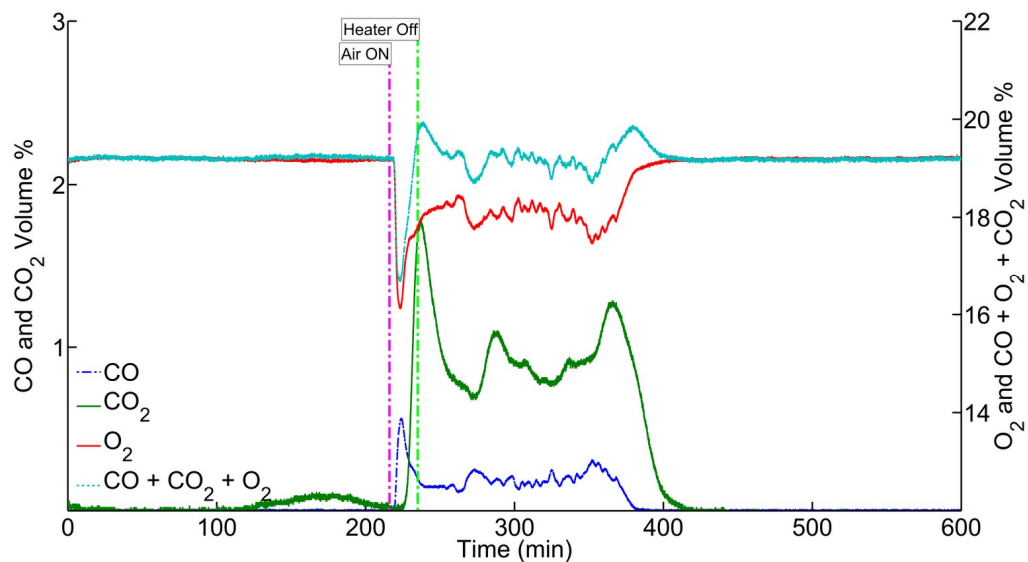
Figure D5: The carbon dioxide (CO₂) (solid green), carbon monoxide (CO) (dashed blue), oxygen (O₂) (solid red), and CO+CO₂+O₂ (dotted light blue) volume % for Experiment No. 28. New drying material was used to dry the emissions prior to analysis, which may have tampered with the emissions measurement
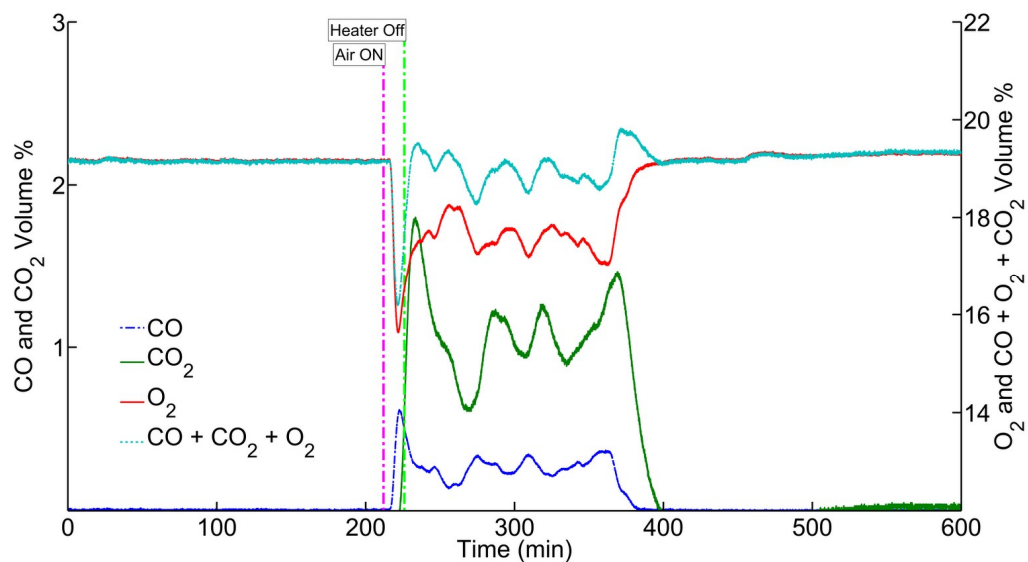

Figure D6: The carbon dioxide (CO₂) (solid green), carbon monoxide (CO) (dashed blue), oxygen (O₂) (solid red), and CO+CO₂+O₂ (dotted light blue) volume % for Experiment No. 29. New drying material was used to dry the emissions prior to analysis, which may have tampered with the emissions measurement.

Table D1: Carbon Monoxide/Carbon Dioxide Measured for Select Experiments

Experiment No.	carbon monoxide / carbon dioxide (% / %)
24	0.010
25	0.013
26	0.028
27	0.031
28[a]	0.025
29[a]	0.017

[a] Values may be unreliable.

References

Barton, P. K., & Atwater, J. W. (2002). Nitrous oxide emissions and the anthropogenic nitrogen in wastewater and solid waste. *Journal of Environmental Engineering, 128*(2), 137-150.

Appendix E: Additional Failure Considerations

Figures E1 to E3 illustrate the temperature profile, mass loss, and mass loss rate profiles from Experiments No. E1 to E3, respectively, which all represent a failure condition, "blow out". Following preheating conditions, the forced air flux was initiated and approximately 50% of the sand and biosolids in Figures E1 and E2 and approximately 30% in Figure E3 were ejected. This is expected to result from the pyrolyzed material formed near the heater clogging the sand pore space and significantly reducing the air permeability (see Figure E4). When the forced air flux was initiated this low permeability caused a pressure build up near the heater that was greater than the weight of the column contents and resulted in a blow out (note the sharp rise in mass and mass loss rate upon air initiation). Initial and corrected biosolids moisture contents (MC) and sand/biosolids mass ratios (S/B) for Experiments No. E1 to E3 are presented in Table E1 and the corrected values are superimposed on the parameter space from Figure 3.5 (Chapter 3) in Appendix F. Lastly, Experiment No. E1 had used slightly finer grained sand (Number 1240S, Bell & Mackenzie Co., mean grain diameter = 0.50 mm, coefficient of uniformity less than 1.50) around the air sparger to promote more uniform air flow. Experiment No. 18 had the same initial conditions as E1, but with coarser grained sand (described in Experimental Conditions in Chapter 3) around the air sparger and resulted in a non-self-sustaining reaction without a blow out. This suggests that the grain size, which is related to the pore size, is involved in the blow out failure condition.
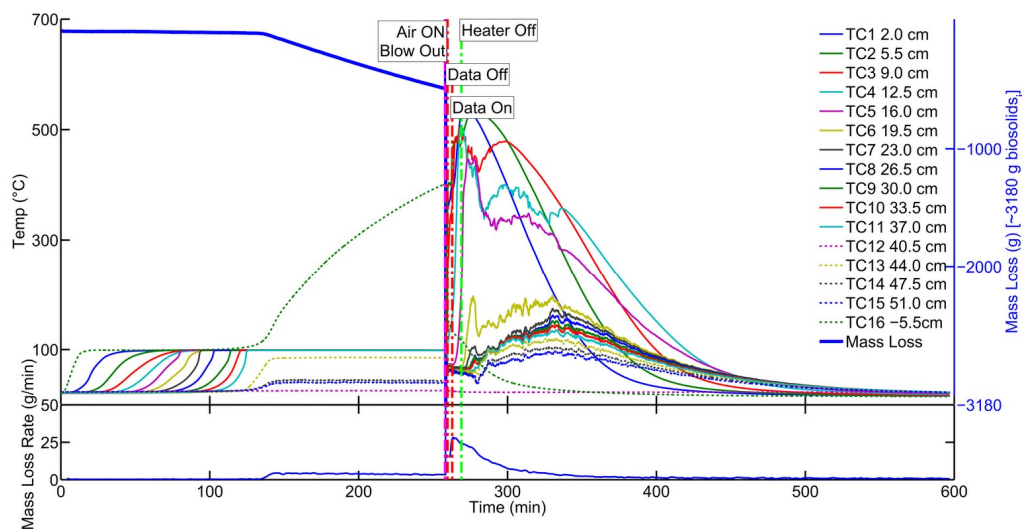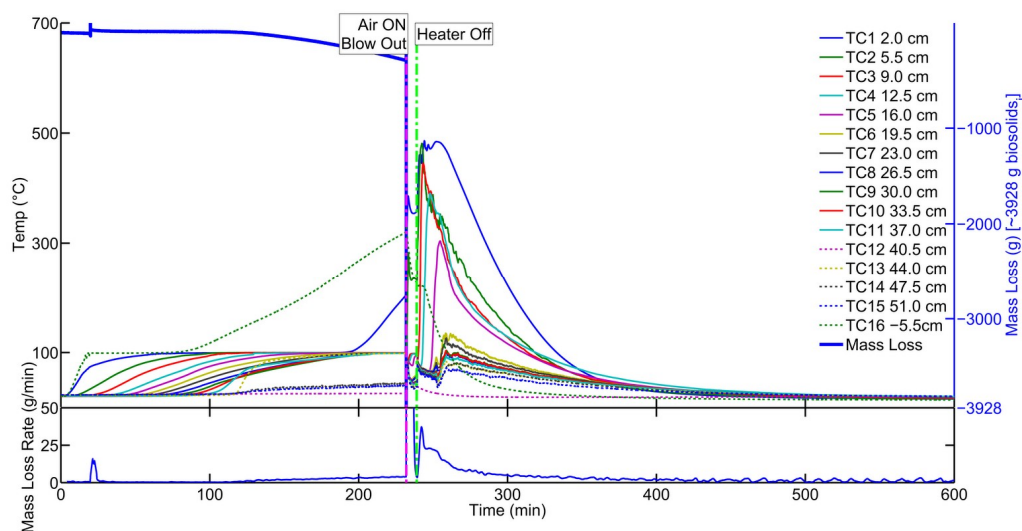
Figure E1: Temperature, mass loss, and mass loss rate profiles for Experiment No. E1, a blow out smouldering experiment with 81% moisture content re-wetted biosolids in a fixed bed at a 3.4 g/g sand/biosolids mass ratio. The solid lines represent thermocouples within the contaminant pack, and the red lines represent when the data logger was turned off in response to the blow out. The left hand main axis shows the initial volatile solids and water mass in the column, 3180 g.

Figure E2: Temperature, mass loss, and mass loss rate profiles for Experiment No. E2, a blow out smouldering experiment with 83% moisture content re-wetted biosolids in a fixed bed at a 2.7 g/g sand/biosolids mass ratio. The solid lines represent thermocouples within the contaminant pack. The left hand main axis shows the initial volatile solids and water mass in the column, 3928 g. The disturbance in the mass data at 20 minutes is due to rearranging equipment.
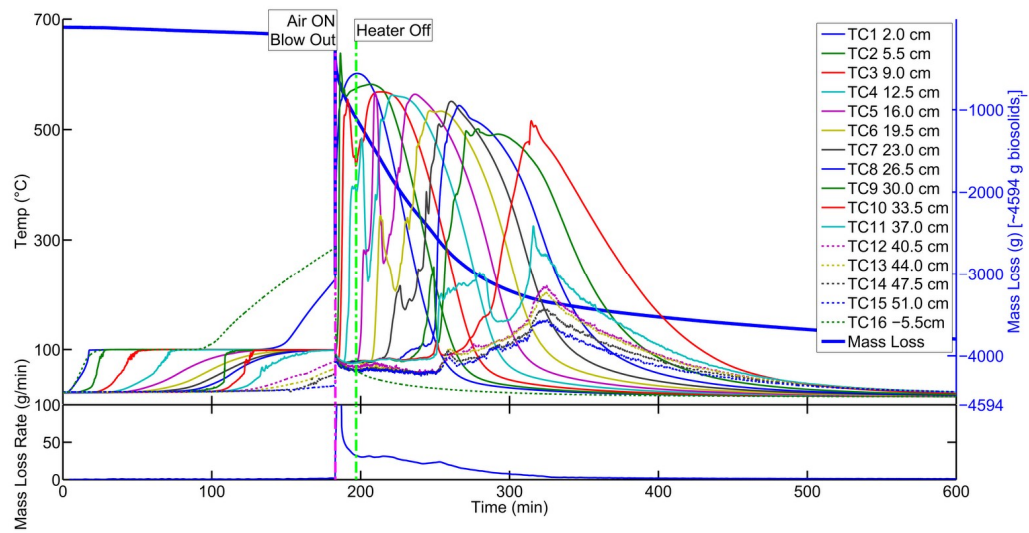

Figure E3: Temperature, mass loss, and mass loss rate profiles for Experiment No. E3, a blow out smouldering experiment with 80% moisture content re-wetted biosolids in a fixed bed at a 2.0 g/g sand/biosolids mass ratio. The solid lines represent thermocouples within the contaminant pack. The left hand main axis shows the initial volatile solids and water mass in the column, 4594 g.

Figure E4: Example photo of the low air permeability crust formed during preheating in Experiment No. 19, which had a very low sand-to biosolids mass ratio but did not blow out.

Table E1: Blow Out Experiments Initial and After-Preheat Conditions

No.	Biosolids Moisture Content % (g_water/g_total)		Biosolids Lower Heating Value (After Preheat) (kJ/g)	Sand / Biosolids (g/g)		Effective System Lower Heating Value (After Preheat) (kJ/g)	Pack Height (cm)	Darcy Air Flux (cm/s)
	Initial	After Preheat		Initial	After Preheat			
E1	83	81	1.37	3.0	3.4	0.31	38	3.3
E2	83	82	1.17	2.5	2.7	0.32	38	3.3
E3	80	80	1.57	2.0	2.0	0.52	40	3.3

Appendix F: Overview of Mass Loss Assumptions

To estimate the corrected biosolids moisture content (MC) and sand/biosolids mass ratio (S/B) after preheating, the mass loss data was used to calculate the amount of water boiled before ignition and remaining below the heater after full combustion. It is noted that very little mass remained after self-sustaining experiments, as the majority of the mixture appeared clean (Figure F1). Figure F2 presents an example of the mass correction superimposed over mass loss data from Experiment No. 29. Experiments No. 27 and 28 had initial false mass readings, so their initial water mass loss was estimated using a boiling mass loss rate of 3.4 g/min, which was estimated by averaging the preheating mass loss from experiments that had identical preheating conditions (Experiments No. 17,26, and 29; Appendix G). Additional details on all experiments are in Table 3.2 in Chapter 3.
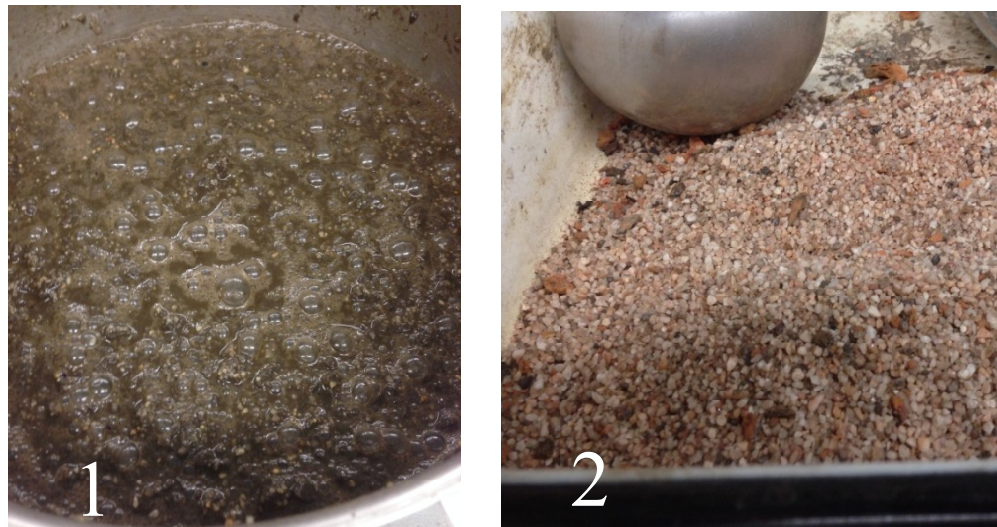

Figure F1: Comparison between (1) mixed sand and biosolids from Experiment No. 16 and (2) a homogenized sample of sand resulting from self-sustaining smouldering after Experiment No. 17. Note the particles larger than the sand in (2) are the biosolids ash.
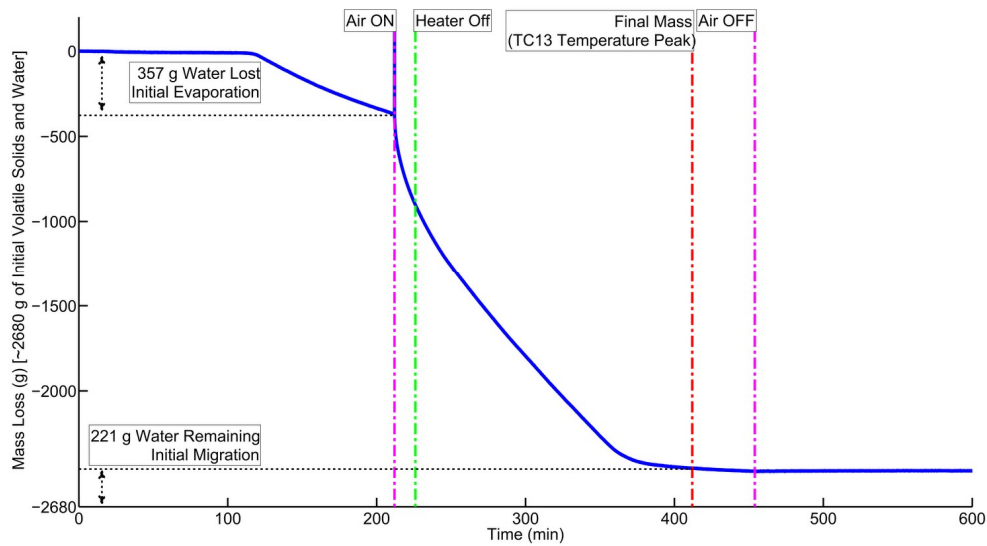
Figure F2: Mass loss from Experiment No. 29, a self-sustaining smouldering experiment with 78% moisture content re-wetted biosolids in a fixed bed at a 4.5 g/g sand/biosolids mass ratio. The sum of the masses of volatile solids and water added into the column is noted as the lower boundary on the y axis, 2680g, and the water lost due to initial boiling and migration downwards is noted on the graph. The air was turned off at 454 min to prevent any water evaporation prior to excavation.

In Figure F2, the initial linear decline in the mass from -10 to -367 g from 119 min until the air flow was turned on (212 min) represents the water boiling out of the column (357 g at 3.8 g/min), driven by the resistance heater. The initial mass loss to -10g is due to rearranging equipment and, as some initial error was present in most experiments, the initial mass reading was always taken after the mass had stabilized (usually near 100 min). The final mass loss (-2459 g) at TC13 peak, the final TC within the sand that denotes the end of full combustion, is 221 g less than the mass of water and volatile solids added to column (2680 g). This remaining 221 g is assumed to be water migrated below the heater during the preheating process, which remained upon excavation. Note the forced air flux was turned off at 454 min to prevent significant evaporation prior to excavation validation of the migration assumption, via a mass balance, and there is an

initial mass spike when the air was turned on due to some low air permeability crust formed around near the heater, which caused an initial increase in pressure and a false spike in the mass data. The initial boiling and migration reduces the biosolids MC from 83% to 78% and raises S/B from 3.5 g/g to 4.5 g/g. It is important to note that these assumptions are not entirely accurate given that: (1) the boiling assumption implies that the early mass loss is exclusively due to boiling water, however, there may be some small amount of initial mass loss due to escaping pyrolysate gas produced near the heater; (2) the migration assumption neglects the char produced due to incomplete combustion around the edges of the column (see Figure F3) and some pyrolysate captured within the top clean sand cap (see Figure F4), which both remained after full combustion.

Figure F3: Top down photo of the pyrolysis char edge formed in Experiment No. 8, a self-sustaining experiment.

Figure F4: Example picture of the top, initially clean sand cap with condensed pyrolysate following full combustion in Experiment No. 29.

Figure F5 illustrates the various zones excavated for a mass balance after Experiment No. 29 to identify where the remaining volatile solids and water persisted after full combustion and Figure F6 presents a photo of the zones. Table F1 presents the results from this mass balance, where the volatile solids and moisture contents are both relative to total mass (i.e., sand, biosolids inert ash, and remaining water/volatile solids). Table F1 which suggests early water migration accounted for 70% of the remaining mass in Experiment No. 29. Table F2 integrates the findings from Table F1 with the mass loss data from Experiment No. 29. It is noted that the unaccounted mass of 1.5% may be due to some small amount of mass lost during sample preparation, prior to packing the column. This mass balance affirms that the initial water boiling and migration assumptions, though not entirely accurate, provide reasonable and conservative approximations for the initial water movement out of the column and present a straightforward method for correcting the biosolids MC and S/B data.
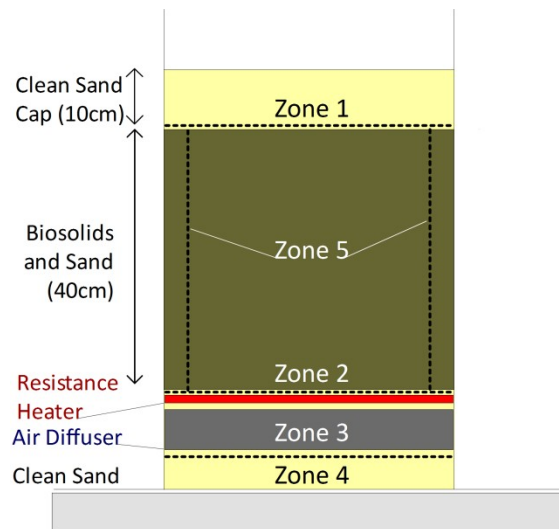
Figure F5: Illustration of the experimental set up with zone numbers labelled for reference to Table F1.
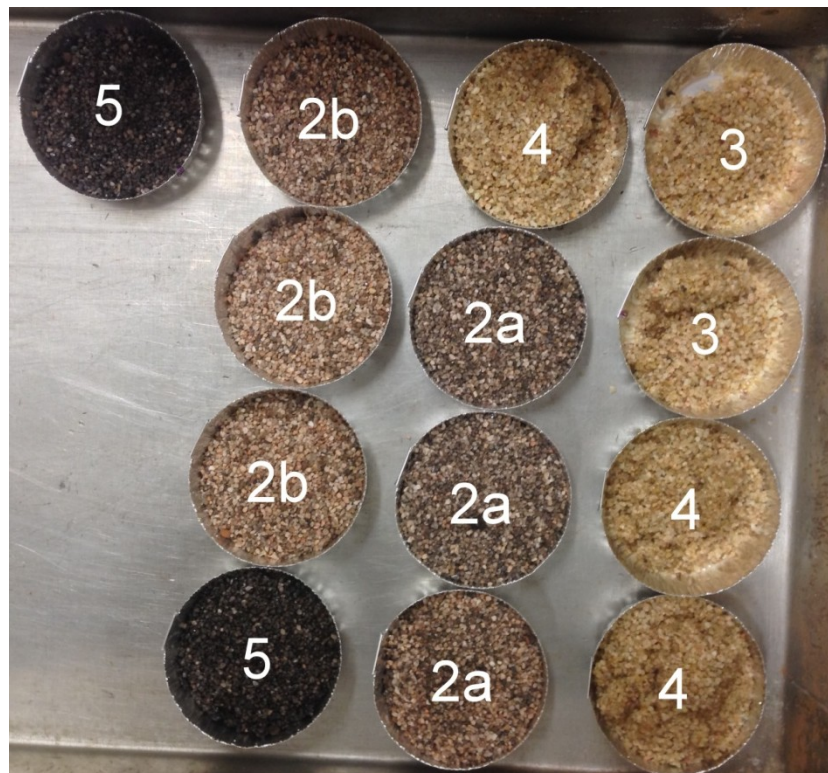

Figure F6: Pictures of the excavated sand and remaining moisture and volatile solids from Experiment No. 29. Each excavated sample has its zone labelled, where 2a represents Zone 2 far from the heater and 2b represents Zone 2 near the heater.

Table F1: Remaining Mass Measured from Experiment No. 29

Section of Column	Sample Initial Weight (g)	Moisture Content (%)	Volatile Solids Content (%)	Total Water (g)	Total Volatile Solids (g)
Initially Clean Top Sand Cap (Zone 1)	2810.6	0.02	0.53	0.7	12.0
Main Contaminant Pack (Zone 2)	10777.2	0.00	0.26	0.0	25.8
Bottom of Contaminant Pack to Air Sparger (Zone 3)	5266.9	0.23	0.19	12.1	8.8
Air Sparger to the Bottom of the Column (Zone 4)	2256.9	5.0	0.29	112.0	9.7
Contaminant Pack Edges (Zone 5)	774.6	0.00	0.77	0.0	4.8
SUM				124.8	54.2

Table F2: Comparing the Mass Balance Results from Table F1 with Mass Loss Date from

Experiment No. 29

Final Mass Loss (g)	Total Remaining Water (Table F1) (g)	Total Remaining Volatile Solids (Table F1) (g)	Initial Water Mass (g)	Initial Volatile Solids Mass (g)	Unaccounted Mass (%)
2459	124.8	54.2	2315	365	1.5

The initial conditions' (i.e., biosolids MC and S/B) variability due to early water boiling and migration have been quantified in Table F3 far from quenching (Experiments No. 4, 24, 25) and near quenching (Experiments. No. 26, 29, 17) (see Results and Discussion and Table 3.2 in Chapter 3 for a full details).

Table F3: Initial Condition Variability Far From Quenching (73% Biosolids Moisture Content, 4.7 g/g Sand/Biosolids Mass Ratio) and Near Quenching (79% Biosolids Moisture Content, 4.4 g/g Sand/Biosolids Mass Ratio)

Experiment No.	Quenching Limit Proximity	Initial Water Boiled (g)	Inferred Water Migration (g)
4		0	28
24		1	94
25	Far	8	126
Average of 3 Repeats		3±164%	83±68%
26		360	260
29		357	255
17	Near	129	311
Average of 3 Repeats		282±53%	275±13%

Though there is significant variability in the initial boiling and migration of water, the variability in the initial conditions is quite low. The variability is due to experimental error from the mixing, packing, and preheating procedures, however, it is expected to be largely governed by the variability in preheating conditions. This is exemplified between Experiments No. 17 and 26, which experienced 129 and 360 g of water boiling and 43 and 96 min of initial preheating time where all TCs were above 98°C (full column boiling), respectively. This full column boiling is significant as it facilitated boiling of water out of the column in these experiments near quenching (see Appendix G). This initial full column boiling drove both the majority of initial boiling and initial migration variability. However, the 95% confidence interval in the biosolids MC and S/B was much lower at 1.1% and 3.4% (far from quenching) and 1.4% and 5.6% (near quenching), respectively. An important conclusion from these results is that with an increase in

moisture content the initial conditions' relative uncertainty does not significantly vary. This means that within this experimental study, greater than 2% change in biosolids MC and 6% change S/B is due to intentionally varying parameters, opposed to experimental variability.

Figures F7a, F7b, and F7c represent the parameter space data points changing upon assuming: (a) no initial boiling or migration, (b) initial boiling but no migration, and (c) initial boiling and migration, respectively. This sequence of figures illustrates the impact that initial water movement has on correctly identifying the smouldering quenching limits where the black dashed lines defining quenching in Regions I and II are kept fixed for reference between parameter space changes. The black lines defining the quenching limits in Regions I and II are drawn closest to the self-sustaining experiments because these data points are fully corrected, as migration could not be estimated for non-self-sustaining or borderline self-sustaining experiments. This implies that the borderline self-sustaining and non-self-sustaining points should actually lie further southeast in Figure F7c. See Results and Discussion in Chapter 3 and Appendix E for further discussion on the parameter space.
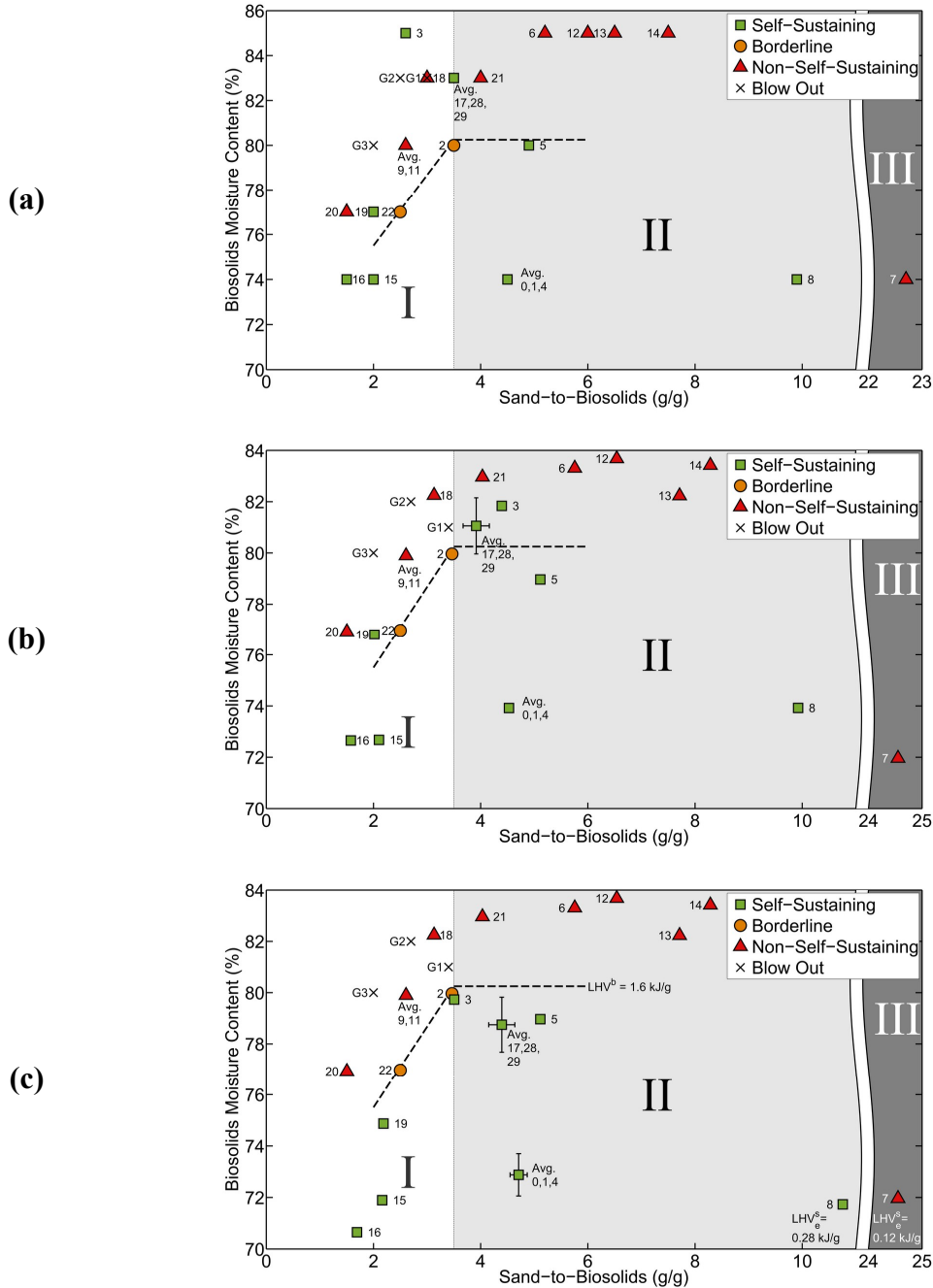
Figure F7: Parameter space illustrating the biosolids moisture content and sand/biosolids mass ratio combinations that facilitates self-sustained smouldering at a Darcy air flux of 3.25 cm/s changing upon: (a) neglecting boiling and migration, (b) neglecting migration, and (c) fully corrected. The error bars denote 95% confidence intervals obtained from three repeat experiments. The quenching limits in Regions I and II (dashed lines) are kept as a reference to compare the data points between F7a, F7b, and F7c. Blow out Experiments No. G1 to G3 are included and all experiments are numbered (see Table 3.2 and Figure 3.3 from Chapter 3 for more details).

Appendix G: Temperature, Mass Loss, and Mass Loss Rate Profiles

All temperature, mass loss, and mass loss rate data, where available, is presented with the

addition of thermocouple data from below the heater (Figure 1) in Figures G2 to G26.

Experiment data not presented here are Experiments No. 0, 4, 9, 10, and 11 (in Appendix

C) and Experiments No. E1 to E3 (in Appendix E). Additional discussion and

information on the presented experiments can be found in Chapter 3.
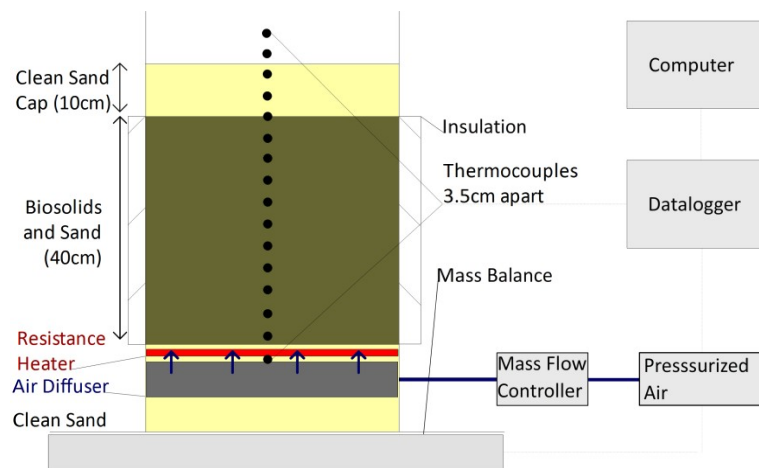
Figure G1: Illustration of the experimental set up with the inclusion of a thermocouple (TC16) below the heater.
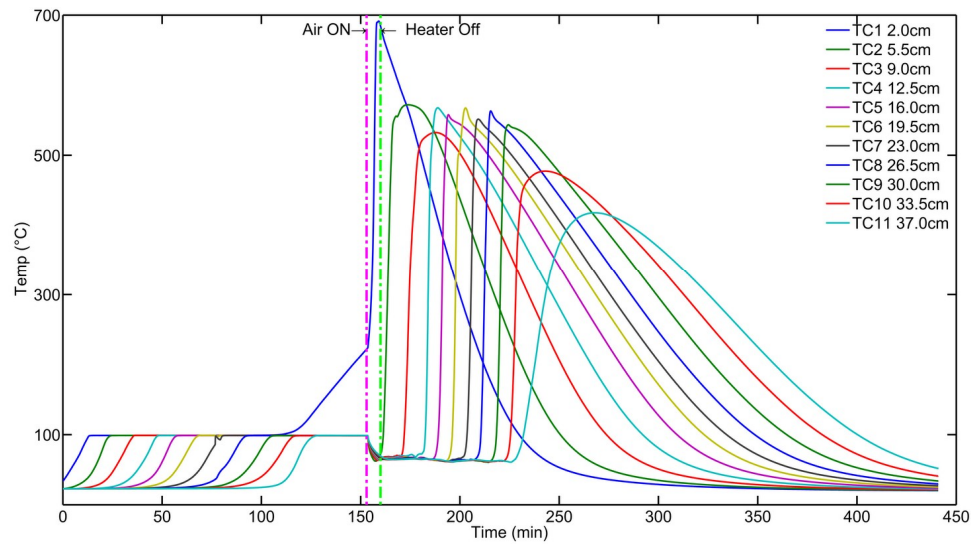
Figure G2: Temperature profile for Experiment No. 1, a self-sustaining smouldering experiment with 74% moisture content re-wetted biosolids in a fixed bed at a 4.5 g/g sand/biosolids mass ratio and an air flux of 3.3 cm/s. All lines represent thermocouples within the contaminant pack.
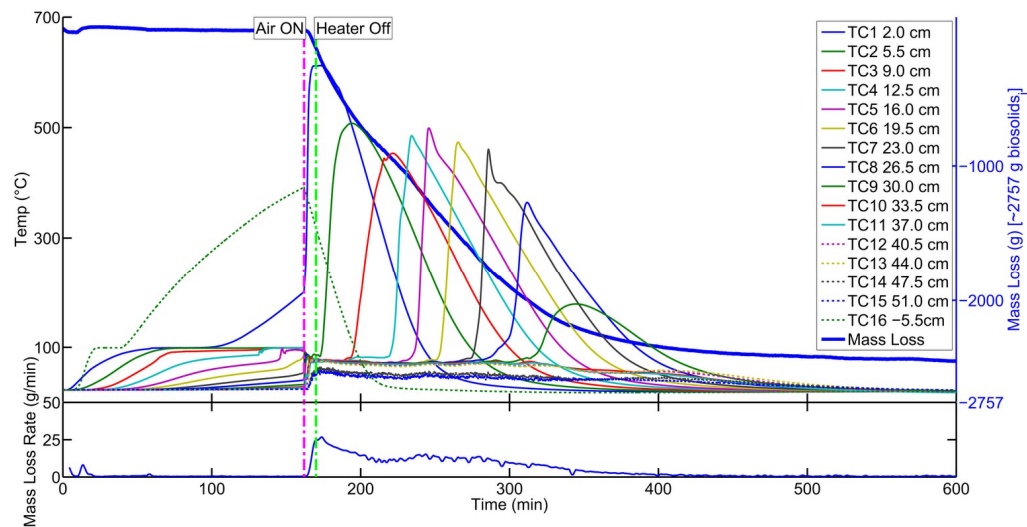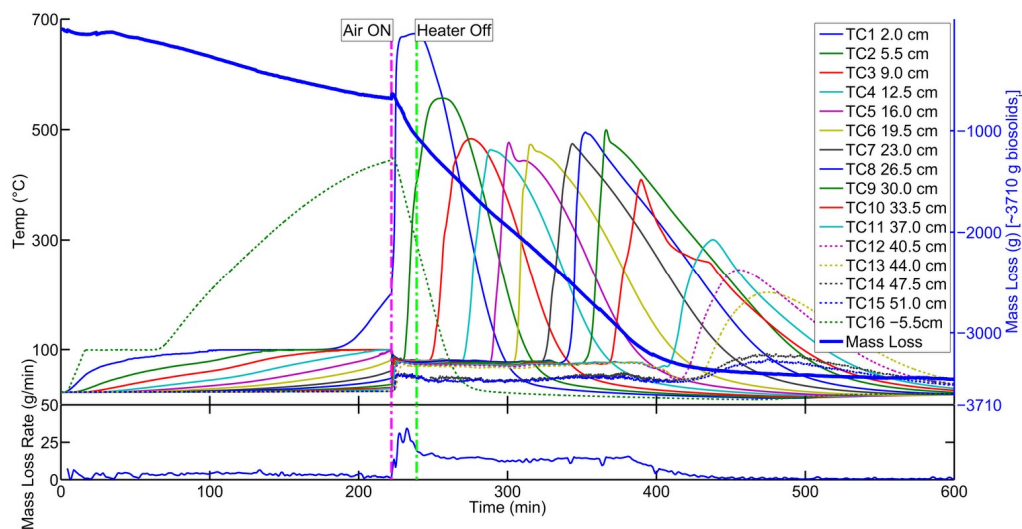

Figure G3: Temperature, mass loss, and mass loss rate profiles for Experiment No. 2, a borderline-self-sustaining smouldering experiment with 80% moisture content re-wetted biosolids in a fixed bed at a 3.5 g/g sand/biosolids mass ratio and an air flux of 3.3 cm/s. The solid lines represent thermocouples within the contaminant pack. The top second y axis (blue) shows the 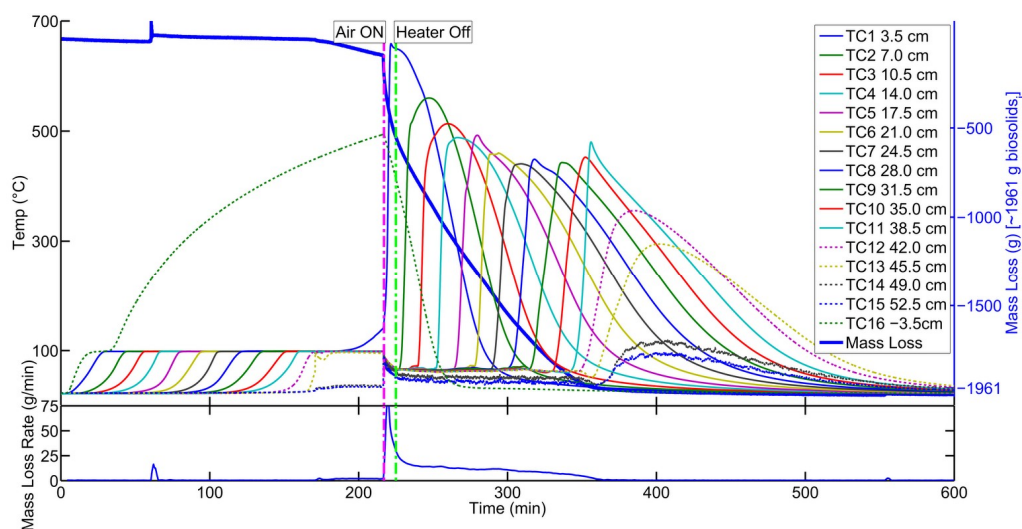initial volatile solids and water mass in the column, 2757 g, and the reaction quenched just before 30 cm up the column (TC9).

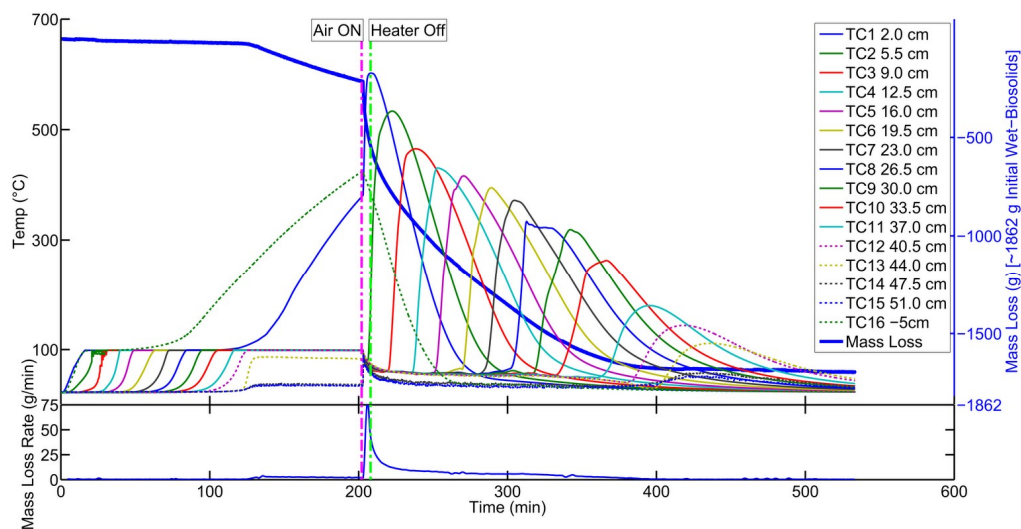**Figure G4: Temperature, mass loss, and mass loss rate profiles for Experiment No. 3, a self-sustaining smouldering experiment with 80% moisture content re-wetted biosolids in a fixed bed at a 3.5 g/g sand/biosolids mass ratio and an air flux of 3.3 cm/s. The solid lines represent thermocouples within the contaminant pack. The top second y axis (blue) shows the initial volatile solids and water mass in the column, 3710 g.**

Figure G5: Temperature, mass loss, and mass loss rate profiles for Experiment No. 5, a self-sustaining smouldering experiment with 79% moisture content re-wetted biosolids in a fixed bed at a 5.1 g/g sand/biosolids mass ratio and an air flux of 3.3 cm/s. The solid lines represent thermocouples within the contaminant pack. The top second y axis (blue) shows the initial volatile solids and water mass in the column, 1961 g. Early disturbance in the mass loss data was due to rearranging equipment. Due to the preheating time over 200 min and high temperature in TC16 (500°C), the air was turned on slightly before TC1 reached 200°C.

Figure G6: Temperature, mass loss, and mass loss rate profiles for Experiment No. 6, a non-self-sustaining smouldering experiment with 83% moisture content re-wetted biosolids in a fixed bed at a 5.8 g/g sand/biosolids mass ratio and an air flux of 3.3 cm/s. The solid lines represent thermocouples within the contaminant pack. The top second y axis (blue) shows the initial volatile solids and water mass in the column, 1862 g.
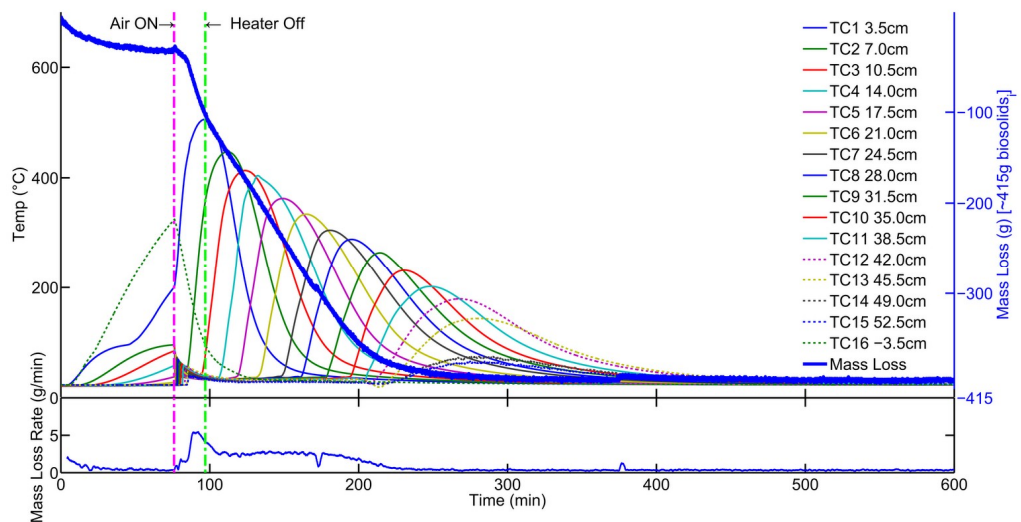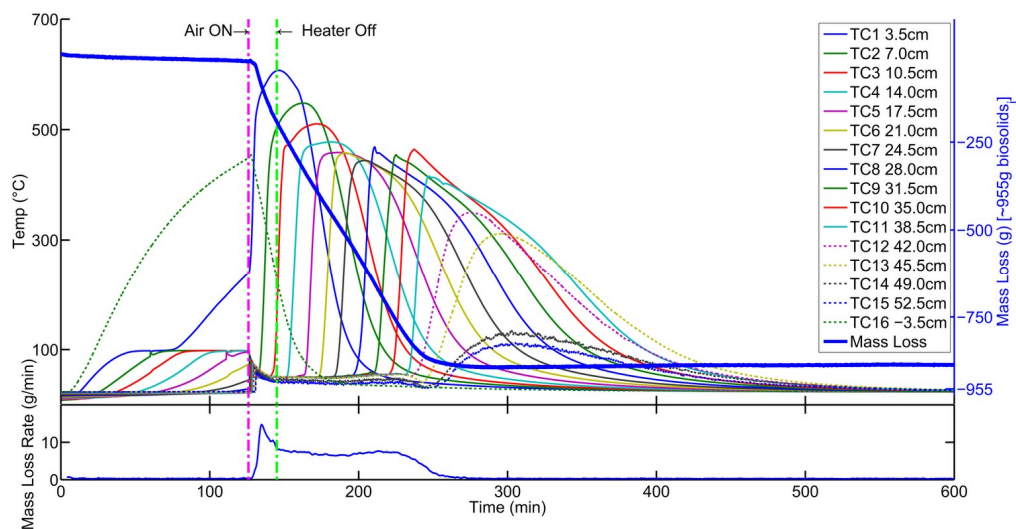

Figure G7: Temperature, mass loss, and mass loss rate profiles for Experiment No. 7, a non-self-sustaining smouldering experiment with 72% moisture content re-wetted biosolids in a fixed bed at a 25 g/g sand/biosolids mass ratio and an air flux of 3.3 cm/s. The solid lines represent thermocouples within the contaminant pack. The top second y axis (blue) shows the initial volatile solids and water mass in the column, 415 g.
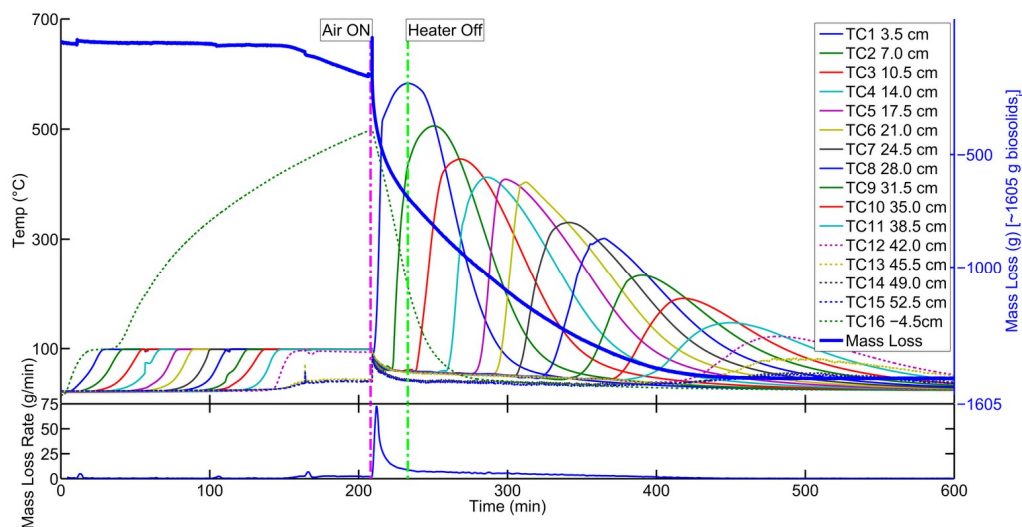
Figure G8: Temperature, mass loss, and mass loss rate profiles for Experiment No. 8, a self-sustaining smouldering experiment with 72% moisture content re-wetted biosolids in a fixed bed at a 11 g/g sand/biosolids mass ratio and an air flux of 3.3 cm/s. The solid lines represent thermocouples within the contaminant pack. The top second y axis (blue) shows the initial volatile solids and water mass in the column, 955 g.
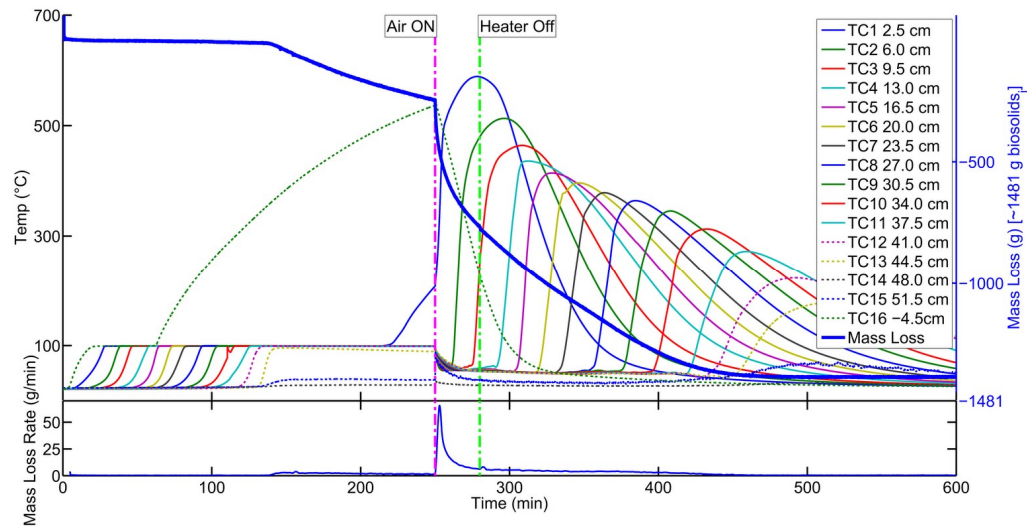

Figure G9: Temperature, mass loss, and mass loss rate profiles for Experiment No. 12, a non-self-sustaining smouldering experiment with 84% moisture content re-wetted biosolids in a fixed bed at a 6.5 g/g sand/biosolids mass ratio and an air flux of 3.3 cm/s. The solid lines represent thermocouples within the contaminant pack. The top second y axis (blue) shows the initial volatile solids and water mass in the column, 1605 g.
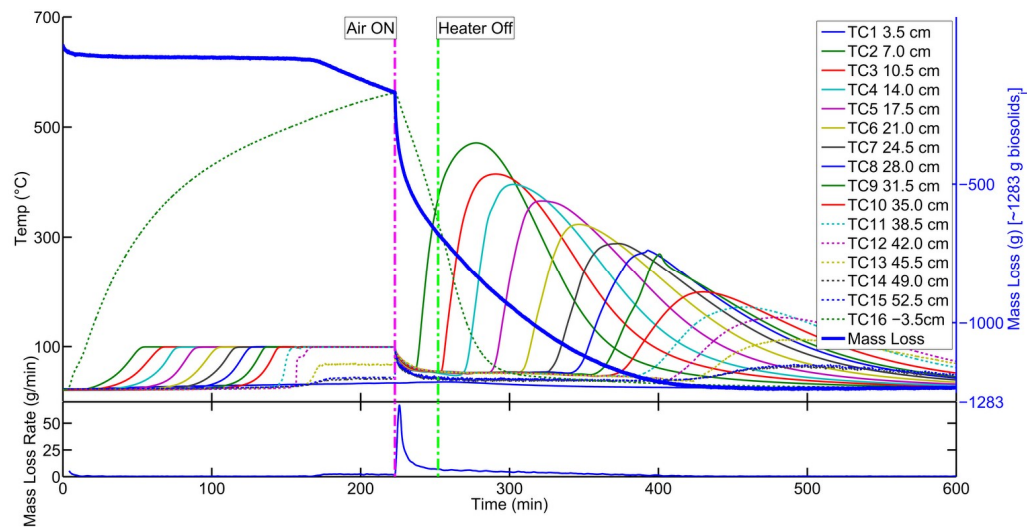
Figure G10: Temperature, mass loss, and mass loss rate profiles for Experiment No. 13, a non-self-sustaining smouldering experiment with 82% moisture content re-wetted biosolids in a fixed bed at a 7.7 g/g sand/biosolids mass ratio and an air flux of 3.3 cm/s. The solid lines represent thermocouples within the contaminant pack. The top second y axis (blue) shows the initial volatile solids and water mass in the column, 1481 g.

Figure G11: Temperature, mass loss, and mass loss rate profiles for Experiment No. 14, a non-self-sustaining smouldering experiment with 83% moisture content re-wetted biosolids in a fixed bed at a 8.3 g/g sand/biosolids mass ratio and an air flux of 3.3 cm/s. The solid lines represent thermocouples within the contaminant pack. The top second y axis (blue) shows the initial volatile solids and water mass in the column, 1283 g. TC1 was broken for this experiment.
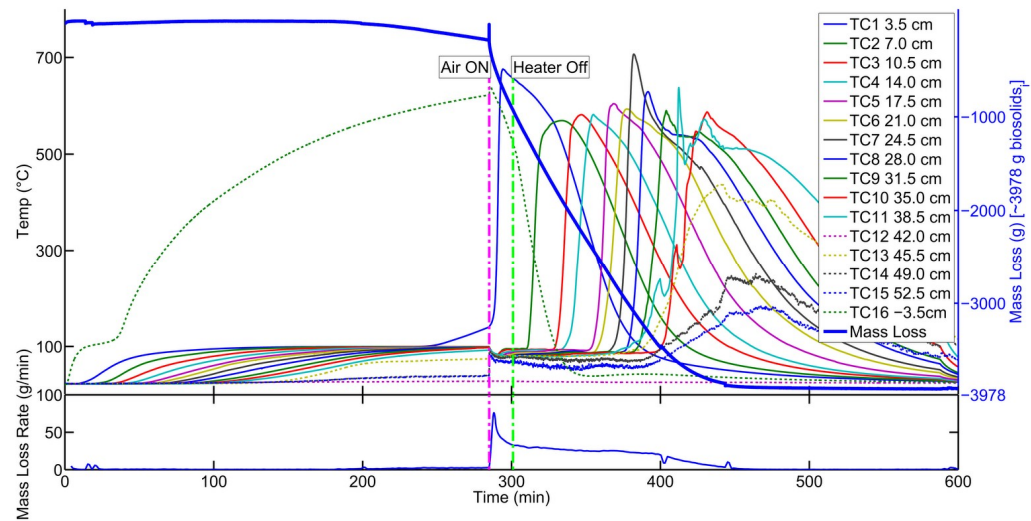
Figure G12: Temperature, mass loss, and mass loss rate profiles for Experiment No. 15, a self-sustaining smouldering experiment with 72% moisture content re-wetted biosolids in a fixed bed at a 2.2 g/g sand/biosolids mass ratio and an air flux of 3.3 cm/s. The solid lines represent thermocouples within the contaminant pack. The top second y axis (blue) shows the initial volatile solids and water mass in the column, 3978 g. The unsteady temperature in TC9 to TC13 is expected to have resulted from water dripping into the reaction front due to the low sand/biosolids mass ratio. TC12 was broken for this experiment.
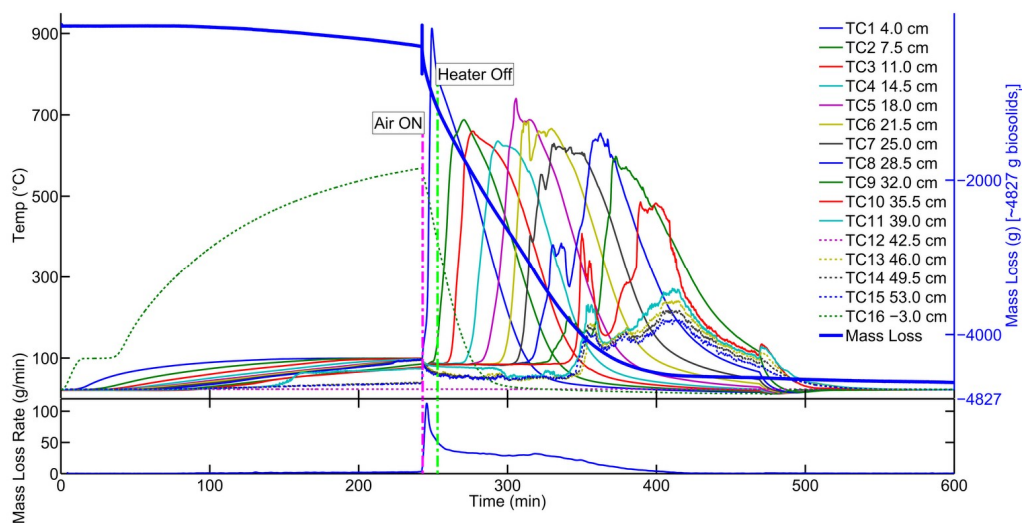
Figure G13: Temperature, mass loss, and mass loss rate profiles for Experiment No. 16, a self-sustaining smouldering experiment with 71% moisture content re-wetted biosolids in a fixed bed at a 1.7 g/g sand/biosolids mass ratio and an air flux of 3.3 cm/s. The solid lines represent thermocouples within the contaminant pack. The top second y axis (blue) shows the initial volatile solids and water mass in the column, 4827 g. The unsteady temperature in TC6 to TC10 is expected to have resulted from water dripping into the reaction front due to the low sand/biosolids mass ratio. Some top sand had been ejected upon air initiation and was corrected in the mass loss data. Due to the ejection, TC11 to 15 were exposed to the atmosphere and represent the air space temperatures above the column upon full combustion. TC12 was broken for this experiment.
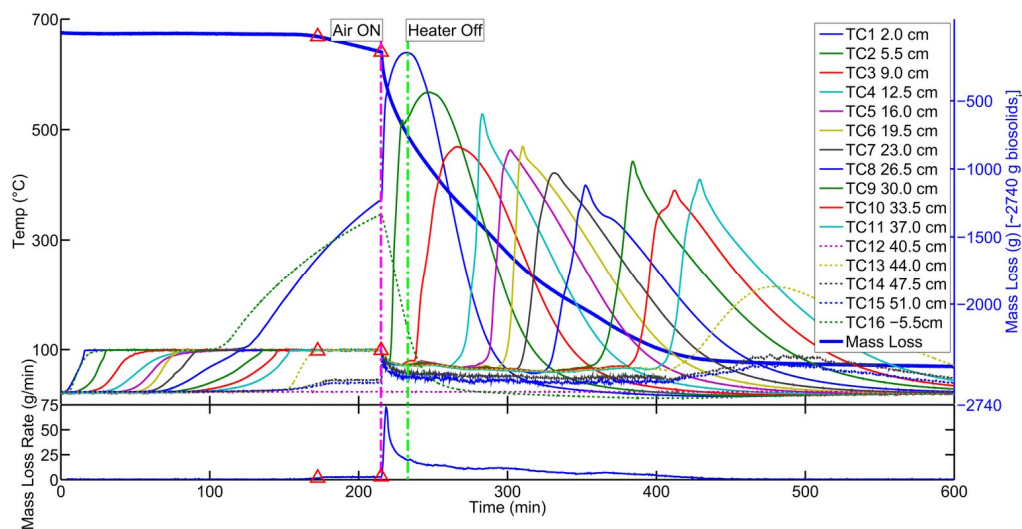
Figure G14: Temperature, mass loss, and mass loss rate profiles for Experiment No. 17, a self-sustaining smouldering experiment with 80% moisture content re-wetted biosolids in a fixed bed at a 4.1 g/g sand/biosolids mass ratio and an air flux of 3.3 cm/s. The solid lines represent thermocouples within the contaminant pack. The top second y axis (blue) shows the initial volatile solids and water mass in the column, 2740 g. The initial water mass loss rate when the full column was boiling was estimated at 2.6 g/min, where the full column boiling period is noted from 172 to 215 min with red triangles. TC12 was broken for this experiment.
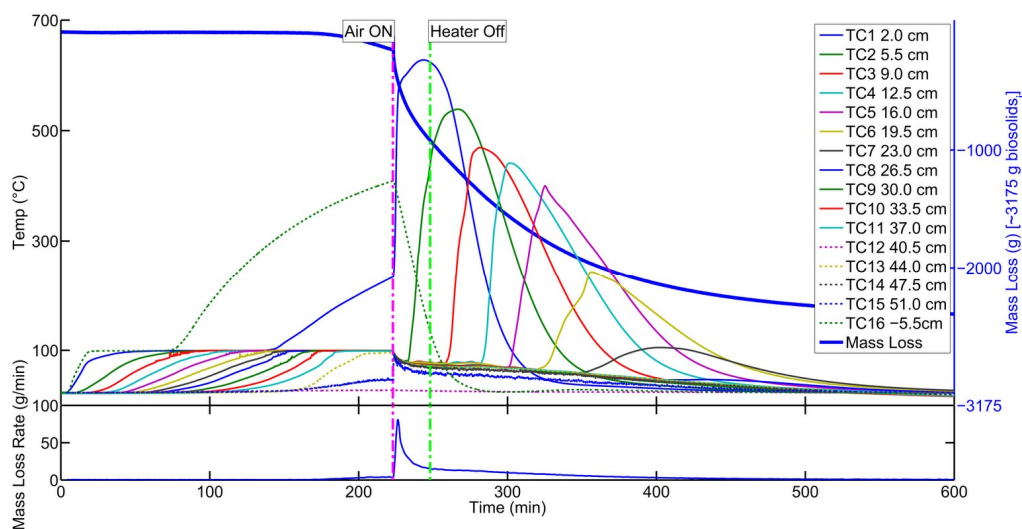

Figure G15: Temperature, mass loss, and mass loss rate profiles for Experiment No. 18, a non-self-sustaining smouldering experiment with 82% moisture content re-wetted biosolids in a fixed bed at a 3.1 g/g sand/biosolids mass ratio and an air flux of 3.3 cm/s. The solid lines represent thermocouples within the contaminant pack. The top second y axis (blue) shows the initial volatile solids and water mass in the column, 3175 g. TC12 was broken for this experiment.
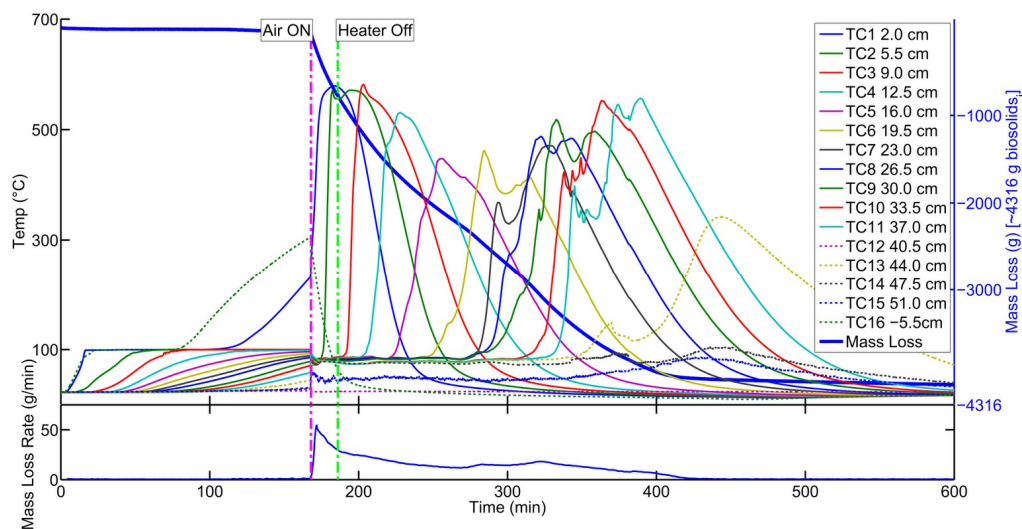
Figure G16: Temperature, mass loss, and mass loss rate profiles for Experiment No. 19, a self-sustaining smouldering experiment with 75% moisture content re-wetted biosolids in a fixed bed at a 2.2 g/g sand/biosolids mass ratio and an air flux of 3.3 cm/s. The solid lines represent thermocouples within the contaminant pack. The top second y axis (blue) shows the initial volatile solids and water mass in the column, 4316 g. Note the 'U' shaped temperature peak and average mass loss rate profiles as the smouldering front passes through the middle 30% of the contaminant pack (TC5 to TC9). TC12 was broken for this experiment.
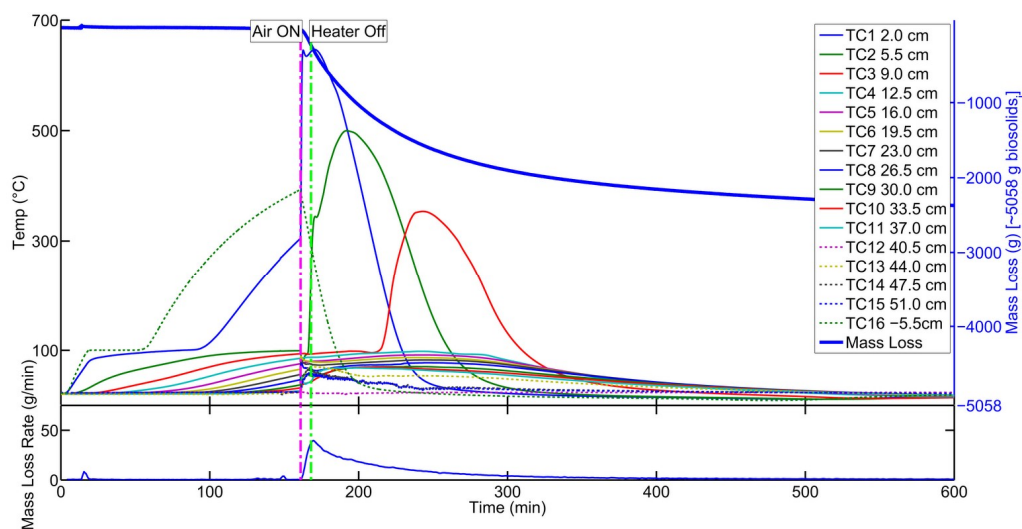

Figure G17: Temperature, mass loss, and mass loss rate profiles for Experiment No. 20, a non-self-sustaining smouldering experiment with 77% moisture content re-wetted biosolids in a fixed bed at a 1.5 g/g sand/biosolids mass ratio and an air flux of 3.3 cm/s. The solid lines represent thermocouples within the contaminant pack. The top second y axis (blue) shows the initial volatile solids and water mass in the column, 5058 g. TC12 was broken for this experiment.
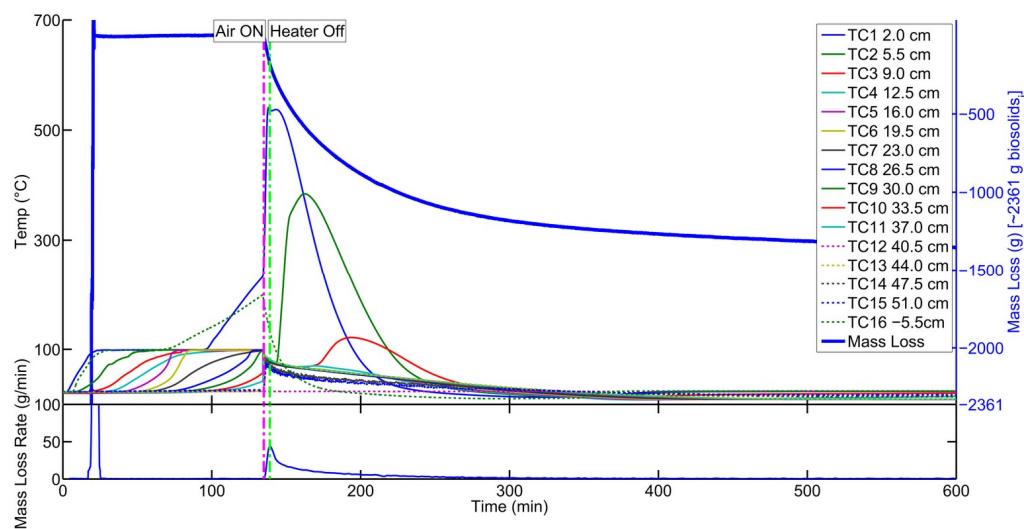
Figure G18: Temperature, mass loss, and mass loss rate profiles for Experiment No. 21, a non-self-sustaining smouldering experiment with 83% moisture content re-wetted biosolids in a fixed bed at a 4.0 g/g sand/biosolids mass ratio and an air flux of 3.3 cm/s. The solid lines represent thermocouples within the contaminant pack. The top second y axis (blue) shows the initial volatile solids and water mass in the column, 2361 g. The early mass disturbance was due to adding the clean sand cap. TC12 was broken for this experiment.
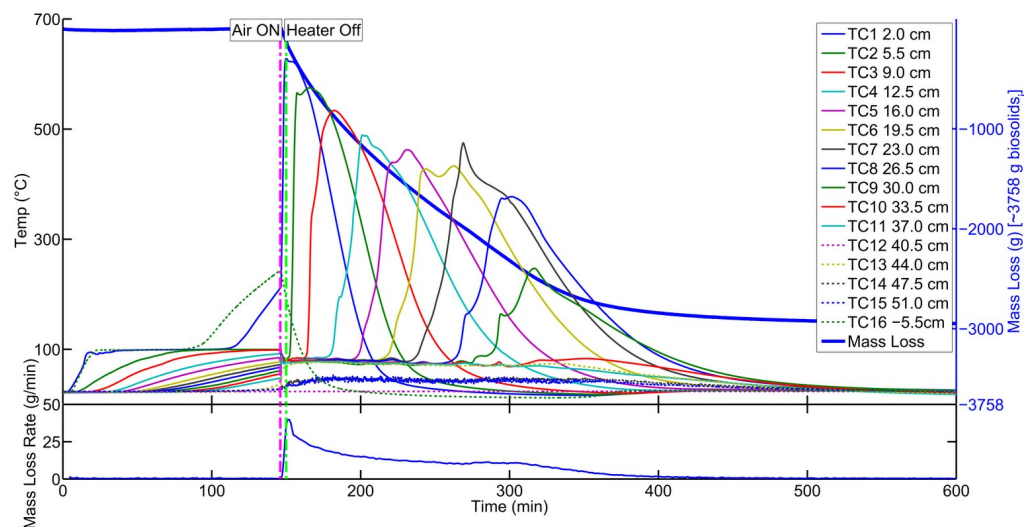

Figure G19: Temperature, mass loss, and mass loss rate profiles for Experiment No. 22, a borderline-self-sustaining smouldering experiment with 77% moisture content re-wetted biosolids in a fixed bed at a 2.5 g/g sand/biosolids mass ratio and an air flux of 3.3 cm/s. The solid lines represent thermocouples within the contaminant pack. The top second y axis (blue) shows the initial volatile solids and water mass in the column, 3758 g, and the reaction quenched just before 30 cm up the column (TC9). TC12 was broken for this experiment.
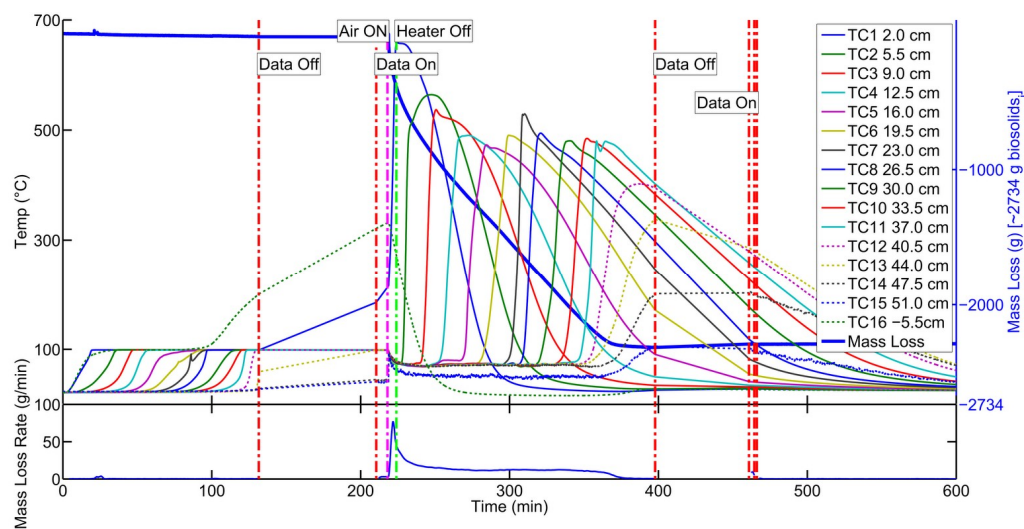
Figure G20: Temperature, mass loss, and mass loss rate profiles for Experiment No. 23, a self-sustaining smouldering experiment with 76% moisture content re-wetted biosolids in a fixed bed at a 4.2 g/g sand/biosolids mass ratio and an air flux of 3.3 cm/s. The solid lines represent thermocouples within the contaminant pack. The top second y axis (blue) shows the initial volatile solids and water mass in the column, 2734 g. The red lines denote an equipment failure where the data logging equipment was temporarily off. All values in between the 'Data Off' to 'Data On' labels are interpolated.
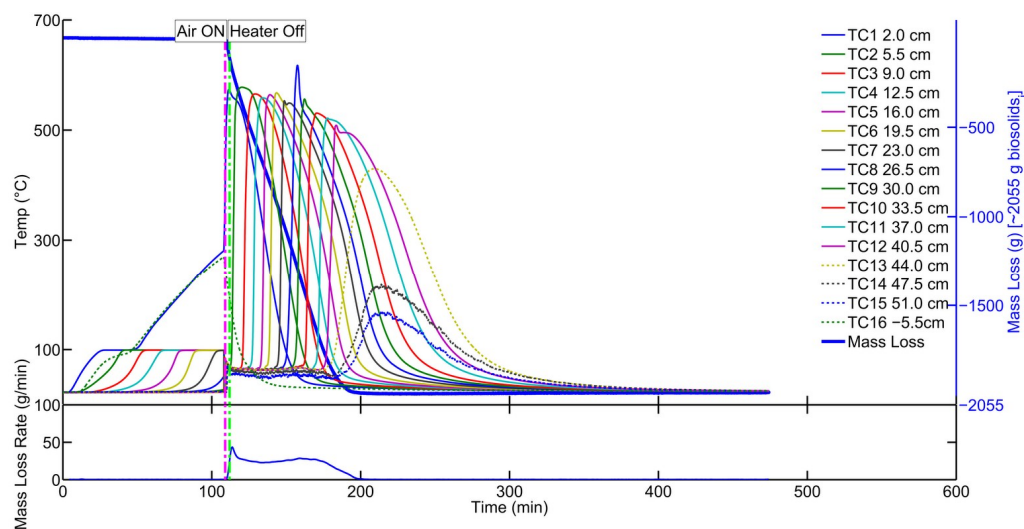

Figure G21: Temperature, mass loss, and mass loss rate profiles for Experiment No. 24, a self-sustaining smouldering experiment with 73% moisture content re-wetted biosolids in a fixed bed at a 4.7 g/g sand/biosolids mass ratio and an air flux of 6.5 cm/s. The solid lines represent thermocouples within the contaminant pack. The top second y axis (blue) shows the initial volatile solids and water mass in the column, 2055 g.
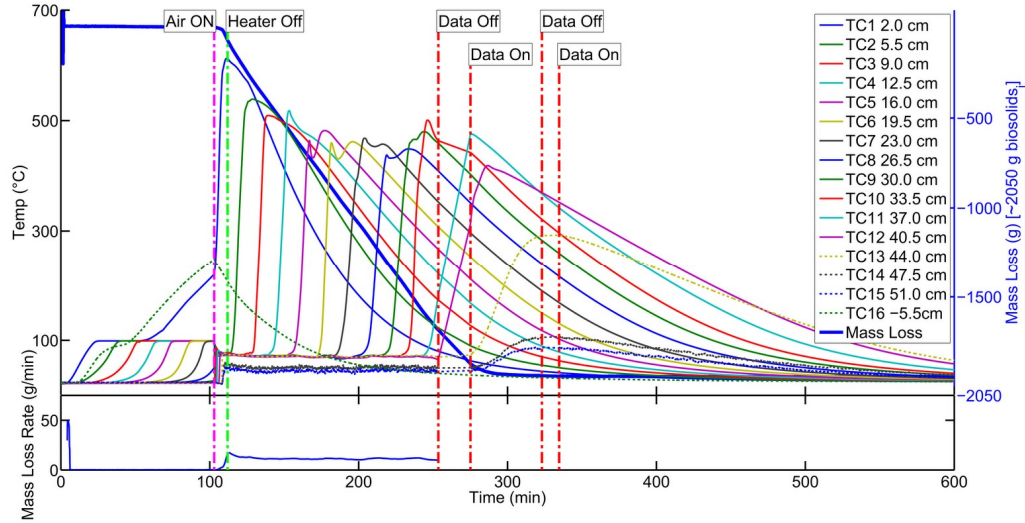
Figure G22: Temperature, mass loss, and mass loss rate profiles for Experiment No. 25, a self-sustaining smouldering experiment with 72% moisture content re-wetted biosolids in a fixed bed at a 4.8 g/g sand/biosolids mass ratio and an air flux of 1.6 cm/s. The solid lines represent thermocouples within the contaminant pack. The top second y axis (blue) shows the initial volatile solids and water mass in the column, 2050 g. The red lines denote an equipment failure where the data logging equipment was temporarily off. All values in between the 'Data Off' to 'Data On' labels are interpolated.
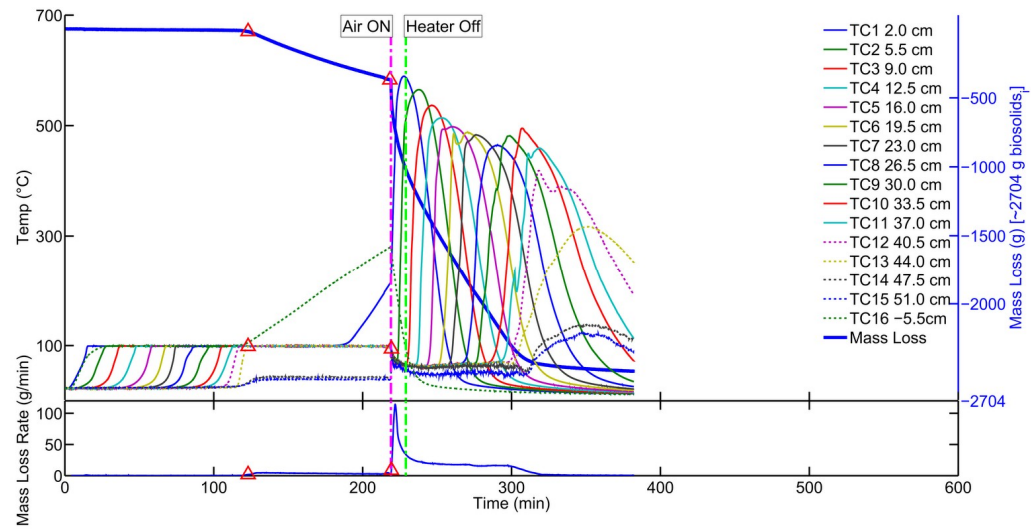
Figure G23: Temperature, mass loss, and mass loss rate profiles for Experiment No. 26, a self-sustaining smouldering experiment with 78% moisture content re-wetted biosolids in a fixed bed at a 3.5 g/g sand/biosolids mass ratio and an air flux of 6.5 cm/s. The solid lines represent thermocouples within the contaminant pack. The top second y axis (blue) shows the initial volatile solids and water mass in the column, 2704 g. The abrupt end in the data before 400 min was due to an equipment error. The initial water mass loss rate when the full column was boiling was estimated at 3.7 g/min, where the full column boiling period is noted from 123 to 219 min with red triangles.
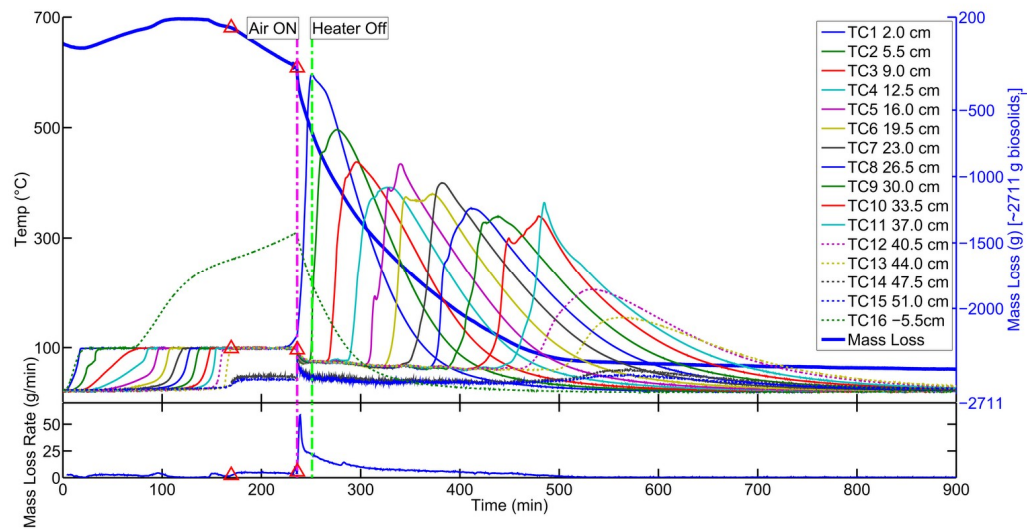
Figure G24: Temperature, mass loss, and mass loss rate profiles for Experiment No. 27, a self-sustaining smouldering experiment with 79% moisture content re-wetted biosolids in a fixed bed at a 4.3 g/g sand/biosolids mass ratio and an air flux of 1.6 cm/s. The solid lines represent thermocouples within the contaminant pack. The top second y axis (blue) shows the initial volatile solids and water mass in the column, 2711 g. The initial rise in mass loss prior to the air turned on was due to an equipment error and so the early water mass loss rate was estimated 3.4 g/min during 170 to 236 min, which is when the full column was boiling (noted with red triangles).
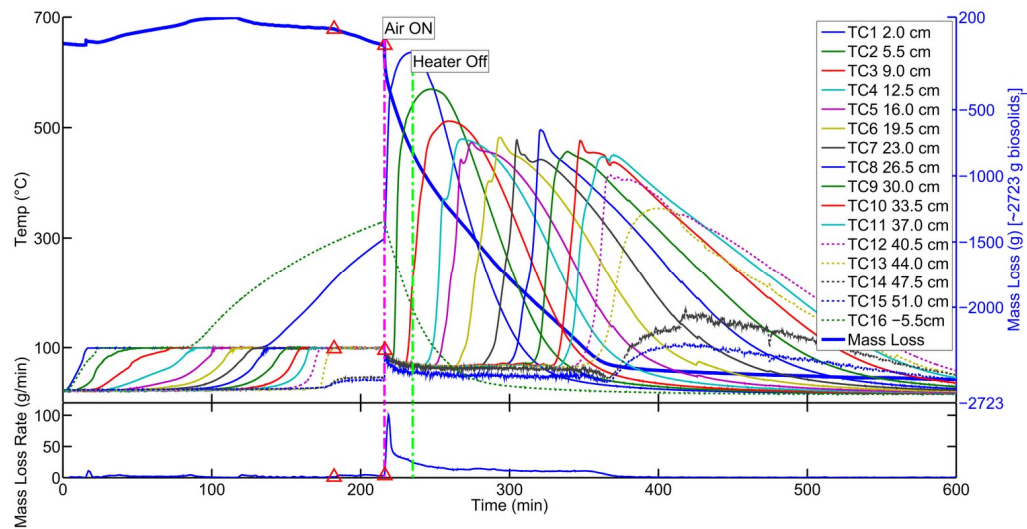
Figure G25: Temperature, mass loss, and mass loss rate profiles for Experiment No. 28, a self-sustaining smouldering experiment with 80% moisture content re-wetted biosolids in a fixed bed at a 4.0 g/g sand/biosolids mass ratio and an air flux of 3.3 cm/s. The solid lines represent thermocouples within the contaminant pack. The top second y axis (blue) shows the initial volatile solids and water mass in the column, 2723 g. The initial rise in mass loss prior to the air turned on was due to an equipment error and so the early mass loss rate was estimated 3.4 g/min during 182 to 216 min, which is when the full column was boiling (noted with red triangles).
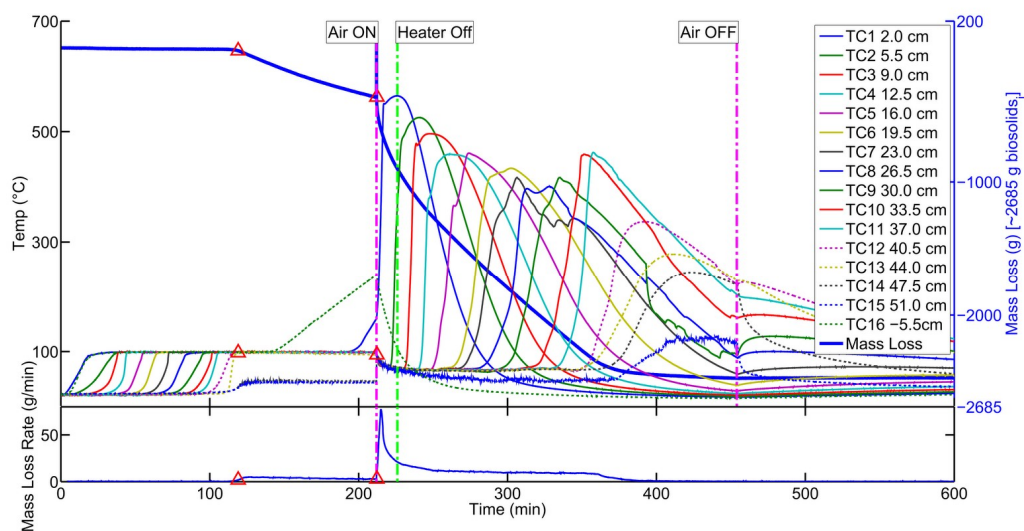
Figure G26: Temperature, mass loss, and mass loss rate profiles for Experiment No. 29, a self-sustaining smouldering experiment with 78% moisture content re-wetted biosolids in a fixed bed at a 4.5 g/g sand/biosolids mass ratio and an air flux of 3.3 cm/s. The solid lines represent thermocouples within the contaminant pack. The top second y axis (blue) shows the initial volatile solids and water mass in the column, 2685 g. The air was turned off at 454 min for a mass balance verification presented in Appendix F. The initial water mass loss rate when the full column was boiling was estimated at 3.8 g/min, where the full column boiling period is noted from 119 to 212 min with red triangles.

Curriculum Vitae

Name: Tarek Lee Rashwan

Post-secondary   The University of Western Ontario
Education and   London, Ontario, Canada
Degrees: 2009-2013 B.E.Sc.

                      The University of Western Ontario
                      London, Ontario, Canada
                      2013-2015 M.E.Sc.

Honours and   Province of Ontario Graduate Scholarship (declined)
Awards: (2014-2015)

                      Natural Sciences Engineering Research Council of Canada Industrial
                      Postgraduate Scholarship
                      (2014-2016)

                      Y.F. Eric Chung and Ruby Chung Graduate Scholarship
                      (2014-2015)

                      Western's Ideas for Sustainability and the Environment, Graduate
                      Competition
                      (2015-2016)

Related Work   Teaching Assistant
Experience: The University of Western Ontario
                      2013-2015

                      Lecture Assistant
                      The University of Western Ontario/Richard Ivey School of Business
                      2013-2015

Publications:

Rashwan, T. L., Gerhard, J. L., Grant, G. (2015, May). *Self-sustaining Smoldering as Energy Efficient Alternative for Managing Biosolids*. Paper presented at the 9th U. S. National Combustion Meeting, Cincinnati, OH.